Use of the *in situ* proximity ligation assay (PLA) for studies of CKS2 interactions in HeLa cells

By Marte Jonsson

45 study points

A dissertation for the Master's degree in Pharmacy
School of Pharmacy
Faculty of Mathematics and Natural Sciences

UNIVERSITY OF OSLO

March 2012

Use of the *in situ* proximity ligation assay (PLA) for studies of CKS2 interactions in HeLa cells

A dissertation in molecular biology/cell biology for the Master's degree in Pharmacy

By Marte Jonsson

Performed at the Department of Radiation Biology
Institute for Cancer Research
The Norwegian Radium Hospital

School of Pharmacy
Faculty of Mathematics and Natural Sciences

UNIVERSITY OF OSLO

March 2012

2012

Use of the *in situ* proximity ligation assay (PLA) for studies of CKS2 interactions in HeLa cells

Supervisors: Heidi Lyng, Kirsten Skarstad

http://www.duo.uio.no/

Trykk: Reprosentralen, Universitetet i Oslo

Abstract

Cyclin-dependent kinases regulatory subunit 2 (CKS2) is overexpressed and associated with aggressiveness of several cancers. The reason for this is not clarified. CKS2 is known to bind the cell cycle regulatory proteins cyclin-dependent kinase 1 and 2 (CDK2 and CDK2) and mitochondrial single-stranded DNA-binding protein (SSBP1). SSBP1 participates in the biogenesis of mitochondria. These interactions have not previously been explored by *in situ* proximity ligation assay (PLA). The purpose of this study was to investigate cellular localization of CKS2 in HeLa cells. Further, co-localization and interactions of CKS2 with CDK1, CDK2 and SSBP1 were explored by immunofluorescence cytochemistry and PLA. Several fixation methods were tested for optimization of the PLA. Immunofluorescence cytochemistry showed that CKS2 was distributed in large foci in the nucleus and in small foci in the cytoplasm. In addition, CKS2 and CDK1 were localized at the centrosomes both in interphase and mitosis. The nuclear CKS2 foci were mainly restricted to weakly Hoechst stained areas, and they were co-localized with CDK1 and CDK2. Co-localization between CKS2, CDK1 and CDK2 was also apparent in the cytoplasm in interphase and mitosis. A small part of the cytoplasmic CKS2 and CDK1 foci co-localized with a SSBP1. PLA functioned well for both formalin and methanol fixated cells. However, formalin fixated cells required treatment with an extra reagent, *e.g*. a detergent buffer or methanol for production of PLA signals in the nucleus. Methanol fixation alone produced reproducible nuclear signals and was used for the examination of CKS2-CDK interactions, whereas combined formalin and methanol fixation were used for studying CKS2-SSBP1 and CDK1-SSBP1 interactions. PLA confirmed that CKS2 interacted with CDK1 and CDK2 in the nucleus and with CDK1, CDK2 and SSBP1 in the cytoplasm. The distribution of the CDK1-SSBP1 interactions in the cytoplasm resembled that of the CKS2-SSBP1 interactions. The results indicated that the large CKS2 foci in the nucleus were localized in euchromatin, which is transcriptionally competent DNA, and thus support the hypothesis that CKS2 has a role in the transcription of DNA. CKS2 probably interacted with CDK1 and CDK2 in these areas. Some of the cytoplasmic CKS2 and CDK1 foci interacted with SSBP1, probably within the mitochondria. In addition, the co-localization of CKS2 and CDK1 at the centrosomes lends support to the hypothesis of CKS-dependent activation and inactivation of the CDK1-CCNB complex prior to and in the mitosis.

Acknowledgements

This Master's thesis was performed at the Department of Radiation Biology, Institute for Cancer Research at the Norwegian Radium Hospital from May 2011 to March 2012.

I would like to express my most sincere gratitude to my supervisor Heidi Lyng for providing me with a stimulating project and for encouragement, inspiration and very helpful feedbacks. Your door was always open for me and my questions. Thank you for sharing your time and your knowledge with me.

Thanks are due to Kirsten Skarstad for being my co-supervisor and for inspiration and positive remarks during the study.

Several colleagues at the MSB group have been helpful in numerous practical ways. In particular Eva-Kathrine Aarnes must be mentioned. She introduced me to practices in the cell lab and answered my never ending questions. I am also grateful to Sebastian Patzke for introducing me to scientific concepts, fluorescence microscopy and for sharing his knowledge. I would like to thank Trond Stokke for helpful feedbacks on the experiments. Thanks are due to all the group members for many interesting talks on and off topic, and for including me in their group.

I would also like to thank my family, especially my parents, for their incredibly support throughout my life. It provided me with a good starting-point for my academic pursuit.

Finally, I would like to thank my fiancée Arild, for always believing in me, and for making this busy period of my life as easy as it could possibly be.

Oslo, 28.03.12

Marte Jonsson

Abbreviations

APC/C – Anaphase-promoting complex/cyclosome

AP site – Apurinic /apyrimidinic site

ATP – Adenosine triphosphate

BER – Base excision repair

BP – Broad-pass

BUB – Budding unhibited by benomyl

CAK – Cdk activating kinase

CCNA – Cyclin A

CCNB – Cyclin B

CCNE – Cyclin E

CDC20 – Cell-division cycle 20

CDC25 – Cell-division cycle 25

CDK – Cyclin-dependent kinase

CKS1 – Cyclin-dependent kinases regulatory subunit 1

CKS2 – Cyclin-dependent kinases regulatory subunit 2

D-loop – Displacement loop

dsDNA – Double-stranded DNA

ETC – Electron transport chain

FBS – Fetal bovine serum

FT – Dichroic beam splitter mirror

HPV – Human papillomavirus

LP – Long-pass

MAD – Mitotic arrest deficient

MMR – Mismatch repair

mRNA – Messenger RNA

mtDNA – Mitochondrial DNA

mtTFA – Mitochondrial transcription factor A

ORF – Open reading frame

PLA – *in situ* proximity ligation assay

POLG – DNA polymerase γ

RB1 – Retinoblastoma

RCA – Rolling circle amplification

RISC – RNA-Induced Silencing Complex

RNAi – RNA interference

ROS – Reactive oxygen species

shRNA – Short hairpin RNA

siRNA – Small interfering RNA

SOD – Superoxide dismutase

SSBP1 – Single-stranded DNA-binding protein

ssDNA – Single stranded DNA

TP53 – Tumor protein p53

Thr 14 – Threonine 14

Tyr 15 – Tyrosine 15

Table of contents

1 Introduction

Cyclin-dependent kinases regulatory subunit 2 (CKS2) is a mammalian protein encoded by the *CKS2* gene [1-3]. It binds to the catalytic subunit of the cyclin-dependent kinases and appears critical for several biological functions [4]. For instance, the protein is assumed to participate in cell cycle control, because of its association with cyclin-dependent kinase 1 and 2 (CDK1 and CDK2) [2]. The CKS2 messenger RNA (mRNA) has been found to be expressed in different patterns through the cell cycle in HeLa cells, which is a cell line derived from cervical cancer [5]. Thus, CKS2 might have a function in cell cycle control. However, the role of CKS2 in the cell cycle is not fully clear. Recently, CKS2 was identified as an interaction partner of single-stranded DNA binding protein 1 (SSBP1) and involved in replication of mitochondrial DNA [6], suggesting that CKS2 have functions other than related to the cell cycle. The *CKS2* gene is up-regulated in several malignancies, including gastric, colorectal, hepatocellular and cervical cancer, and its expression correlates with aggressiveness and poor prognosis of the cancer [7-10]. The importance of CKS2 for cancer progression has not been clarified.

Protein interactions appear essential for cellular biological processes [11]. Knowledge of CKS2 interactions with other proteins in cancer cells can provide insight into active signaling pathways in these cells. By that, more knowledge of CKS2 protein interactions can be one step on the way to ascertain which pathways that contribute to the development and aggressiveness of, for instance, cervical cancer. Such pathways can be attractive targets for the development of cancer therapies [12].

There are several methods that can be used to study interactions between proteins in cells. Immunofluorescence cytochemistry is a suitable method for co-localization experiments, and for examination of the spatial distribution of the proteins [13]. Recently, a new method, in situ proximity ligation assay (PLA), was developed to study protein-interactions in cells [14, 15]. PLA is a sensitive method that relies on the simultaneous binding of two antibodies against two target proteins, and utilizes a proximity ligation technique coupled to an amplification reaction to detect the antibodies whenever they are in close proximity, *i.e.* in cases of interaction. Both immunofluorescence cytochemistry and PLA require specific staining of the proteins in fixated cells [16, 17]. Fixation may influence the availability and change the structure of the antigen [18]. It is uncertain which fixation method will provide the best and

most reproducible results for the present experiments, but methanol, formalin and combinations of these have been used. The PLA method requires access of two antibodies, and might therefore be sensitive for fixation methods.

The purpose of this thesis was to detect interactions between CKS2 and its known interaction partners in different cellular compartments of HeLa cells. In order to achieve this, the subsidiary aims were to:

- Study cellular localization of CKS2 and its co-localization with CDK1, CDK2 and SSBP1 with immunofluorescence cytochemistry
- Optimize the PLA technique for studies of CKS2 interactions with respect to different fixation methods
- Use the optimized protocol to search for CKS2 interactions with CDK1, CDK2 and SSBP1 in relation to cellular compartments

2 Biological background

2.1 The Cell Cycle

The cell cycle is the life of a cell from the time it is formed by a dividing parent cell until its own division in two cells [19]. The entire DNA is duplicated before a cell divides. At division, the two copies of the DNA are allocated to opposite parts of the cell, and the cell splits in two. The daughter cells therefore end up with a complete genome, which is the genetic equivalent of the parent genome.

The cell cycle is divided in the interphase and the mitotic (M) phase [19]. The cell grows by producing proteins and organelles, such as mitochondria and the endoplasmatic reticulum, during the three subphases (G1, S and G2; figure 1). During the G1 phase, the cell prepares for DNA synthesis, but the chromosomes duplicate only during the S phase [20]. The S phase is followed by the G2 phase, during which the cell prepares for the mitosis.

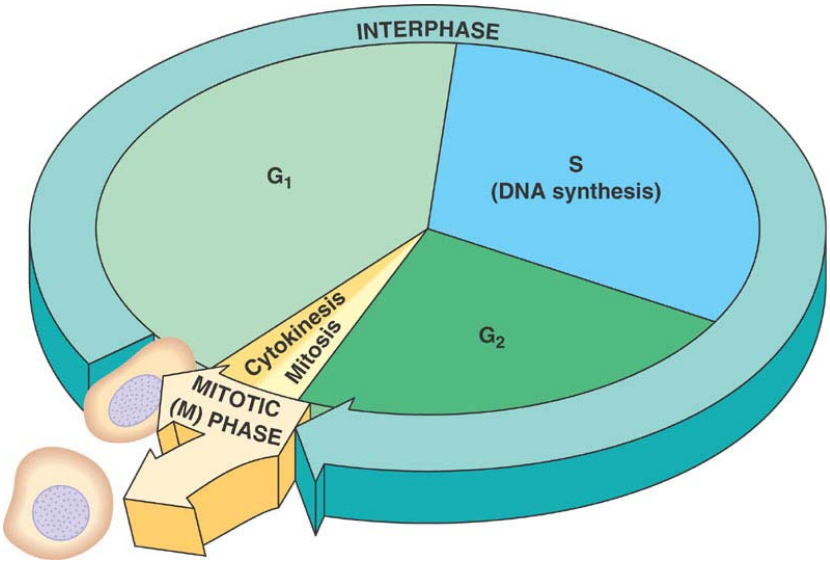

Figure 1. The different phases of the cell cycle. The interphase accounts for about 90 % of the duration of the cell cycle, and is subdivided in the G1 phase (first gap), S phase (synthesis), and G2 phase (second gap) [19]. The interphase is followed by the M phase (mitosis).

The interphase alternates with the mitotic (M) phase, which includes mitosis and cytokinesis [19]. Mitosis is the division of the nucleus, whereas cytokinesis is the division of the cytoplasm. The mitosis is divided in five stages: prophase, prometaphase, metaphase,

anaphase and telophase (figure 2). The cytokinesis overlaps with the latter stages, and completes the cell cycle.

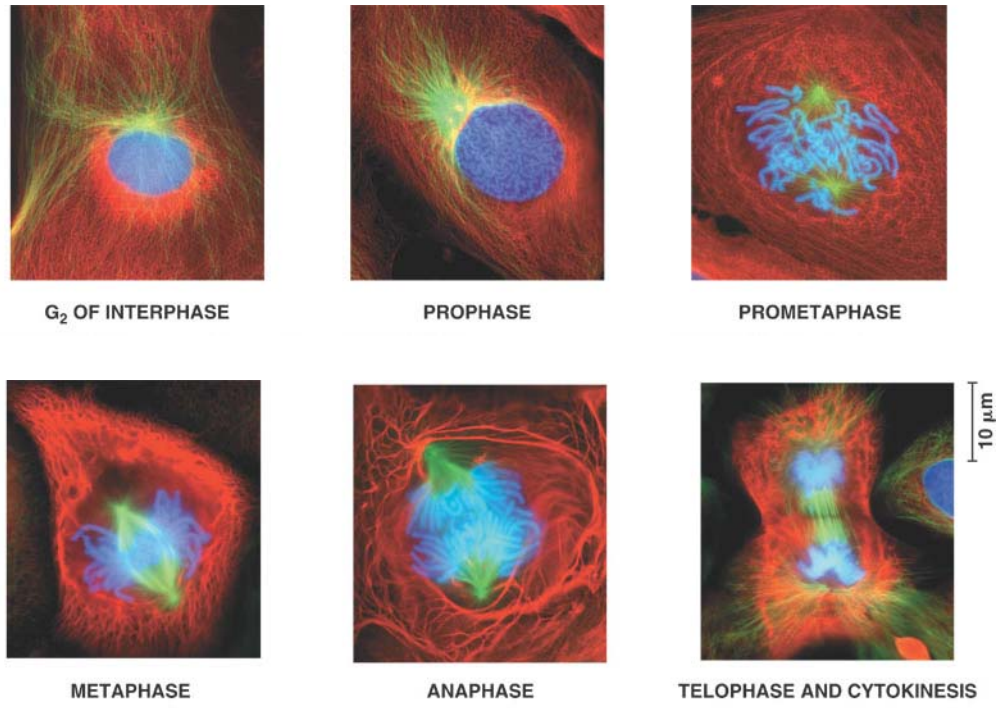

Figure 2. The mitotic division of a mammalian cell [19]. Chromosomes are stained blue, microtubules green and intermediate filaments red.

When a cell is not dividing and during DNA replication, the DNA is kept in the form of a thin fiber [19]. After DNA replication, the DNA is coiled up in a condensed form. During prophase, the chromatin fibers become more tightly coiled, condensing in discrete chromosomes. The formation of the mitotic spindle begins during prophase at the centrosomes, which are organelles that organize the cell's microtubules. The nuclear envelope breaks down during the prometaphase and the spindle microtubules invade the nuclear area and interact with the chromosomes. At metaphase, the centrosomes are located at opposite ends of the cell. At this stage, the chromosomes are settled midways between the two spindle poles and forms a plane called the metaphase plate of the cell. During anaphase, proteins holding the two sister chromatids together are inactivated, and the chromosomes are pulled in opposite directions. Two daughter nuclei begin to form during telophase and the chromosomes become less condensed. Cytokinesis is well underway by late telophase. A furrow appears near the old metaphase plate. It is created by a contractile ring of actin filaments, which interact with the protein myosin and pinches the cell in two. This produces two completely separated daughter cells.

2.1.1 CDK-cyclin complexes: key drivers of the cell cycle

Cells reproduce themselves with extreme precision. This ensures normal growth and development [19]. Each event of the cell cycle has to be completed successfully for the cell to continue through the cycle. This is controlled by several checkpoints. Mammalian cells have built-in stop signals that halt the cell cycle until the cell receives triggering signals. The signals are produced when crucial processes have been completed. Checkpoints can also register chemical and physical signals. For instance, cells fail to divide if nutrients or specific growth factors are lacking, or if the DNA is damaged [19, 21].

Three important checkpoints are located in G1, G2 and M phases [19]. If the cell receives a stimulating signal during the G1 checkpoint, it will usually complete the S, G2 and the M phase. If not, it will exit the cycle and enter G0 phase. Cell cycle control molecules are proteins of two main types: kinases and cyclins. Kinases are enzymes that inhibit or activate other proteins through phosphorylation. The kinases circulate in an inactive form until they interact with cyclins. They are therefore called cyclin-dependent kinases (CDKs). The name cyclins originates from their fluctuating concentration during the cell cycle, which causes rhythmic fluctuations in the activity of the CDKs. This results in the initiation of cell cycle events. Different types of cyclins are produced at different cell cycle phases.

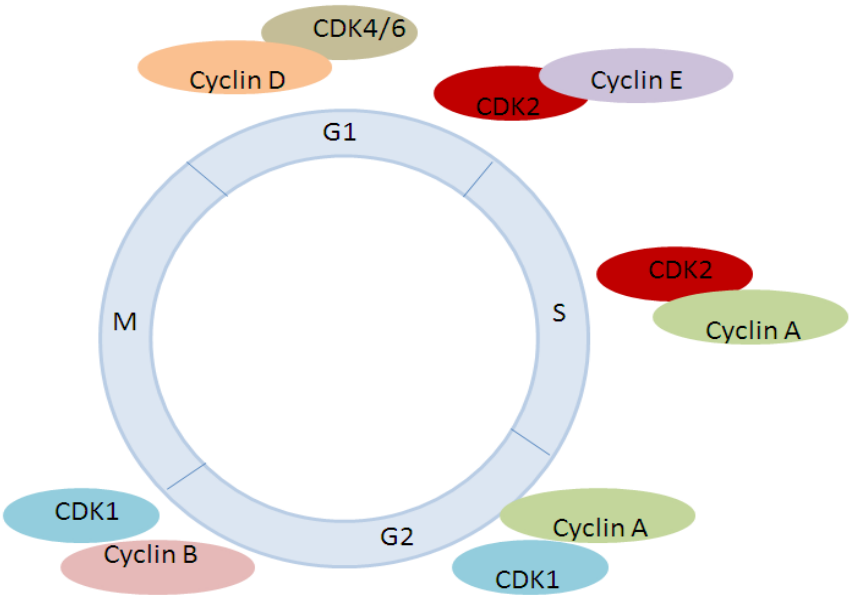

Figure 3. CDK-cyclin complexes direct progression through the cell cycle. The sites of activity of the CDK-cyclin complexes in the various cell cycle phases are indicated.

At formation, the CDK-cyclin complexes are inactive [19, 22]. First, they are phosphorylated at specific sites by kinases. Phosphorylation of some sites are required for its activity, others inhibit its activity. Second, the inhibitory phosphate groups are removed by phosphatases. Once activated, the CDK-cyclin complexes can activate more complexes and create an explosive increase in CDK-cyclin activity.

Progression through G1 is regulated by CDK4, CDK6 and CDK2 and their cyclins (cyclin D and E) (figure 3) [23]. Cyclin E (CCNE) is required to activate CDK2 for proper completion of G1 phase and is thought to be essential for initiating DNA replication. CCNE is silenced once the S phase is begun to avoid re-replication of DNA. Then, CDK2 interacts with newly synthesized cyclin A (CCNA), which is required for proper completion and exit from the S phase. At the end of the S phase, CCNA associates with CDK1. During G2, CCNA is degraded by ubiquitin-mediated proteolysis and cyclin B (CCNB) is actively synthesized. The CDK1-CCNB complex is activated in G2 and triggers the cell into M phase. The complex activates key proteins, which cause the chromosomes to condense, the nuclear envelope to break down, and the mitotic spindle to form [19]. Inactivation of CCNB is regulated by the anaphase-promoting complex/cyclosome (APC/C) and is required for proper exit from the mitosis [23].

CDK1, originally identified as a mitosis promoting kinase, appears to have a master role in the cell cycle. CDK1 can compensate for the loss of CDK2 by binding in a complex with CCNE to drive cells through the G1-S transition [24]. In addition, a study revealed that CDK1 is sufficient to drive the eukaryotic cell cycle in early embryogenesis and in mouse embryonic fibroblasts [25].

2.1.2 Checkpoints of the cell cycle

The cell cycle control system is self-regulating [19]. If one step, for instance the mitosis, is delayed, the cell will not proceed into cytokinesis with the cromosomes half segregated. The system has molecular breaks that stop the cell cycle at specific checkpoints, as mentioned in chapter 2.1.1.

One major checkpoint in G1 halts the cell cycle if the DNA is damaged [19, 22]. This ensures that the cell do not replicate damaged DNA. Otherwise, the cell mutates and may become cancerous. DNA damage causes an increase in the regulatory tumor protein p53 (TP53), which activates the transcription of the CDK inhibitor protein p21. The protein inhibits

CDK2-CCNE and prevents entry into S-phase. The cell can then repair the damaged DNA and continue the cell cycle. If TP53 is defective, replication may occur, leading to accumulation of mutations. Mutations in TP53 are found in half of all diagnosed cancers.

The G2 checkpoint, also known as the G2/M checkpoint, prevents cells from entering mitosis with damaged DNA [20]. The checkpoint inhibits the activity of CDK1-CCNB by inhibitory phosphorylations. This is achieved by the checkpoint kinase 1 and 2 (CHK1 and CHK2), which are activated during DNA damage and phosphorylate cell division cycle 25 (CDC25) phosphatases. This prevents CDC25 proteins from activating CDK1-CCNB, by removing inhibitory phosphate groups, and mitotic entry. DNA damage also activates TP53, which increases transcription of the CDK inhibitor p21.

A checkpoint called the spindle checkpoint stops the cell cycle during M phase if the chromosomes are not properly attached to the mitotic spindle in metaphase [20]. Activation of the spindle checkpoint is achieved by proteins called mitotic arrest deficient (MAD) and budding uninhibited by benomyl (BUB), which inhibit the CDC20 subunit of the APC/C. This restrains the APC/C from targeting CCNB and prevents metaphase-anaphase transition [26].

2.2 CKS proteins

CKS2 is a member of the cyclin-dependent kinase subunit (CKS) family [7]. CKS proteins are expressed in all eukaryotic lineages [27]. In mammals, there are two homologs, CKS1 and CKS2, which participate in the cell cycle regulation [7]. CKS2 is overexpressed in many human malignancies, including colorectal [9], gastric [7], cervical [28] and hepatocellular cancer [10]. Moreover, Lyng et al [8] have reported that high CKS2 expression was correlated with poor progression free survival and associated with metastatic phenotypes, rapid proliferation and tumor size in patients with uterine cervical cancer.

The function of CKS2 in mammalian cells is not well understood. Mice lacking CKS2 are sterile, because the germ cells fail to progress past the first metaphase-anaphase transition during meiosis [29]. Mice that lack CKS1are viable and fertile, but a double nullizygous genotype is lethal [2].

CKS proteins consist of four-stranded anti-parallel β-sheets chapped at one end by two short α-helices [30]. X-ray diffraction structural determinations exhibit that CKS2 exist as

monomers, dimers or hexamers [4]. The hexamer form is a trimer of strand-exchanged dimers, which forms a ring structure [4, 30]. However, experiments suggest that monomeric CKS2 binds strongly to CDKs, whereas the dimer and hexamer sterically precludes binding with CDKs [31-33]. CKS2 appears to be involved in several cellular functions, for instance in regulating the APC/C and the mitochondrial single stranded DNA binding protein (SSBP1) [6, 34]. The interaction with CDK proteins, especially with CDK1, is most extensively studied. The significance of CKS2s binding to CDK2 is poorly known. However, overexpression of CKS2 in cancer cells is shown to maintain CDK2 in an active state in spite of inhibitory phosphorylations on Tyrosine-15 (Tyr-15) caused by activation of the S-phase checkpoint [27].

2.2.1 CKS2 is involved in the G2-M transition of the cell cycle

CKS2 appears to affect the G2-M transition of the cell cycle, and it is known to interact with CDK1-CCNB [35, 36]. During interphase, CDK1 is inactive because of inhibitory phosphorylation on Tyr-15 and Threonine-14 (Thr-14) by WEE1 and MYT1 [37, 38]. When the conditions are appropriate for mitosis, CDC25 proteins remove both inhibitory phosphates, thereby activating CDK1. CKS proteins are necessary for proper function of CDK1 in several species [39, 40]. In egg extracts of *Xenopus* (an African frog genus), a CKS2 homolog called XE-p9 is required for entry into and exit from mitosis and facilitate substrate recognition by CDK1-CCNB [38]. Also, immunodepletion of XE-p9, henceforth termed CKS2, prevents entry into mitosis with an accumulation of inactive phosphorylated CDK1. This suggests a role for CKS2 in regulating dephosphorylation of CDK1. Furthermore, CKS2 stimulates the ability of CDK1-CCNB to down-regulate CDC25, MYT1 and WEE1. Thus, CKS2 appears to affect the activation of CDK1-CCNB at the G2-M transition. The initial activation of CDK1-cyclin B, which involves dephosphorylation by CDC25, occurs at the centrosome [41, 42].

Since CDK1 appears to have a master role in the cell cycle regulation [25], it is not unlikely that CKS2-CDK1 complexes may also be involved in regulating other cell cycle phases. However, to date this remains poorly known.

2.2.2 CKS proteins affect activation of the APC/C and mitotic exit

CKS proteins have roles in regulating both the activation and function of the ubiquitin ligase APC/C [34, 43]. The APC/C regulates some of the cell cycle transitions, including metaphase-anaphase transition and the exit from the mitosis [26]. An APC/C activator, CDC20, binds to APC/C and activates its ubiquitin ligase activity. In addition, APC/C needs to be phosphorylated by CDK1-CCNB in order to become active [44-46]. During mitosis, the APC/C-CDC20 complex ubiquitylates PTTG (securin) and mitotic CCNs, leading to their destruction by the 26 S proteasome (figure 4) [26, 47, 48]. Degradation of PTTG and CCNB triggers cleaving of the cohesion complexes between the sister chromatids, separation of the sister-chromatids, inactivation of CDK1 and mitotic exit. However, if some chromatids are not attached to the mitotic spindle, a group of proteins, denoted spindle checkpoint proteins, inhibit the function of CDC20 and thus the activation of APC/C. In *Drosophila* embryos and HeLa cells, the disappearance of CCNB in the mitosis commences at the centrosomes [49, 50].

Experiments performed by Zon et al [34] indicate that CKS proteins activate APC/C by promoting CDK1-CCNB-dependent phosphorylation of APC/C. Furthermore, in metaphase after the spindle checkpoint has been released, CDK1-CCNB needs to bind to CKS proteins to ensure processing of CCNB1 by APC/C. CKS1 and CKS2 have overlapping roles in mitosis [2, 43]. Zon et al reported that depletion by either CKS1 or CKS2 alone had no effect on CCNB and PTTG destruction. This indicates that both CKS1 and CKS2 regulate this function.

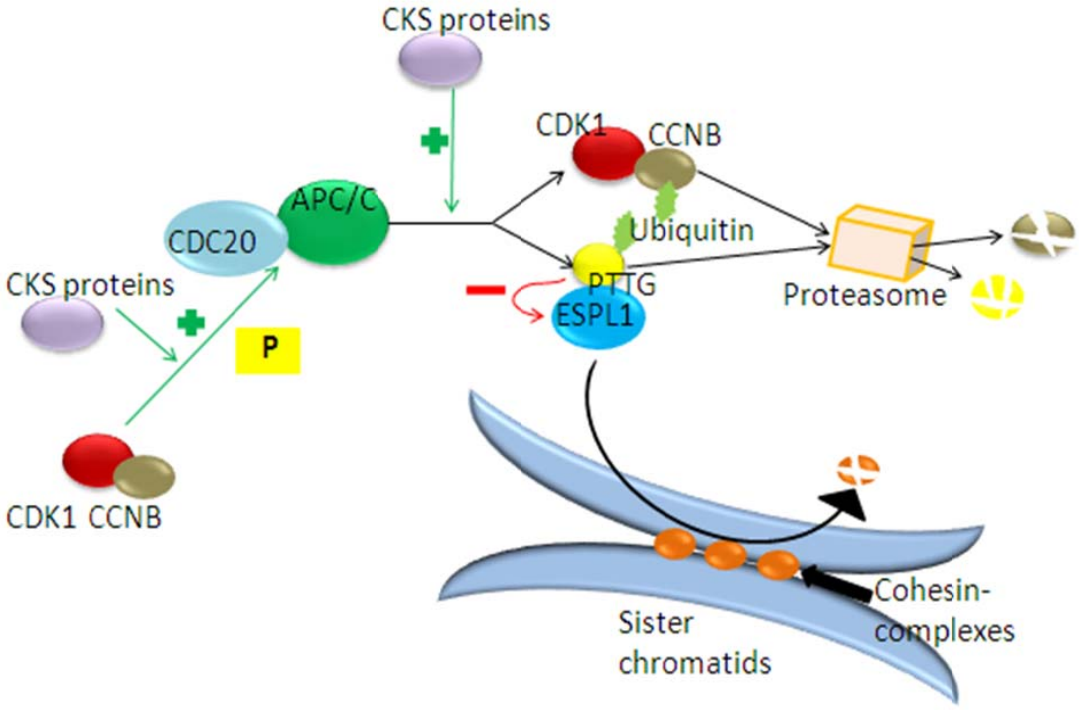

Figure 4. The APC/C-CDC20 complex is activated by CKS dependent phosphorylation performed by CDK1-CCNB. APC/C-CDC20 ubiquitylates CCNB and PTTG when all chromatids are attaches to the mitotic spindle and the spindle assembly checkpoint is released. Ubiquitination functions as a marker for degradation by the proteasome. The degradation of PTTG (which inhibit (red arrow) ESPL1 (separin)) and CCNB, activate ESPL1, which cleaves cohesin complexes and trigger sister-chromatid separation. CKS proteins promote APC/C dependent destruction of CCNB and PTTG [34].

2.2.3 CKS proteins affect the degradation of CCNA

In conflict with the view that the spindle checkpoint must be released before the APC/C-CDC20 is activated, is the observation that CCNA is targeted for destruction by the proteasome already in prometaphase [51]. Studies by Wolthuis et al [43] show that CCNA is capable of binding to CDC20 already in G2 phase and that CKS1 or CKS2 is required for the degradation of CCNA. CCNA binds CDC20 with sufficient affinity to oust the spindle checkpoint proteins. A CKS protein promotes the degradation of CCNA by binding CCNA-CDC20 to the APC/C (figure 5) [52].

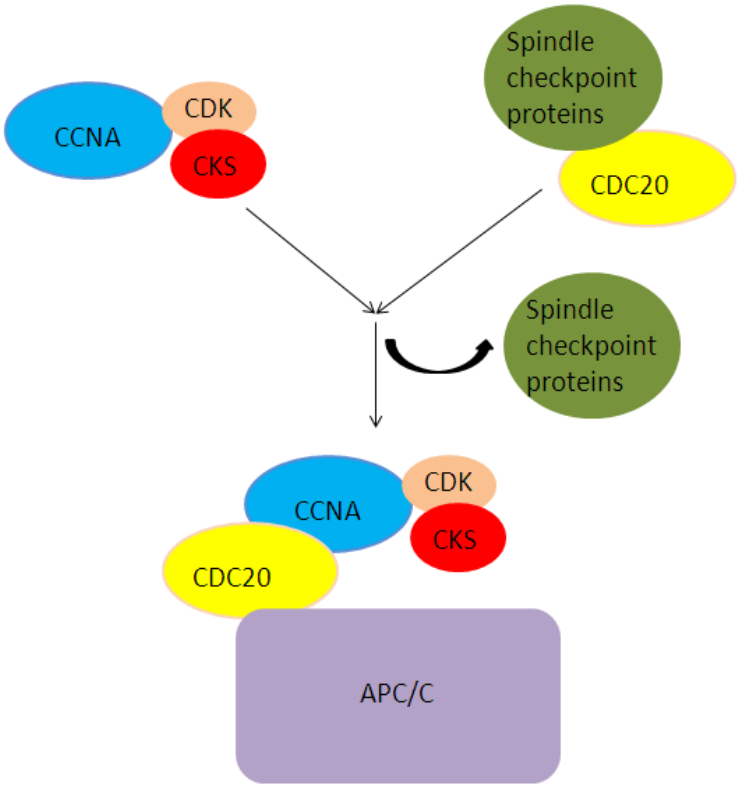

Figure 5. The CKS-CDK-CCNA complex binds CDC20 by out-competing the spindle checkpoint proteins. The CKS sub-unit recruits CCNA to the APC/C. Modified from [52].

2.2.4 CKS2 may be involved in the transcription of CDK1 and CCNB genes

CKS2 is chromatin-bound, as previously exhibited by chromatin immunoprecipitation experiments [2]. In both S-fase and in a G2 enriched population, CKS2 was associated with *CCNB* and *CDK1* genes. Furthermore, there was an increase in the association of CKS2 with *CCNB* and *CDK1* promotors and open reading frames in the G2-phase that correlated with an increase in RNA polymerase II. Thus, CKS2 proteins might be involved in transcription of *CDK1* and *CCNB* genes.

Depletion of both CKS proteins by small interfering RNAs (siRNAs), led to impaired proliferation with G2 phase arrest in mouse embryonic fibroblast (MEF) cells [2]. Over time, these G2 arrested cells were capable of undergoing an additional round of replication without division, *i.e*, tetraploidization. This phenotype has been attributed to impaired transcription of the genes encoding CCNB1, CCNA2 and CDK1 proteins.

2.2.5 CKS2 regulates a mitochondrial function

CKS2 interact with SSBP1, which have a role in mitochondrial biogenesis and replication [53]. This interaction is described at section 2.6.6 “CKS2 in mitochondria”.

2.3 Cancer

Cancer is a set of diseases in which cells divide and grow without control [19]. This may result from mutations in genes that normally regulate cell growth and division during the cell cycle. The cancer-causing genes are called oncogenes (from Greek *onco*, tumor). The normal genes, from which they transform, are called proto-oncogenes. Genetical alterations may result from random spontaneous mutations or environmental influences, such as chemical carcinogens, X-rays and certain viruses. Scientists have recognized a number of tumor viruses, which cause cancer in various species, including humans.

In addition to genes that normally promote cell division, cells contain genes encoding proteins that inhibit cell division [19]. Such genes are called tumor-suppressor genes, because their encoded proteins prevent uncontrolled cell growth. Any mutations in these genes that decrease the normal activity, may therefore lead to cancer. The tumor suppressor proteins have normally various functions, such as repairing damaged DNA. This prevents the cell from accumulating cancer-causing mutations. An example of this is the product of the gene *TP53,* TP53, which halts the cell cycle when DNA damage is spotted and turns on genes involved in DNA repair. When the damage is irreparable, TP53 promotes cell death by apoptosis. If mutations in *TP53* accumulate, cancer may ensue.

2.3.1 Cervix cancer

The incidence and mortality from cervical cancers in general are rising. However, there has been a decrease in incidence and mortality in Norway during the last decades [54]. In 2008, cervical cancer was ranked as the 9th most frequent cancer among Norwegian women [55]. The decreasing trend parallels the introduction of a screening program that aims at detecting precancerous changes in the cervix at an early stage. These precancerous lesions can be treated before they lead to cancer.

The risk of developing cervical cancer is elevated in women with multiple sex partners [56, 57]. Infection with human papillomavirus (HPV) is a major etiological factor in cervical

carcinogenesis. Whilst HPV infection is necessary, other co-factors are required, which may include long term use of oral contraceptive pills, smoking, high parity, diet, co-infection with human immunodeficiency virus, herpes simplex virus and *Chlamydia trachomatis* infection [58].

Human papillomavirus (HPV) is a double-stranded DNA virus [58]. Over 150 types of HPV have been identified, whereby 40 infect the squamous epithelium of the anogenital tract. Among these, 15 are characterized as high risk in association with cervical intraepithelial neoplasia and cervical cancer (HPV 16, 18, 31, 33, 35, 39, 45, 51, 52, 56, 58, 59, 68, 73 and 82) [59, 60]. Two of these high risk types, HPV 16 and 18, remain the most common HPV types in cervical lesions, and cause 60-80 % of all cervical cancers [58].

The HPVs, which are sexually transmitted, infect cells in the basal layer of the squamous epithelia [61]. Most HPV infections are cleared by cell-mediated immune mechanisms. However, in a minority of cases, the infection persists and the HPV DNA integrates into the host DNA. Open reading frames (ORFs) of the HPV are genomic transcription sites responsible for viral activity [60]. Two ORFs of HPV, *E6* and *E7*, are oncogenes involved in the transformation from normal cells to cancer cells.

E7 proteins are best known for the inhibition of the tumor suppressor protein retinoblastoma (RB1) [61]. RB1 is responsible for regulating many genes involved in cell cycle progression, differentiation, mitosis and apoptosis. In addition, E7 contributes to immortalization of keratinocytes by binding to key proteins, resulting in a high CDK2 activity, which promotes cell cycle progression.

One major consequence of targeting the cell cycle regulators by high risk E7 proteins is an increase in the level of the tumor suppressor TP53[61]. TP53 is involved in preventing cancer by increasing the cell's susceptibility to apoptosis. To restrain this, E6 proteins cause proteasomal degradation of TP53 and block transcription by interfering with its DNA-binding activity.

In all, E6 and E7 promote proliferation and evasion of apoptosis of suprabasal cells [61] (figure 6). The oncoproteins also degrade and inactivate TP53 and RB1, and cause genetic instability. This leads to the accumulation of DNA damage and mutations, which may result in transformation and development of carcinomas.

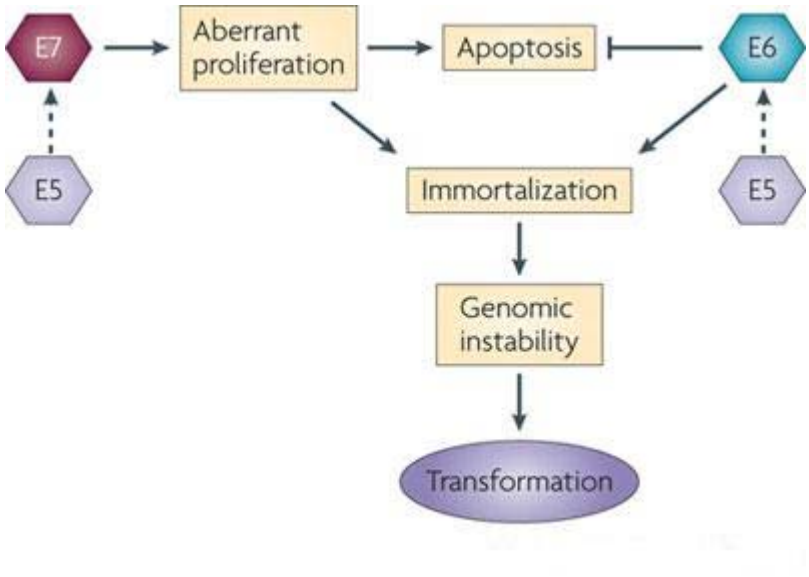

Figure 6. Molecular mechanisms by which HPV induces cervical carcinogenesis. Proliferation caused by E7 initiates apoptosis (programmed cell death), which is repressed by the oncoprotein E6. Together, E6 and E7 immortalize cells, cause genomic instability and thereby transform cells and develop carcinomas. The functions of E6 and E7 are augmented by the viral protein E5 [61].

2.4 Mitochondria and cancer

2.4.1 Introduction to mitochondria

Mitochondria are organelles that perform essential functions in cellular metabolism and regulation of cell death [62]. They are involved in regulating important processes such as ATP production, ion storage, apoptosis and anabolic and catabolic metabolism [63]. It is assumed that the mitochondria originate from aerobic heterotrophic prokaryotes, which became endosymbionts [19]. The term endosymbiont refers to a symbiotic cell that lives inside another, called the host cell. Thus, it is not surprising that mitochondria have double membranes and possess their own genome accompanied by a mitochondrial transcriptional and translational machinery to produce their own RNAs and proteins [62]. Mitochondrial genes have been integrated into the nucleus genome throughout evolution, and today about 99% of the roughly 1000 mitochondrial proteins are encoded by nuclear DNA and transported into mitochondria [62, 63].

The human mitochondrial genome is a circular double-stranded DNA molecule of 16.6 kb, which encodes 13 polypeptides of the electron transport chain (ETC) and 22 tRNA and 2 rRNA genes necessary for its own protein synthesis [64]. Each mitochondrion contains 2-10 copies of its genome [62]. The replication of the mitochondrial DNA is not coordinated with the S-phase of the cell cycle. However, the overall number of mitochondria remains constant during proliferation. This suggests that the generation of mitochondria is affected by extra-mitochondrial signals. This hypothesis is supported by the fact that new mitochondria are continuously formed even when the mitochondrial DNA is deleted.

2.4.2 Metabolism and the generation of reactive oxygen species

The best characterized function of the mitochondrion is the production of energy, in the form of adenosine triphosphate (ATP) [62]. This process, called oxidative phosphorylation, is completed by a series of protein complexes (numbered I to IV [19]) termed the respiratory chain. Electrons, originally derived from the breakdown of fuel (proteins, carbohydrates and lipids), are transported through the respiratory chain, also called ETC [19]. Some electrons may leak from the electron transport complexes and react with molecular oxygen to form superoxide radicals, $O_2^{\bullet -}$ [62]. These radicals are then converted to other reactive oxygen species (ROS). In fact, the mitochondrial ETC is considered a major source of ROS [64].

2.4.3 Mutation and DNA repair

Human mitochondrial DNA, which lacks protective histones, is continuously exposed to ROS produced by the mitochondria, and has a 10 fold higher rate for accumulation of mutations than nuclear DNA [64]. Mitochondrial DNA lacks sizeable introns, so most mutations occur in the coding regions. Some mutations lead to changes in the multiprotein complexes of the ETC, reduce their affinity for electrons and result in an increased ROS production [62].

Elevated level of ROS is associated with a cascade of redox signaling, which leads to DNA damage [64]. Redox signaling has been defined as "entire chains involving cascades of redox reactions, eventually leading to changes in gene expression" [65]. The mutations caused by the persistent oxidative stress may lead to cancer promotion and metastasis [64].

Cells have a number of ways to defend themselves from ROS induced damage [64]. They possess ROS scavengers and anti-oxidant enzymes, such as superoxide dismutases (SOD), catalases, and glutathione peroxidases. SOD reacts with H+ and converts $O_2^{\bullet -}$ to H_2O_2 and O_2 [66]. H_2O_2 is not a radical, but can diffuse across membranes and form hydroxyl radicals ($OH^{\bullet -}$) [64]. Glutathione peroxidase and catalase are enzymes that counteract this by reducing H_2O_2 to H_2O.

Mitochondria also contain their own DNA repair systems, for instance base excision repair (BER), mismatch repair (MMR) and mitochondrial DNA (mtDNA) degradation in response to damage [67]. A DNA polymerase, called polymerase-γ (POLG), is assumed to function in mitochondrial BER, which is the best characterized repair process [68]. The BER proteins repair the damaged DNA and restore genome integrity [69]. The inappropriate base is excised by a DNA glycosylase (figure 7). This results in an apurinic/apyrimidinic (AP) site cleaved by an AP endonuclease, creating a strand break with a 3´-hydroxyl end and a 5´-deoxyribose phosphate (dRP) sugar moiety. POLG fills the nucleotide gap and eliminates the 5´dRP fragment. The DNA nick is then sealed by DNA ligase. Several DNA glycosylases have been identified in mitochondria including UNG1 (active on uracil), OGG1 (guanine oxidation) and NEIL1 (pyrimidine oxidation).

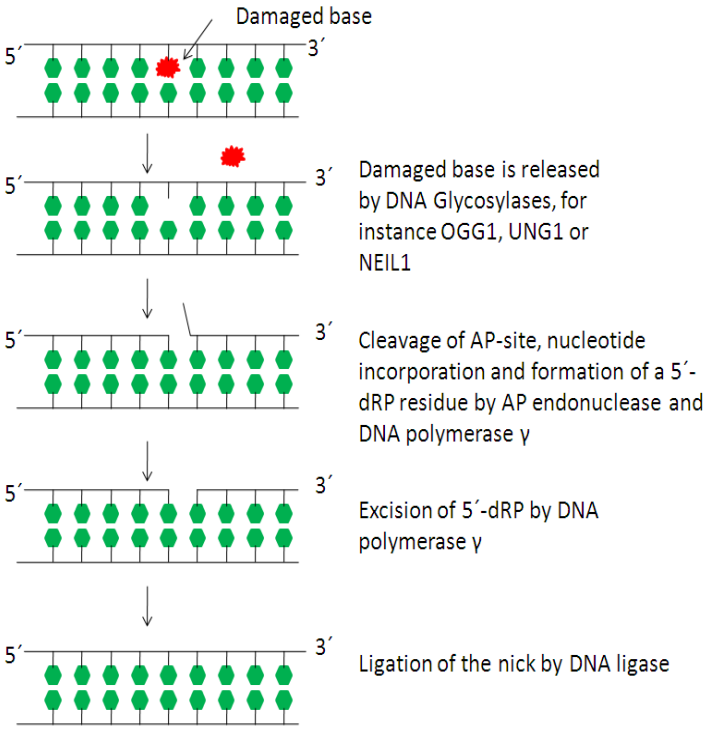

Figure 7. A representation of the base excision repair pathway in the mitochondria. Modified from [69].

2.4.4 ROS-induced oncogenic transformation

Mitochondrial dysfunction is presumed to be involved in age-related diseases like neurodegerative diseases, type 2 diabetes and cancer [63, 70, 71]. Here, the focus will be on mitochondrial defects in cancer. As explained above, the mitochondrial ETC produces ROS as a byproduct [63, 64]. Mitochondria are one of the major sources of ROS and research has revealed that ROS have important roles in regulating events such as proliferation, differentiation and migration [72]. In addition, redox signaling is accepted to be involved in regulating normal processes and disease progression, including angiogenesis, oxidative stress, aging, and cancer.

Often, cancer cells possess higher levels of ROS than normal cells ([72] and references therein). If a small amount of cells overcome cellular senescence, factors like hypoxia and/or lack of glucoses can trigger transformation to malignancy. Prolonged hypoxia and glucose deprivation are drivers of elevated mitochondrial ROS production, and prolonged hypoxia activates signaling pathways that leads to stabilization and activation of the hypoxia inducible factor HIF-2alpha. This enables cells to survive with sustained levels of elevated ROS.

However, HIF-2alfpha represses DNA mismatch repair processes and the cells accumulate ROS-induced oxidative damage and mutations, which lead to malignant transformations. Experiments have shown that inhibition of HIF-2alpha expression by short hairpin RNA (shRNA) prevents in vivo growth and tumorigenesis in different cancers, regardless of mutational status and tissue of origin [73]. Furthermore, HIF-2alpha expression seems to promote hypoxic cell proliferation by enhancing transcriptional activity of the protooncogene MYC, which in turn promotes altered glucose metabolism, suppression of apoptosis, cell growth and survival [72].

2.4.5 Mitochondrial single-stranded DNA binding protein (SSBP1)

Single-stranded DNA binding proteins (SSBs) attach to single-stranded DNA with high affinity [74]. They are involved in replication, recombination and repair of DNA. In humans, there are two different groups of SSBs, nuclear (RPA, hSSB1, hSSB2) and mitochondrial (SSBP1) [75].

SSBP1 is involved in mitochondrial DNA replication

SSBP1 is an extremely well preserved protein related to prokaryotic SSBs [75]. It exists in the mitochondria of all eukaryotes, from yeast to humans. SSBP1, POLG and PEO1, a DNA helicase at the mitochondrial replication fork, form the replication machinery (figure 8) [74]. Human SSBP1 stimulates the DNA unwinding rate of PEO1 [76]. In addition, an 8 fold stimulation of POLG has been noted with human SSBP1 [77]. These interactions with replication proteins suggest that SSBP1 has a role in the replication of mtDNA. In HeLa and *Drosophila* cells, RNA interference (RNAi) of SSBP1 caused loss of mtDNA [78, 79]. This may indicate that SSBP1 is essential for the maintenance of mtDNA.

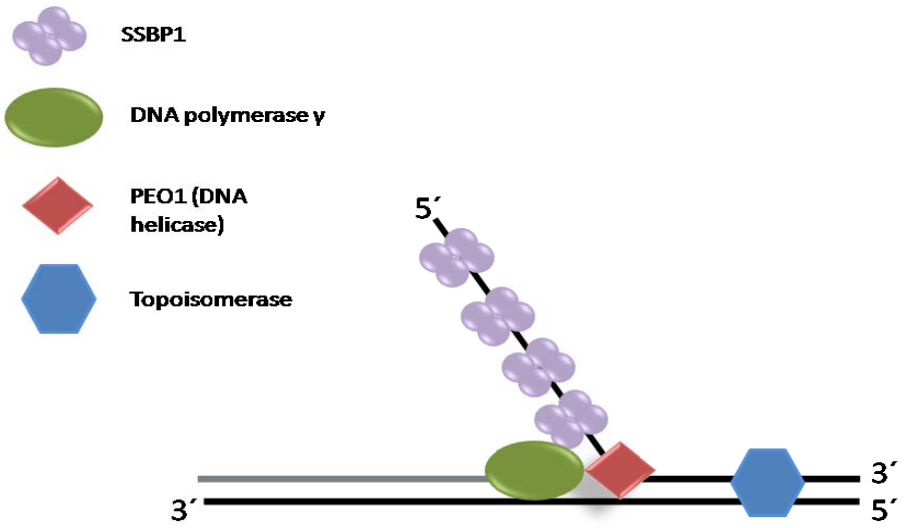

Figure 8. A sketch of the mitochondrial replisome illustrating the role of SSBP1 in replication. The new DNA strand (gray) is synthesized by DNA polymerase γ (green). The mitochondrial DNA helicase (blue) unwinds DNA and SSBP1 (purple) binds to the single-stranded DNA. Topoisomerase relieves superhelical tension. Modified from [80].

A part of the mitochondrial DNA holds three DNA strands [79]. This triple-stranded structure is called a displacement loop (D-loop) [81]. The D-loop is assumed to be involved in regulating mtDNA replication. A small segment of the heavy strand in mtDNA is replicated twice [82]. This short strand, which is located in the D-loop, is known as 7S DNA. SSBP1 is presumed to stabilize the D-loop and the long stretches of single-stranded DNA created during replication [83, 84]. In experiments, reduction of SSBP1 protein was linked to a rapid decrease of 7S DNA in HeLa cells [79]. Inhibition of mitochondrial DNA synthesis by 2′,3′-dideoxycytidine treatment, which inhibits POLG [85], did not result in such reduction of 7S DNA [79]. From these experiments, it is therefore hypothesized that SSBP1 is required for the synthesis of 7S DNA.

SSBP1 affects repair of damaged mitochondrial DNA

SSBP1 serves vital roles in repair of mtDNA [74]. It is involved in several DNA repair mechanisms, for instance in BER and in potentiation of the exonuclease activity of TP53 in mitochondria [83, 86, 87].

Daily, hydrolytic deamination of cytosine produce 70-200 uracil bases in the DNA [88]. DNA polymerase does not distinguish U from T in the template. This produces G:C to A:T transition mutations. Uracils in U:G mismatches are 100 % mutagenic if not repaired. Single-stranded DNA (ssDNA) has 140-300 fold higher rate of deamination than double-stranded DNA (dsDNA). Mammalian cells possess uracil-DNA glycocylases, which counteract this and initiate BER (figure 7). The only known uracil-glycocylase in mitochondria is UNG1.

Given that the nuclear SSB protein, RPA, interacts with several DNA repair proteins, it has been speculated whether SSBP1 interacts similarly in the mitochondria [83]. Experiments have been performed to check if SSBP1 affects the repair of deaminated, oxidized and methylated DNA bases in ssDNA. Steen et al [83] observed that the uracil-glycolase UNG1 had a preference for ssDNA over dsDNA, but that there was a complete excision of uracil only in the dsDNA substrates. The majority of uracils in ssDNA remained unprocessed. Additional experiments demonstrated that uracil excision was reduced when SSBP1 was added to the samples, and that UNG1 directly binds the SSBP1-DNA complex. Futhermore, *in vitro* SSBP1 also inhibited the repair of 3-methylcytosine in ssDNA by the metyl-removing enzyme ABH1. However, NEIL1 glycosylase, which excise oxidatively damaged DNA bases, was only partially inhibited by SSBP1.

Since SSBP1 inhibits uracil excision by UNG1, it may seem paradoxical that SSBP1 recruits UNG1 to single stranded mitochondrial DNA[83]. However, this may indicate that SSBP1 facilitates accumulation of UNG1 at mtDNA, but inhibits excision of uracil until dsDNA is restored after replication is finished. A possible explanation is that this delayed processing avoids formation of double strand breaks as mitochondria have limited homologous recombination that produce error-free processing of nicks at the replication fork.

The DNA excision repair proteins ERCC8 and ERCC6 interact with the BER protein OGG1 and SSBP1, which are in a complex with mitochondrial DNA, as has been shown in co-immunoprecipitation experiments on oxidatively stressed mitochondria [87]. The interaction did not occur in non stressed mitochondria. It is known that mitochondrial OGG1 has a role in repair of oxidative DNA damage [89]. From the co-immunoprecipitation results, it is therefore proposed that the ERCC6, ERCC8, OGG1 and SSBP1 complex is involved in protection from oxidatively induced mtDNA mutations [87].

The tumor suppressor TP53 translocates into mitochondria and interacts with POLG in response to mtDNA damage caused by endogenous and exogenous insults, such as ROS [74].

Loss of TP53 increases vulnerability of mtDNA to exogenous damage, leading to increased frequency of mtDNA mutations in vivo [86]. Wong et al [74] identified TP53 as a novel interaction partner of human SSBP1 *in vitro*. SSBP1 bound to its transactivated domain, enhanced the 3'-5' exonuclease activity of TP53, particularly in hydrolyzing 8-oxo-7,8-dihydro-2'-deoxyguanosine (8-oxodG), a well-known marker of oxidative stress. Therefore, SSBP1 appears to be involved in a mitochondrial repair process performed by TP53. Whether SSBP1 affects other repair functions caused by TP53 in mitochondria remains poorly elucidated.

2.4.6 CKS proteins in mitochondria

Radulovic et al [6] discovered SSBP1 as a new interaction partner of CKS proteins in mitochondria. By using pulldown assay, an in vitro method used to determine physical interactions between proteins, they found that SSBP1 only binds to CKS2 which are in complex with CDK.

Futhermore, Radulovic et al [6] reported that knockdown of both CKS1 and CKS2 by shRNA did not reduce protein levels or expression of SSBP1 mRNA. However, CKS knockdown cells exhibited reduced amount of mtDNA. In addition, CKS knockdown cells showed abnormal mitochondrial morphology with increased fragmentation. Hence, CKS proteins seem to be involved in protection of mitochondrial genome integrity. They also demonstrated that SSBP1 is a substrate for CDK, and that CKS knockdown cells do not phosphorylate SSBP1. Furthermore, application of roscovitine, which is a CDK1, CDK2 and CDK5 inhibitor, abolished SSBP1 phosphorylation and inhibited mtDNA replication. Thus, the experiments indicated that SSBP1 undergoes CKS-CDK dependent phosphorylation, and that inhibition of SSBP1 phosphorylation leads to defective replication of mtDNA.

3 Methodological background

3.1 Fluorescence

Fluorescence is a short-lived type of light created by electromagnetic excitation [90]. A fluorescent substance absorbs light energy at a shorter wavelength (higher energy) than it emits. This phenomen was first observed in 1852 by Sir George G. Stokes with the mineral fluorspar, thereof the term fluorescence.

The fluorophore (a molecule that can generate fluorescence) absorbs energy in the form of photons from the external source, creating an excited singlet electronical state [91]. A portion of this excited energy is emitted as fluorescence, and the fluorophore returns to its ground state. The difference in energy or wavelength of absorption and emission is termed the Stokes shift.

Absorption of light (photons) by a molecule and emission of energy in the form of fluorescence, occur only at characteristic wavelength for a given molecule, *i.e.* each fluorescent molecule have its own excitation and emission spectrum (figure 9) [92].

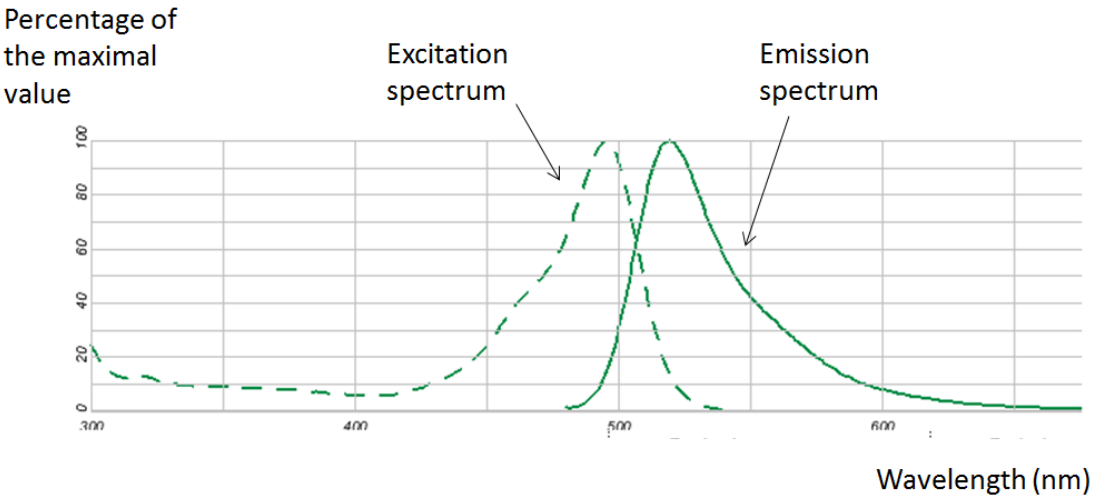

Figure 9. An illustration of an excitation and emission spectrum. Modified from [93].

3.2 Antibodies and immunofluorescence

Antibodies are glycoproteins, naturally produced by human and animal effector B lymphocytes in response to infection [94]. Their function is to bind pathogenic components and microorganisms, thereby, rendering them innoxious. They bind to specific structures, called epitopes, in an antigen. Structurally, they look like the letter Y. The fragments binding to the antigen (the "arms") are called Fab (Fragment antigen binding). The stem is called Fc (Fragment crystallizable), referring to the first experiments where it was observed to crystallize.

In general, each antibody consists of two identical heavy and light polypeptid chains [94]. The tips of the Y's arms show extensive variation, and are therefore called the variable regions. Antibodies are divided into five isotypes: IgA, IgD, IgE, IgG and IgM. They are distinguished by the type of stem in the molecule. All antibodies of the same class have an identical stem, and this part is therefore called the constant region.

Antibodies bind strongly and with specificity to its antigen and they are therefore useful for detecting and quantifying proteins [94]. They can be made commercially, and are used widely in biological research and as medical drugs. Traditionally, antibodies are produced by immunizing animals with a particular antigen and one can prepare antisera from their blood. A more modern approach is to fuse the desired B lymphocyte from an immunized animal with a tumor cell to form hybridoma cells. They are immortal and can divide and produce antibodies indefinitely. This type of antibodies descends from the same clone of B lymphocytes, and is therefore called monoclonal antibodies.

Antibodies that bind to a specific target molecule are called primary antibodies [95]. The primary antibody can be labeled with a fluorescent tag, which produces a visible signal that allows direct detection of the target antigen. Alternatively, the primary antibody can be connected to a secondary antibody, which is labeled with a fluorescent tag or an enzyme producing visible light. The method of labeling proteins by fluorescently tagged antibodies is called immunofluorescence [16]. Using secondary antibodies provides several advantages over direct detection with labeled primary antibodies [95]. First, primary antibodies are expensive, and by exposing primary antibodies to labeling procedures, researchers may risk poor recovery or inactivation of the antibodies. Second, primary antibodies may have several epitopes to which secondary antibodies can bind, and therefore produce signal amplification.

Primary antibodies are produced in a few different host animal species, for instance in mice, rabbits, rats and goats [96]. They are often of the isotype IgG. Secondary antibodies have specificity for the antibody species and isotype of the primary antibody. They are produced by injecting harvested primary antibodies, into a different animal species. For instance, anti-mouse antibodies are raised by injecting mouse antibodies into an animal other than mouse. When a goat is immunized with mouse antibodies, goat anti-mouse antibodies are generated.

3.3 Fluorescence microscopy

Fluorescence microscopy is one of the techniques used in this thesis. It allows the examiner to focus on the target of interest with a high degree of selectivity [97]. Researchers have developed many thousand fluorescent probes for labeling different cellular, sub-cellular or molecular components. A brief synopsis of the properties of the fluorescence microscope is outlined below.

The light source

Correct illumination of the specimen is very important for obtaining high quality images [98]. In fluorescence microscopy, various light sources can be used, including mercury- and xenon arc lamps [99]. However, metal halide illumination sources are rapidly emerging as a serious challenger of mercury- and xenon arc lamps. The fluorescence microscope (Zeiss AxioImager Z1) used in the present experiments was equipped with a metal halide lamp (HXP-120).

The metal halide lamp emits light in the ultraviolet, violet, blue, green, and yellow regions (figure 10) with spectral lines at 365, 405, 436, 546, and 579 nm [99]. The spectral lines arise from elemental excited state transitions in mercury vapor.

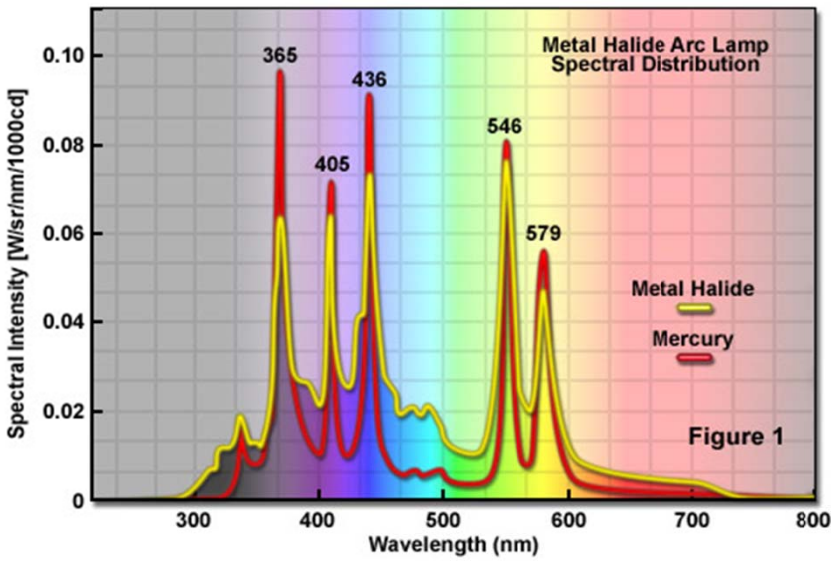

Figure 10. The spectral distribution of the metal halide arc lamp. The lamp emits white light with prominent emission lines [99].

The beam path and filters of the fluorescence microscope

Fluorescence microscopy permits the delivery of excitation energy to the specimen and separate weaker emitted fluorescence for observation from brighter excitation light [92]. The light beam from the metal halide lamp travels through 3 filters before the fluorescence is observed through the binoculars or imaged by the camera (figure 11) [100]. The exciter filter in the Zeiss Axio Imager.z1 is either a band pass (BP) filter or a broad pass filter (table 1). The former transmit light within a certain wavelength interval, the latter transmit light at an unspecific distance from the main excitation wavelength (bell-shaped transmission curve) [101]. A dichroic beam splitter (FT) reflects short-wave excitation light into the specimen. The emission produced by the excitation of the fluorophore is transmitted through the dichroic beam splitter, which only transmits light of longer wavelengths than the excitation light. Any remaining excitation is filtered out by an emission filter, which is either a BP or a long-pass (LP) filter. The latter is transmits light above the specified wavelength [101].

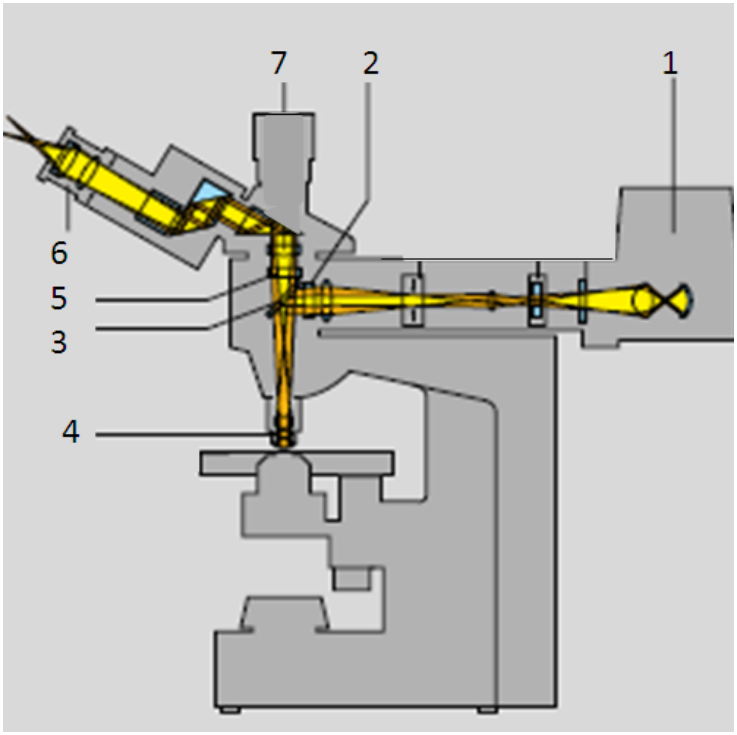

Figure 11. The beam path in the fluorescence microscope. The light flows from the light source (metal halide lamp) (1) via an exciter filter (2) to a beam splitter (3). The objective (4) gathers the light and passes it to the specimen. From the specimen, the light transmits through the dichroic beam splitter (3) to an emission filter (5). The fluorescent light can be observed either through the binoculars (6) or a camera (7) [100].

Table 1 The different filters in the Zeiss AxioImager.Z1 microscope.

Filters[a]		
Exciter filter[b]	Beam splitter[b]	Emission filter[b]
365	FT 395 [c]	BP 445/50
BP 395-440[c]	FT 460	LP 470[c]
BP 470/40	FT 495	BP 525/50
BP 550/25	FT 570	BP 605/70
BP 640/30	FT 660	BP 690/50

[a] The fluorescence microscope have 3 filters (exciter filter, beam splitter and emission filter), which ensure separation of the fluorescence for observation from the excitation light.

[b] The wavelengths or wavelength intervals that the filters transmit (nm)

[c] BP: band pass filter, FT: dichroic beam splitter mirror, LP: Long-pass filter

The ApoTome

Image quality in fluorescence microscopy is compromised when signals originating from the focal plane are overlaid with image information arising from remote areas [102]. An ApoTome is a slider module for fluorescence microscopy. By using this module an image of improved quality can be generated from the various focal planes of the specimen as an image stack.

The ApoTome (figure 12) consists of a grid, which is inserted into the illumination pathway of the fluorescence microscope and projected onto the specimen [102]. The grid is relocated over the specimen by a glass plate, which is tilted back and forth in the light path. A minimum of three images of the specimen is acquired with the grid located at different positions. The grid is visible in the focal plane, and no fluorescence is generated in regions where no light reaches the specimens. The images are then processed by the microscope software, which determines grid contrast as a function of location and removes the out-of focus image information before superimposing the three images into a final optical section. An optical section is an image of the specimen that only extracts information from the region that corresponds to the objective depth of field.

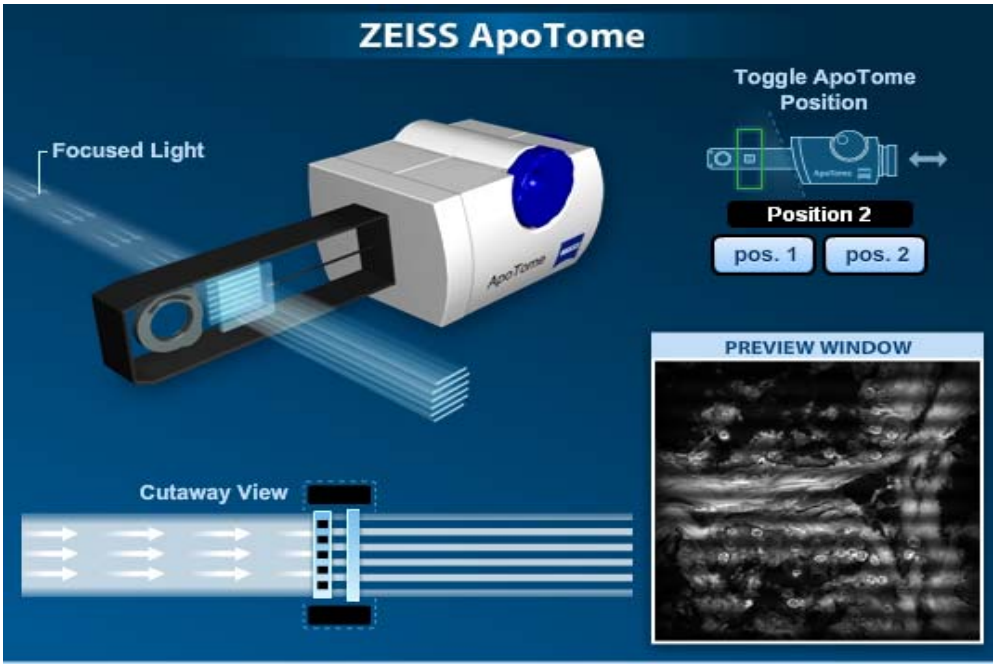

Figure 12. The ApoTome consists of two plates, which are positioned in the light path. The grid pattern is imprinted on the excitation light. A glass plate, located parallel to the gridded plate, is tilted back and forth. This motion moves the "grid" excitation light back and forth in the specimen [102].

3.4 *In situ* proximity ligation assay

PLA is a method to monitor interactions of endogenous proteins in cells and tissues with high specificity [103]. The principles outlined below describes *in situ* PLA applied for detection of interaction between two proteins using Olink® Bioscience's Duolink II reagents. Typical samples are tissue sections, cytospin preparations or adherent cells fixated on a glass slide [17]. The samples are incubated with primary antibodies, produced in different animals species, directed against the two target proteins (figure 13A). The secondary antibodies with specificity for the species of the primary antibodies are connected to oligonucleotides, which are designated proximity probes (figure 13B) [103]. If the two target proteins are in proximity (maximum 30-40 nm apart), they will create a signal [104]. The oligonucleotides on the proximity probes, serve as templates for circularization of so-called connector oligonucleotides by enzymatic ligation (figure 13C) [103]. Then, DNA polymerase and nucleotides are added to the sample. One of the oligonucleotides serves as a primer for DNA polymerase, which uses the ligated circle as a template for rolling circle amplification (RCA) [17]. The other oligonucleotide has three mismatched RNA nucleotides at the 3' end that prevents it from serving as a primer [103]. This produces a single-stranded product, composed of up to 1000 repeated sequences, complementary to the DNA circle. Fluorescently labeled oligonucleotides, added to the sample, bind to the single-stranded product and produce a fluorescent spot which can be visualized by fluorescence microscopy (figure 13D) [17]. For proteins located at a larger distance, the connector oligonucleotides will not hybridize and no signal will appear.

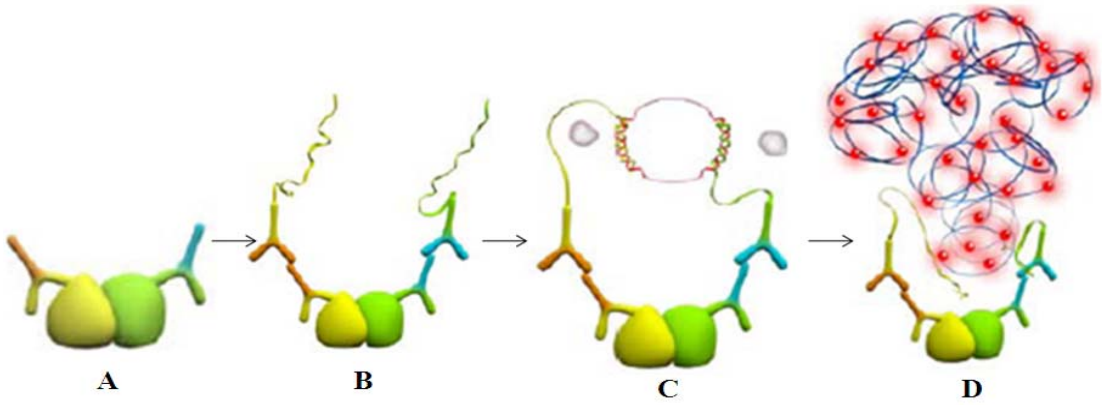

Figure 13. The principle of the assay. A. The primary antibodies bind to their protein targets. B. Secondary antibodies, conjugated with oligonucleotides (PLA probes), bind to the primary antibodies. C. Ligase and oligonucleotides hybridize the two PLA probes and join a closed circle. D. Polymerase uses the circle as a template for rolling circle amplification (RCA). Fluorescently labeled oligonucleotides hybridize with the RCA product. Modified from [17].

3.5 Fixation of cells

High quality cell preparation for microscopic examination presupposes proper cell fixation [105]. This renders it possible to examine the preparation at a later point of time. It "freezes" the cells, so they appear the same in the microscope as when they were alive. The fixative used must allow access of the antibodies to the cells and not alter the antigen in a way that inhibits subsequent binding of antibodies [18].

There are three main methods used to preserve the cells and retain their structural organization[106]:

- Fixation by cross-linking
- Fixation by precipitation
- Fixation by freezing (cryofixation)

Cryofixation is probably the best method for cellular preservation and often employed for electron microscopy [106]. It involves rapid freezing of tissues or cells followed by cross linking reagents. However, the technique requires equipment which is absent in many laboratories. As cryofixation was not an option in this thesis, it will not be discussed any further.

3.5.1 Fixation by cross-linking

Cross-linking reagents involve chemicals with aldehyde groups, such as formaldehyde and glutaraldehyde [107]. The reagents bind to proteins and lipids and form intermolecular bridges between reactive groups. They generally work by binding aldehydes to free amino groups and thereby creating a network which links cellular components together and keeps them in place [108]. The cross-linkers preserve cell morphology better than organic solvents [109]. They also prevent molecules from being washed out of the cell. A disadvantage, however, is that the resulting cross-linking may inhibit antibodies from entering into the cells [107] and therefore requires a permeabilization step to allow antibodies to access intracellular structures [109]. For permeabilization, detergents or organic solvents are used [110]. Detergents comprise dilute solutions (0.05-0.5%) of for instance Trition X-100 or Igepal ca-630, which solubilize the phospholipids of cellular membranes. However, these are harsh

detergents [111], and milder detergents such as saponin or digitonin may be required for specific applications [110]. Organic solvents, such as methanol or acetone can also be used. Aldehyde fixation should be performed at room temperature or warmer [108]. Cold temperatures can disrupt cytoskeletal elements and result in altered cellular size, shape and interrelationships of subcellular organelles.

Formaldehyde, CH2O, binds to amino acids, peptides, proteins and some lipids and crosslink amine-, sulfhydryl-, and hydroxylgroups [107]. There are two different sources of formaldehyde, formalin and paraformaldehyde. Formalin is produced by oxidation of methanol, and contains 37 % formaldehyde along with impurities such as methanol, formic acid and other aldehydes and ketones. Working fixatives are produced by dilution to a 10 % formalin solution, which contains 3.7 % formaldehyde. Paraformaldehyde is a powder, which consists of polymers of formaldehyde. When mixed with NaOH and heated, paraformaldehyde depolymerizes to monomer formaldehyde (figure 14). Hence, a paraformaldehyde solution is pure formaldehyde.

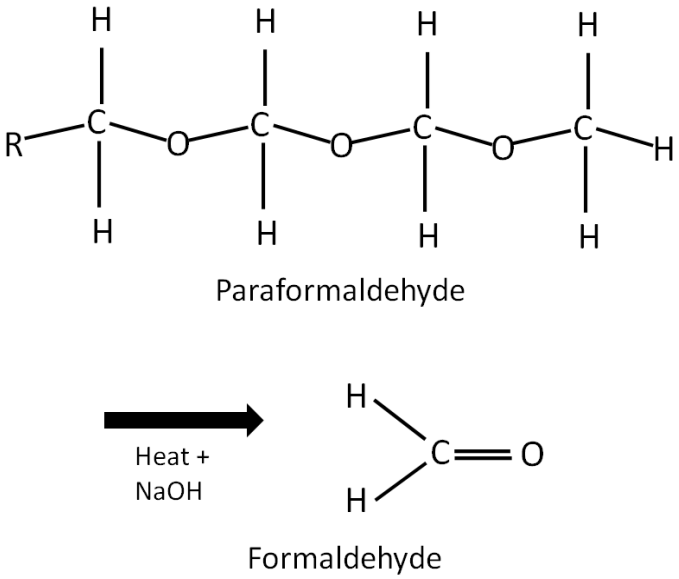

Figure 14. The chemical reaction for production of formaldehyde from paraformaldehyde [107].

3.5.2 Fixation by precipitation

Fixation by precipitation includes use of organic solvents like cold alcohols and cold acetone [107, 109]. The fixatives dehydrate and precipitate the proteins within the cells [108, 109]. The solvents destroy the structure of the cellular molecules. If extensive three dimensional

structures or networks of structures are to be explored, these fixatives may shrink the samples and thus alter the localization of some antigens [110]. Proteins are denatured because the fixatives break hydrophobic bonds, and lipids in membranes are dissolved into micelles [107]. This permeabilizes the membrane, and enhances the access of antibodies to intracellular antigens [108]. A disadvantage of this method is that molecules are washed out of the cell during fixation and processing and may cause false negative results[107].

4 Materials and methods

4.1 Cell specifications and maintenance

4.1.1 Cell line

HeLa cells were used in the experiments. These cells were the first cultured human cell line grown in vitro (in a "test tube") [112]. The cells originate from a lady, named Henrietta Lacks. They were isolated from an aggressive, cervical glandular-adenocarcinoma on the 8th of February 1951 at The Johns Hopkins Hospital in Baltimore, Maryland. Later, her cells have been distributed worldwide and are widely used in cancer cell studies. They have also been used in biochemical research to study biochemical pathways in human cells.

HeLa cells are adherent, which means that they stick to surfaces. They have a doubling time of about 24 hours [113]. The cell line contains human HPV-18 sequences [114], and they exhibit a low expression of TP53, normal levels of RB1 and overexpress the MYC gene [115].

4.1.2 Cell cultivation and counting

The HeLa cells were cultivated in a T75 tissue culture flask with 5 % CO_2 at 37 °C, similar to the temperature the body. The cells were grown in DMEM + Glutamax™ (Life Technologies) added 10% fetal bovine serum (FBS, Life Technologies), 1% L-glutamine (PAA) and 1% Penicillin-Streptomycin solution (100 U/mL penicillin and 100 µg/mL streptomycin, PAA). The cell culture was split and passed on to new T75 culture flasks twice a week.

Before splitting and experiments, the cells were microscopically examined to ensure that they were healthy and growing as expected. Attached cells should be slightly elongated in shape at low density and more pavement stone-like when approaching confluence.

The cells were split at approximately 80 % confluence (see Appendix 1). An aseptic technique was used to reduce the likelihood of contamination by microorganisms and the procedure was carried out in a clean LAF bench with sterile equipment and solutions. Old growth medium was removed, and the cells were washed with 5-8 mL sterile Dulbecco's PBS (PAA) prior to trypsinization to remove any residual from the growth medium. This is necessary because

FBS in the growth medium contains trypsin inhibitor [116]. Trypsin (Sigma-Aldrich) was added to the culture cell flask, distributed over the entire cell surface and the culture flask was placed in a 37 °C CO_2 incubator until the cells detached from the surface. Trypsin may damage the cells, so it was important to examine the cells every few minutes. If necessary, the loose cells were dislodged by gently knocking on the cell bottle with the palm of the hand without causing cell aggregation. Trypin was inactivated by adding fresh culture medium to the flask at the required split ratio and the content was gently mixed. One ml cell suspension or about 1 million cells were transferred into a new flask and filled with fresh culture medium.

Cells were counted with a coulter counter (Beckman Coulter, Z2 Coulter Counter) before they were plated out for experiments (see Appendix 2). In the coulter counter cells were moved, one at a time, through an electrical current. The coulter counter identifies and counts the individual cells through measuring the electrical conductivity, which differs between the cell and the suspending fluid [117]. Before the cells were counted the cell suspension was diluted 1:100 in isoton water. The coulter counter was flushed with the same liquid, and the counter adjusted so that only live cells were counted.

4.2 Microscopy

4.2.1 Seeding cells for microscopic examination

Cells were seeded on coverslips for the immunocytochemistry experiments and on glass slides for the PLA experiments in a petri dish. The coverslips and glass slides were sterilized by autoclavation prior to the experiments. The number of cells seeded depended on the size of the petri dish (table 2).

The amount of cell suspension needed for each petri dish was calculated from the formula:

Total number of cells in the petri dish / (the counted number of cells / mL cell suspension) = X mL cell suspension per petri dish. The dish was then filled with growth medium (37 °C) to the desired volume (table 2).

The cells were grown overnight at 37°C in a CO_2 incubator.

Table 2. Account of the sample preparation.

Seeding cells on coverslips			
Petri dish size[a]	Number of coverslips/dish	Number of cells	Amount of growth medium
35 mm 60 mm	3-4 6-7	120 000 250 000	2.5 mL 5 mL
Seeding cells on slides			
Petri dish size[a]	Number of slides/dish	Number of cells	Amount of growth medium
100 mm 150 mm	1 5	1 000 000 3 000 000	10 mL 30 mL

[a] The diameter of the petri dishes

4.2.2 Experimental design

A flow chart of the experiments is shown in figure 15. Cells were fixated with either formalin or methanol and stained with various antibodies (against CKS2, CDK1, CDK2 and SSBP1 proteins), and analyzed by fluorescence microscopy. The distribution of the proteins, in the nucleus and the cytoplasm, was also examined. Then, co-localization of proteins was examined by double staining of cells with antibodies (CKS2 with CDK1/CDK2/γ-tubulin or SSBP1, and CDK1 with SSBP1). Localization studies were performed at least 3 times for each fixative, and the co-localization experiments were conducted at least 2 times for each combination of antibodies. A qualitative evaluation of how the fixatives affected the staining was performed. Possible interactions between proteins were further analyzed with PLA. In order to establish PLA, cells were suspended in 4 different fixation and permeabilization solutions before they were stained with CKS2 and CDK1 antibodies. The results were quantified and compared by statistical analysis of the data. Then, based on these results and the staining patterns examined by immunocytochemistry, the most suitable fixation methods were selected. The selected fixation methods were used for subsequent PLA studies, which examined interactions between CKS2 and CDK1, CDK2 or SSBP1, and between CDK1 and SSBP1. The PLA experiments were performed at least 4 times for each combination of antibodies.

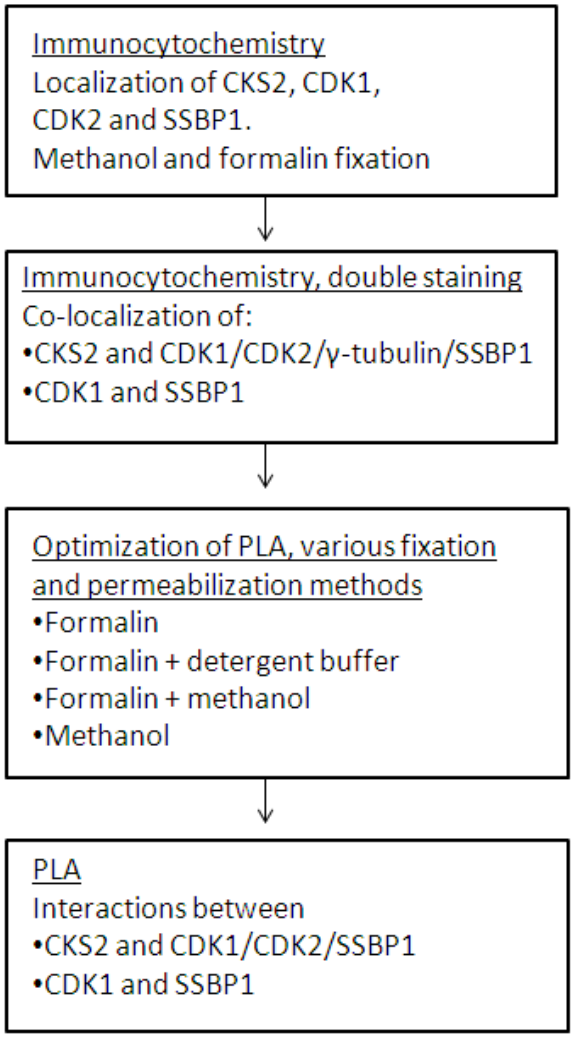

Figure 15. Flow chart of the experimental design.

4.2.3 Immunocytochemistry

The coverslips used for cell seeding were round, 12 mm in diameter and 0.17 mm thick (Assistant, no 1.5). Choosing the correct coverslip thickness is crucial to good image resolution. In these experiments, cells were fixated in two different ways in order to evaluate how this affected the staining of the antigen depending on the nature of the antigen examined:

- Methanol fixation for 10 minutes at -20 °C
- Formalin fixation for 10 minutes at room temperature

The protocol for the immunocytochemistry staining is describes in detail in Appendix 3. All antibodies used in this thesis were tested in both formalin and methanol fixated cells, except for the anti-γ tubulin antibody, which has been used by other group members and is known to work only in methanol fixated cells. All incubations were carried out at room temperature.

The coverslips were placed with the cell side up on a sheet of parafilm in a humidified chamber. The parafilm avoided dispersion of reagents placed on the coverslips. The humidified chamber consisted of a petri dish (diameter of 150 mm) with three layers of wet filter paper. PBS-AT (1% BSA (Sigma-Aldrich), 0.5 % Triton-X100 (Sigma-Aldrich) in PBS) was used as blocking, permeabilizing agent and antibody diluent. The coverslips were incubated with the primary antibody against CKS2 (Life Technologies), CDK1 (Santa Cruz Biotechnology or Lifespan Biosciences), CDK2 (Santa Cruz Biotechnology), SSBP1 (Sigma-Aldrich) or γ-tubulin (kind gift from Stephen Doxey, Worcester) for 2 hours and the secondary antibody donkey anti-mouse 549 (Jackson ImmunoResearch) or donkey anti-rabbit 488 (Jackson ImmunoResearch) for 40-60 minutes. The secondary antibodies were fluorophore-conjugated with emission at 549 nm and 488 nm respectively and had to be protected from light. Technical controls without primary antibody were also prepared. In the co-localization experiments, cells received two primary antibodies with appropriate secondary antibodies. Thus, controls were prepared that only received one primary antibody and the secondary antibody produced in the other animal species. DNA was stained with Hoechst 33258 (0.6 μg/mL) (Sigma-Aldrich) for 1-2 minutes. The coverslips were dried carefully and mounted on slides with 5 μl ProLong ® Gold Antifade Reagent (Life Technologies), which suppresses photo bleaching [118].

4.2.4 *In situ* proximity ligation assay

The Duolink II orange starter kit was used for the experiments. The starter kit contained secondary PLA probes, a blocking solution, an antibody diluent, a ligation solution, an amplification solution, wash buffers, mounting medium and the enzymes ligase and polymerase. The various functions of the PLA solutions are accounted for in Appendix 4, table 2.

After seeding, cells were washed with warm (37 °C) Dulbecco's PBS, and fixated with one of the following methods:

- Methanol for 10 minutes at -20 °C
- 10% neutral buffered formalin for 10 minutes at room temperature
- 10 % neutral buffered formalin for 10 minutes at room temperature followed by methanol for 10 minutes at -20 °C

- 10 % neutral buffered formalin for 10 minutes at room temperature followed by detergent buffer for 1 hour on ice (0°C)

After fixation, cells were washed three times with Dulbecco's PBS and the methanol fixated cells were soaked in PBS for 2-3 minutes for rehydration. A reaction area of 1 cm^2 was outlined on the slides with a hydrophobic barrier pen (ImmEdge ™ Pen). All incubations were performed in a humidified chamber and all incubations, except with primary antibody, were carried out at 37 °C. A detailed protocol describing incubation time, temperature, antibody- and reagent dilutions is presented in Appendix 4, and the detergent buffer formula is shown in Appendix 5. The mounting medium contained DAPI, which stained DNA in the nucleus. A technical negative control omitting primary antibodies was included in the experiments, which examined the unspecific binding of the PLA probes. Ideally, a negative control with a cell line that did not express one or both of the target proteins should have been included. Such a control would have given information on the specificity of the primary antibodies [17]. siRNA experiments for knockdown of CKS2 were performed. However, CKS2 knockdown in HeLa cells appeared to up regulate apoptosis and complicated the introduction of a negative control. These results are therefore not included in the thesis.

4.2.5 Fluorescence microscopy

A Zeiss AxioImager z1 microscope was used to capture images of the stained cells (Appendix 6). Three fluorescent dyes were used for the immunofluorescense studies: Dylight549 donkey anti-mouse, which is excited by light of 549 nm (figure 16), Dylight488 donkey anti-rabbit, which is excited by light of 488 nm (figure 17) and Hoechst 33258, which is excited by light of 352 nm (figure 18) [119]. The spectra below show that there is no significant overlap in the excitation or emission spectra of the three fluorochromes in the regions that are allowed to pass through the filters of the fluorescence microscope.

The PLA interactions were assessed by fluorescently labeled oligonucleotides, which are excited at 554 nm and emit light of 579 nm. The fluorochrome was used with the same filter as with Dylight 549. The specimens were mounted with 0.17 mm thick coverslips (Assistent). Since 63x and 100x oil objectives (NA 1.4; Carl Zeiss) were used, a drop of immersion oil was applied on top over the coverslips (figure 19).

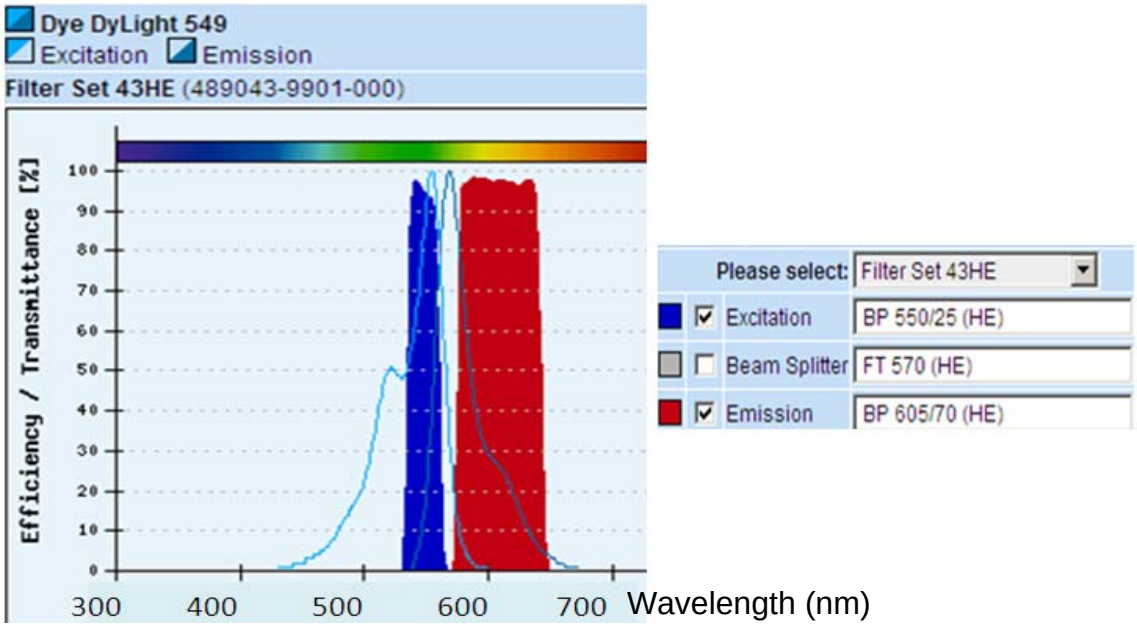

Figure 16. Excitation- (light blue curve to the left) and emission (light blue curve to the right) curves of Dylight549. The excitation filter (550/25) used with this fluorochrome allows transmission of wavelengths in the dark blue scattered area, whereas the emission filter allows only wavelengths in the red area to pass [119].

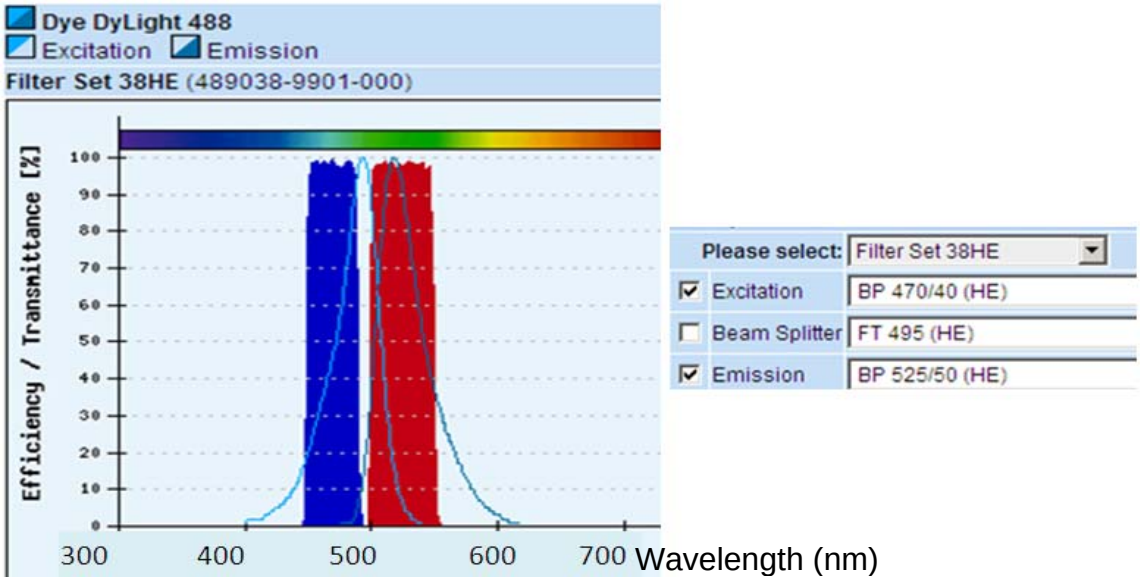

Figure 17. Excitation- (light blue curve to the left) and emission (light blue curve to the right) curves of Dylight488. The excitation filter (470/40) used with this fluorochrome allows transmission of wavelengths in the dark blue scattered area, whereas the emission filter (525/50) allows only wavelengths in the red area to pass [119].

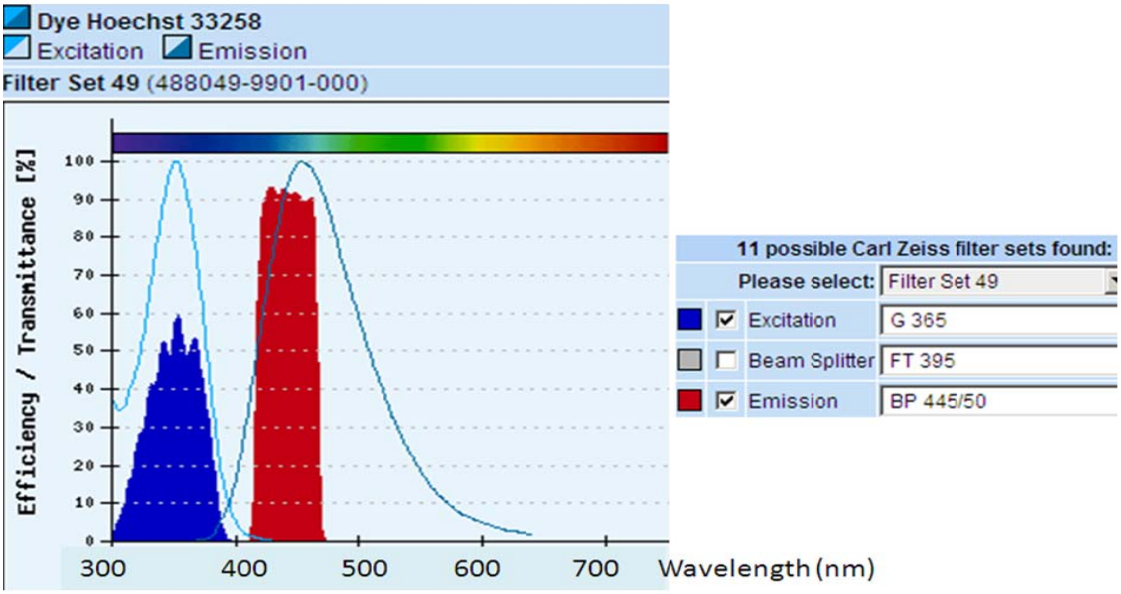

Figure 18. Excitation- (light blue curve to the left) and emission (light blue curve to the right) curves of Hoechst 33258. The excitation filter 365 used with this fluorochrome allows transmission of wavelengths in the dark blue scattered area, whereas the emission filter 445/50 allows only wavelengths in the red area to pass [119].

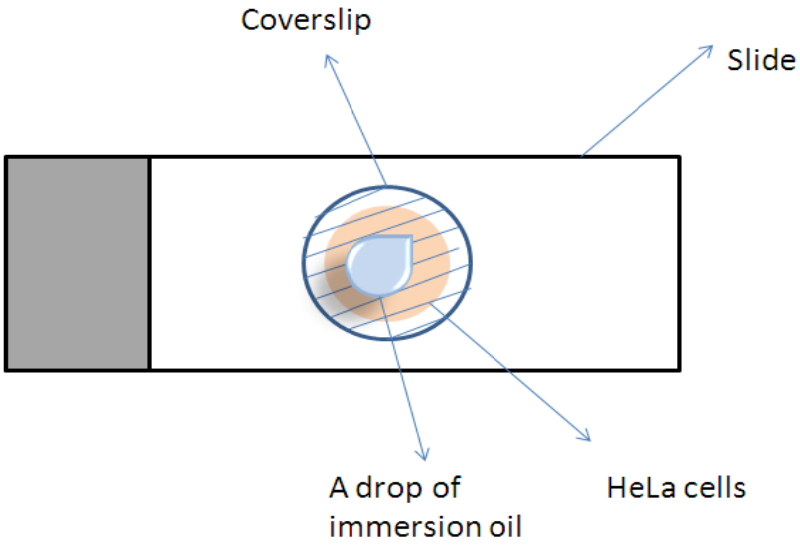

Figure 19. A sketch of a specimen prepared for microscopic examination. A drop of immersion oil was deposit on the top of the specimen's coverslip when using 63x and 100x oil objectives.

4.2.6 Qualitative evaluation of immunocytochemistry images

The staining of the cells, which were fixated with either formalin or methanol, was compared. The cytoplasmic and nuclear stainings were evaluated separately. The strength of the signal was classified as weak, intermediate, strong or intensive. The distribution of the staining was assessed as either evenly distributed or in foci. The staining was classified as variable, when differing among cells. Qualitative evaluations are subjective. When signals stood out clearly from the background, they were categorized as intensive. Here, strong and intermediate signals in the nucleus were distinguished by evaluating the fluorescence intensity and staining of foci.

4.2.7 Quantification of PLA foci

Proper permeabilization of the antibodies was required for obtaining PLA signals in the nucleus. The duolink PLA antibody diluent contained a permeabilizing agent with unspecified content. In order to establish PLA, interactions between CKS2 and CDK1 in the nucleus were quantified for the four different fixation methods.

This PLA experiment was performed three times, and about 70 cells from each fixation method, randomly chosen from all three experiments, were photographed. Foci in the nucleus were counted for one focal plane with distinct nucleoli per cell. Some cells had overlapping PLA foci. In these cases, a focus was assumed to be 0.5 μm in diameter, and the number of foci was counted accordingly.

4.2.8 Statistics

Vertical histograms of number of PLA foci in the nucleus were plotted by use of SigmaPlot (Systat Software). The distributions were not normally distributed (Shapio-Wilk test, $P<0.05$). Possible differences in number of PLA foci due to fixation method, were tested by use of SigmaStat, applying a Mann-Whitney Rank Sum test. This test is an alternative to the t-test, but does not require normally distributed data. A significance value of 0.05 was used. As the data were not normally distributed, median values are given, instead of the mean, as the middle value of the distribution.

5 Results

5.1 Localization and co-localization of CKS2, CDK1, CDK2 and SSBP1 by immunocytochemistry

Cells for immunocytochemistry studies were fixated with either formalin or methanol. The images shown here are of methanol fixated cells. The formalin fixated cells are shown in Appendix 7. Representative images of the stained cells were chosen. Controls for the immunocytochemistry and PLA experiments are given in Appendix 8.

5.1.1 Localization of CKS2

CKS2 was located in both the cytoplasm and the nucleus (figure 20). Some large and small CKS2 foci were observed in the nucleus of interphase cells, but there was no CKS2 in the nucleoli. However, CKS2 were uniformly distributed in foci over the entire cytoplasmic compartment. Some cells exhibited two intensively coloured foci close together in the interphase. They appeared to be located in the cytoplasm close to the nucleus. The diameter of each of the points (of the double-point) was approximately 0.9 µm (figure 20D).

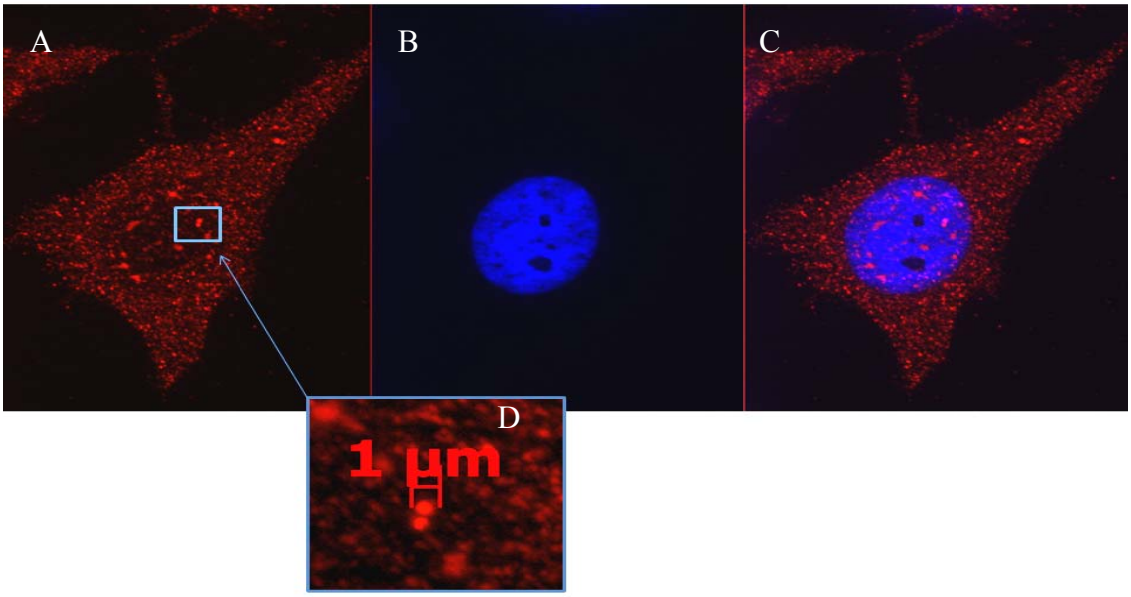

Figure 20. Localization of CKS2 in a methanol fixated HeLa cell in interphase. A. Red colour gives the distribution of CKS2. B. Blue colour gives the distribution of DNA in the nucleus. C. Stained CKS2 superimposed on the nuclear DNA staining. D. CKS2 staining visualized a double-point in some cells.

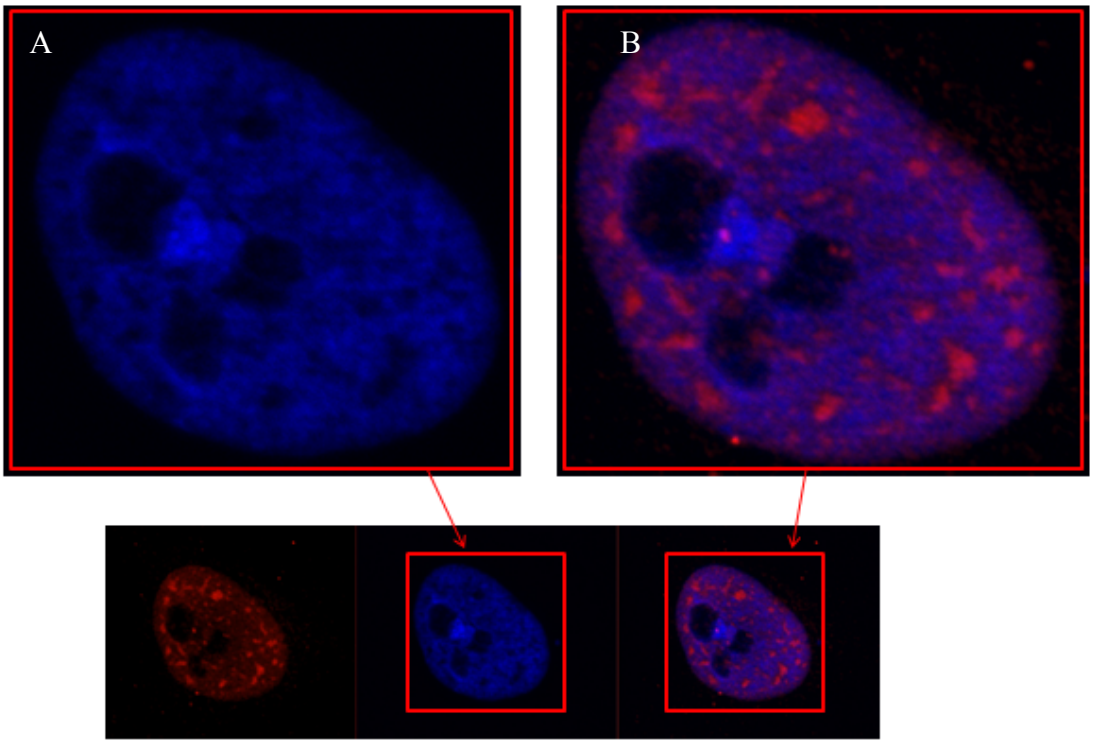

Figure 21. Distribution of CKS2 in the nucleus of a formalin fixated HeLa cell. A. Magnified nucleus with stained DNA (blue). B. Magnified nucleus with stained CKS2 (red).

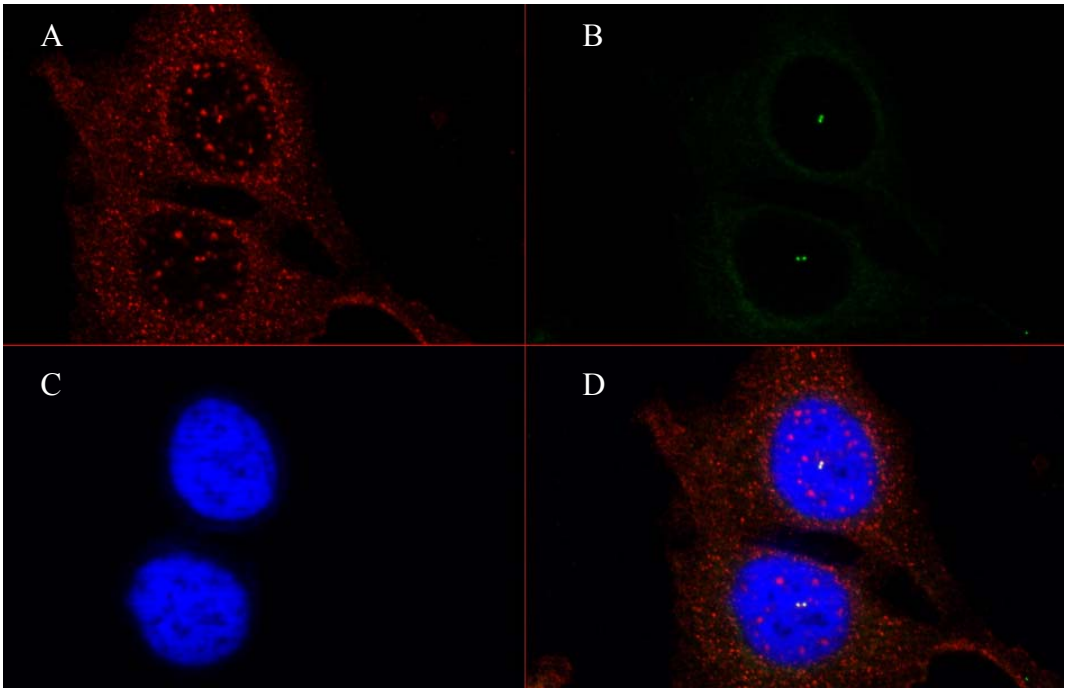

Figure 22. Localization of CKS2 and γ-tubulin in a methanol fixated HeLa cell in interphase. A. CKS2 (red), B. γ-tubulin (green), C. DNA in the nucleus (blue) and D. All three images superimposed on each other.

In the nucleus, it was observed that CKS2, to a large extent, localized to dark areas except for the nucleoli (figure 21).

Cells simultaneously incubated with anti-CKS2 and anti-γ tubulin antibodies are shown in figure 22. The latter intensively stained one or two foci located in the cytoplasm close to the nucleus. CKS2 stained foci were positioned at the same location. The co-localization is shown as yellow foci in the image (figure 22D). CKS2 stained foci co-localized with γ-tubulin in all the observed cells.

5.1.2 Co-localization of CKS2 with CDK1 and CDK2

CDK1 proteins were well distributed throughout most parts of the cell both in the nucleus and the cytoplasm, but were not seen in the nucleoli (figure 23). CDK1 and CKS2 appeared to be co-localized both in the cytoplasm and in the nucleus, as can be seen as yellow signals in the merged CKS2 and CDK1 images (figure 23 and 24). This was also seen in formalin fixated cells (Appendix 7, figure 1). In the interphase cells, the co-localization of CKS2 and CDK1in the nucleus is apparent (figure 24). An intensively stained large, green CDK1focus was located outside the nucleus (figure 23). This was clearly visible in methanol fixated cells, but less so in formalin fixated cells (Appendix 7, figure 1). Two CKS2 foci were located on the same spot.

In mitosis, both CKS2 and CDK1 were mainly distributed in the cytoplasm. There were no intensively stained CKS2 or CDK1 foci in the nucleus (figure 24). In the prometaphase cell, two green CDK1 foci were located on both sides of the DNA. Two CKS2 foci appeared to be located on the same spot.

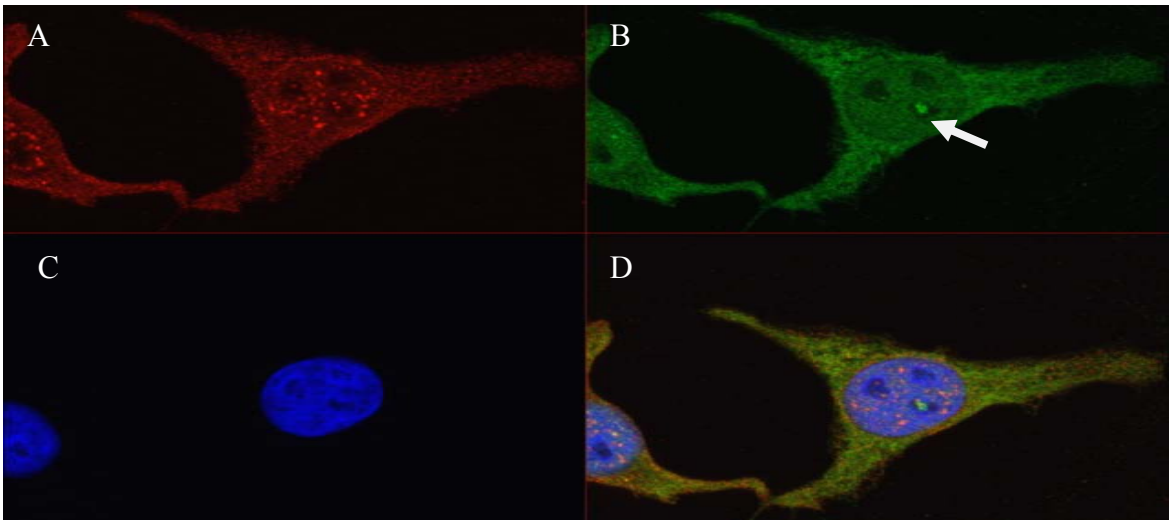

Figure 23. Localization of CKS2 and CDK1 in a methanol fixated HeLa cell in interphase. A. CKS2 (red), B. CDK1 (green), C. DNA in the nucleus (blue) and D. All three images superimposed on each other. The arrow in B indicates two green CDK1 foci found in many cells.

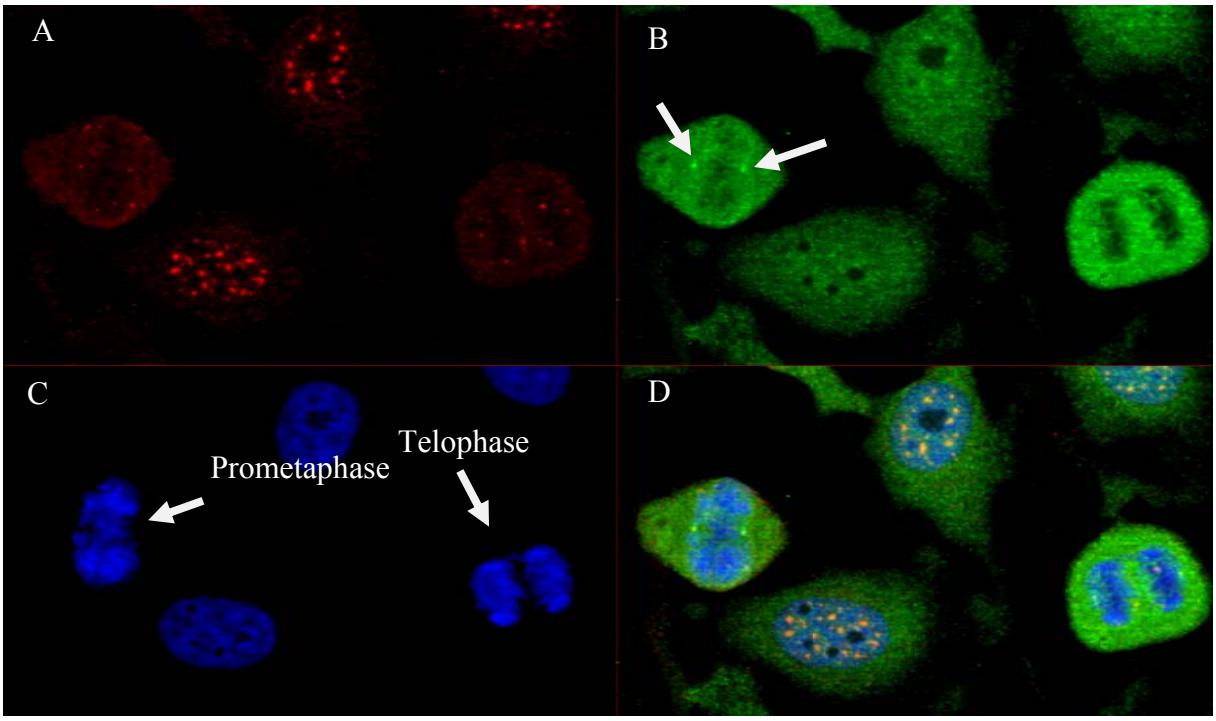

Figure 24. Localization of CKS2 and CDK1 in methanol fixated HeLa cells in interphase and mitosis. Mitotic (prometaphase and telophase) cells are indicated on the DNA image (C). A. CKS2 (red), B. CDK1 (green), C. DNA in the nucleus (blue) and D. All three images superimposed on each other. Yellow dots are areas where CKS2 and CDK1 typically co-localize. The arrows point at two CDK1 foci.

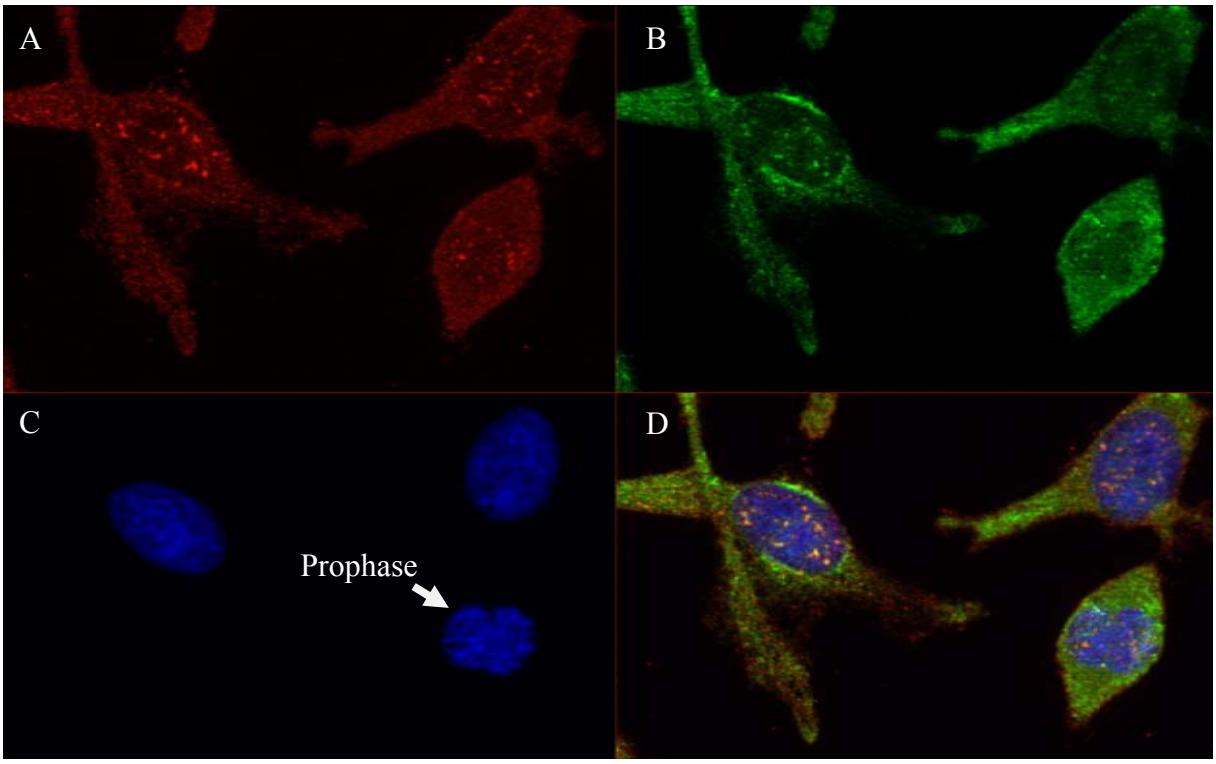

Figure 25. Localization of CKS2 and CDK2 in methanol fixated HeLa cells in interphase and mitosis. A mitotic (prophase) cell is indicated on the DNA image (C). A. CKS2 (red), B. CDK2 (green), C. DNA in the nucleus (blue) and D. all three superimposed on each other. Yellow dots are areas where CKS2 and CDK2 typically co-localize.

As for CDK1, CDK2 was also well distributed throughout most parts of the cell, both in the nucleus and the cytoplasm (figure 25). No CDK2 staining was observed in the nucleoli. CKS2 and CDK2 appeared to be co-localized both in the cytoplasm and in the nucleus, as can be seen as yellow signals in the merged CKS2 and CDK2 image. This was also seen in formalin fixated cells (Appendix 7, figure 2). In interphase cells, the co-localization of CKS2 and CDK2 in the nucleus was apparent. CDK2 formed foci in the nucleus of interphase cells. This was not visible in formalin fixated cells (Appendix 7, figure 2). In mitosis, the CKS2 and CDK2 signals appeared to be most dense in the cytoplasm. However, some CKS2 and CDK2 foci were distributed in the nucleus.

5.1.3 Co-localization of CKS2 with SSBP1

SSBP1 was located only in the cytoplasm, visible as green foci in the stained cells (figure 26). Sometimes the foci appeared to lie in lanes. Most of the protein was located close to the cell nucleus. This was also seen in formalin fixated cells (Appendix 7, figure 3). The SSBP1 foci

were often more abundant in formalin fixated cells. A large part of CKS2 in the cytoplasm appeared not to be co-localized with SSBP1. Only a few yellow signals are seen on the image. However, the SSBP1 signal in the cytoplasm was very strong and may drown the CKS2 signal. This was also seen in formalin fixated cells (Appendix 7, figure 4), although the yellow signals were more abundant in these cells.

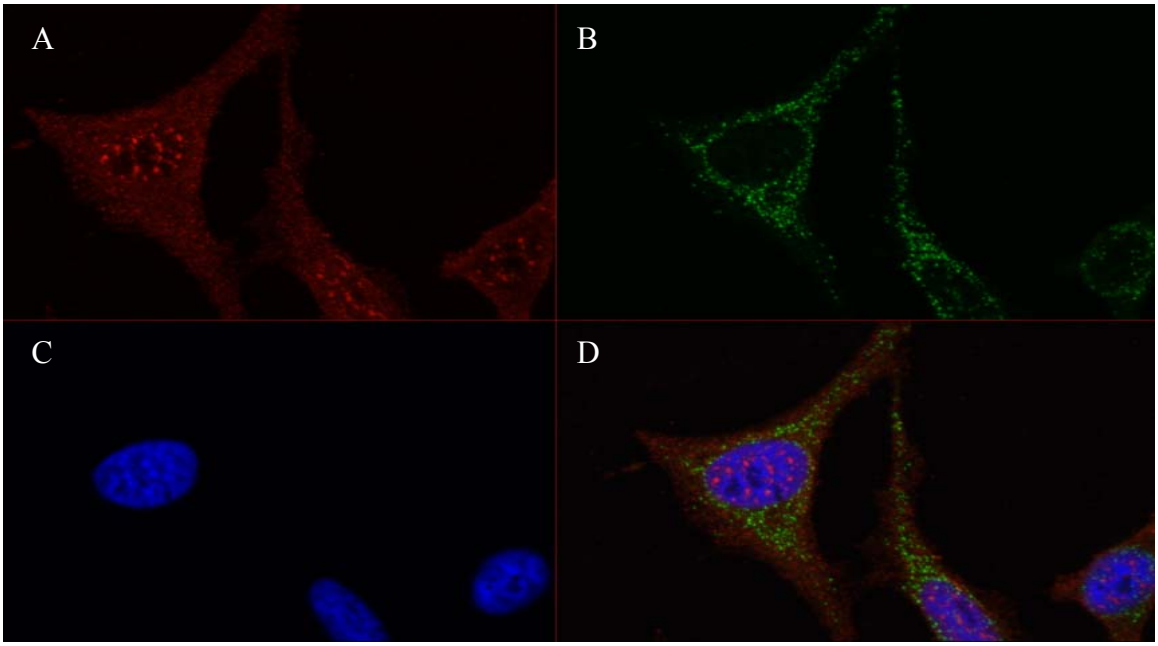

Figure 26. Localization of CKS2 and SSBP1 in methanol fixated HeLa cells in interphase. A. CKS2 (red), B. SSBP1 (green), C. DNA in the nucleus (blue) and D. all three superimposed on each other.

5.1.4 Co-localization of CDK1 with SSBP1

For co-localization of CDK1 with SSBP1, a mouse CDK1 antibody was used. CDK1 was localized in the cytoplasm and the nucleus (figure 27). Moreover, stained cells exhibited intensively stained foci usually appearing in pairs. They were localized in the cytoplasm close to the nucleus. This is in agreement with the foci seen with the CDK1 rabbit antibody (figure 23). Most of the CDK1 proteins in the cytoplasm appeared not to be co-localized with SSBP1. However, the SSBP1 signal in the cytoplasm was very strong and may drown the CDK1 signal. Thus, only a few yellow spots were visible in the cytoplasm. These yellow spots were abundant in formalin fixated cells (Appendix 7, figure 5).

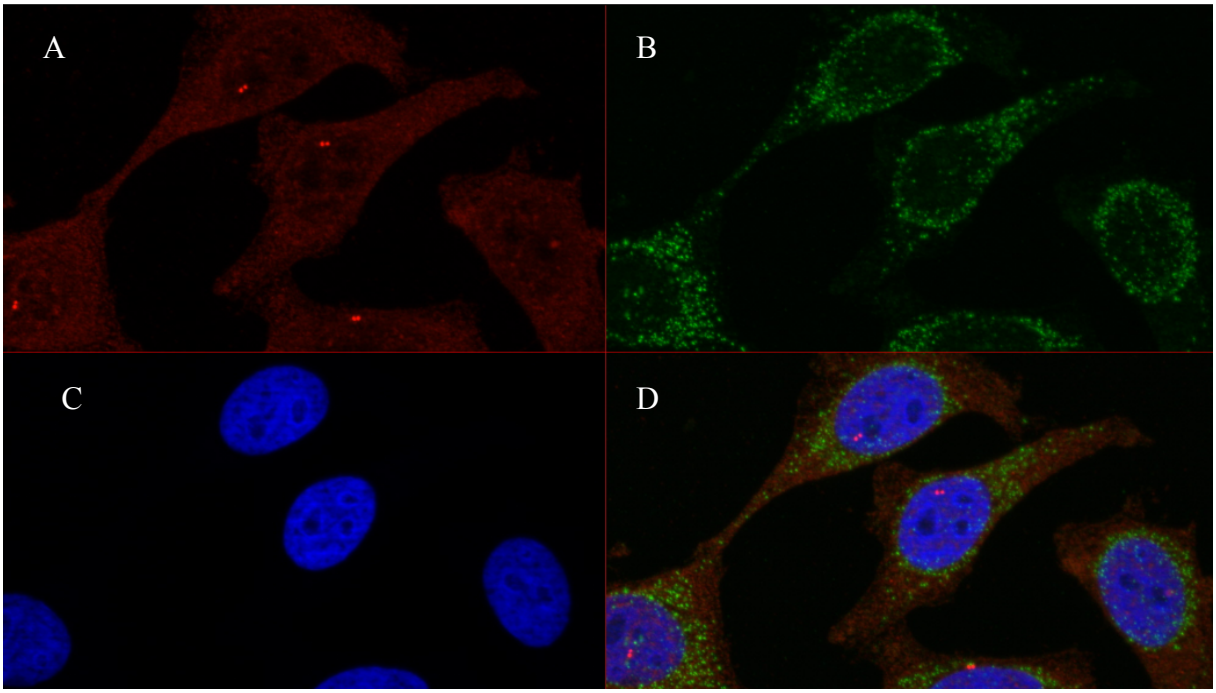

Figure 27. Localization of CDK1 and SSBP1 in formalin and methanol fixated HeLa cells in interphase. A. CDK1 (red), B. SSBP1 (green), C. DNA in the nucleus (blue) and D. All three superimposed on each other.

5.1.5 Controls for immunocytochemistry experiments

Images of the technical negative controls are shown in Appendix 8. The negative controls were incubated with mouse anti-CKS2 (figure 1), rabbit anti-CDK1 (figure 2), rabbit anti-CDK2 (figure 3), rabbit anti-SSBP1 (figure 4), mouse anti-CDK1 (figure 5), donkey anti-rabbit (figure 6), donkey anti-mouse (figure 7) or rabbit anti-γ tubulin (figure 8). The control cells exhibited very weak signals.

5.1.6 Comparison of staining in formalin versus methanol fixated cells

Formalin retained the structure of the nuclear content better than methanol. The intensity of the nuclear staining was stronger from the mouse CKS2, rabbit CDK2 and mouse CDK1 antibodies in methanol fixated cells. In addition, the cytoplasmic CKS2 and CDK1 stained double-foci were more visible in methanol fixated cells. However, the density of the SSBP1 signal appeared to be highest in formalin fixated cells. Thus, both formalin and methanol

fixation could be used in staining with the various antibodies in this thesis. The choice of fixative depended on which cellular structures that were examined (table 3).

Table 3 Qualitative comparison of the signals produced with various antibodies in formalin and methanol fixated cells

	Staining in formalin		Staining in methanol	
Antibody	Cytoplasm	Nucleus	Cytoplasm	Nucleus
Mouse anti-CKS2	Intermediate, no cells with intensive foci	Strong, large foci	Intermediate, some cells with intensive foci	Intensive, large foci
Rabbit anti-CDK1	Intermediate. Few cells with intensive foci	Intermediate	Intermediate. Many cells with intensive foci	Intermediate
Rabbit anti-CDK2	Intermediate	Intermediate, no cells with large foci	Intermediate	Strong. Many cells with large foci
Rabbit anti-SSBP1	Strong	Weak	Strong, variable	Weak
Mouse anti-CDK1	Intermediate, but variable staining of foci	Intermediate, variable	Intermediate, all cells have intensive foci	Strong signal

5.2 Establishment of PLA

5.2.1 Proximity of CKS2 with CDK1

When using formalin for fixation, few PLA foci where visible in the cytoplasm and no foci was found in the nucleus (figure 28). To test if this was caused by the fixation reagent, four different fixation methods were used. This was formalin, methanol, formalin and detergent buffer, and formalin and methanol. The number of PLA foci in the nucleus was counted and plotted in histograms (figure 29). No foci in the nucleus was observed in formalin fixated cells. Number of foci increased when methanol or formalin followed by detergent buffer were used. The median values were 66 and 64, respectively. The number of foci was highest when formalin and methanol was applied in sequence, achieving a median value of 94. The distribution of number of cells with different number of PLA foci differed among fixatives. The distribution of methanol- and formalin and detergent buffer fixated cells ranged from approximately 30-160 PLA foci, whereas formalin and methanol fixated cells ranged from 20-230 PLA foci. The distribution of the PLA foci of formalin fixated cells peaked at 0 PLA foci, methanol- and formalin followed by detergent buffer fixated cells peaked at approximately 50 PLA foci, and formalin and methanol fixated cells peaked at approximately 100 PLA foci. The distribution of the latter exhibited an additional peak at 50 PLA foci.

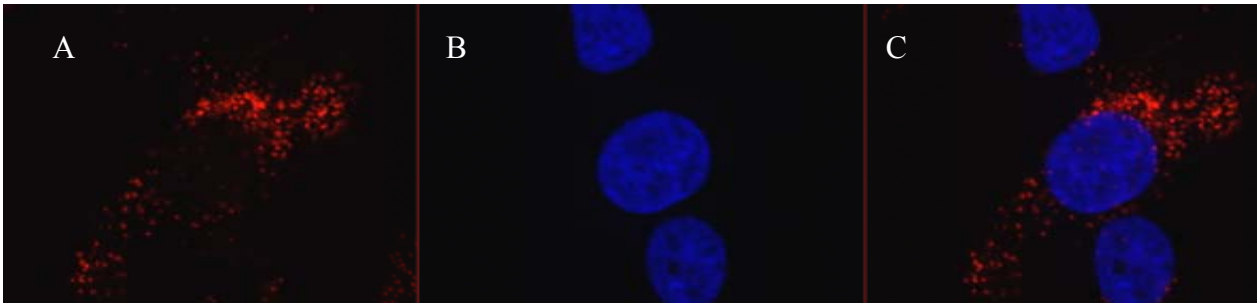

Figure 28. Localization of PLA foci (proximity of proteins) in formalin fixated HeLa cells in interphase. The distribution of co-localized CKS2 and CDK1 (A), DNA in the nucleus (B) and the two superimposed on each other (C).

When comparing the number of PLA foci in the nucleus among fixation methods, significant differences were found for all fixatives except between methanol and formalin followed by a detergent buffer (table 4).

The present results were used to determine fixatives for the further experiments to explore interactions. The immunocytochemistry staining of CKS2, CDK1 and CDK2 in methanol fixated cells exhibited an applicable staining in the cytoplasm and the nucleus. Additionally, the variation in number of PLA foci in methanol fixated cells was smaller than for formalin followed by methanol fixated cells. In the further experiments, the intention was not to quantify the number of PLA foci, but to find a sensitive method to identify the signals. Thus, methanol was used as fixative for subsequent PLA experiments exploring proximity of CKS2 and the CDK proteins. Formalin and detergent buffer would have given a similar result, but was not chosen because earlier master theses on CKS2 function have been performed with methanol fixation. The immunocytochemistry staining of SSBP1 in formalin fixated cells produced a denser signal compared to methanol fixation. Thus, formalin followed by methanol was used as fixative for the PLA experiments exploring interactions of CKS2 and CDK1 with SSBP1.

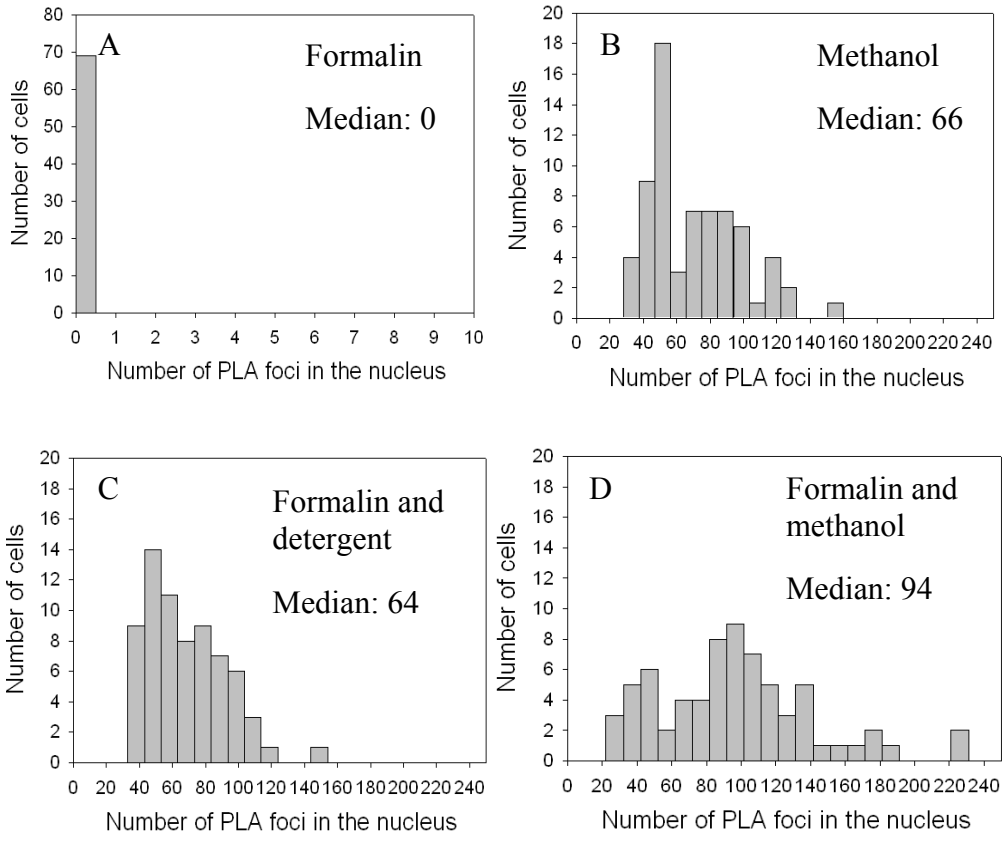

Figure 29. Number of CKS2-CDK1 PLA foci in the nucleus of about 70 HeLa cells. Fixation with A. formalin, B. methanol, C. formalin and detergent and D. formalin and methanol.

Table 4. Pairwise comparison of CKS2-CDK1 PLA foci in the nucleus of HeLa cells between experiments using different fixatives

Fixative[a]	U-value[b]	P[c]
Formalin and methanol vs. formalin and detergent	1446.5	<0.001
Formalin and methanol vs. methanol	1537	<0.001
Methanol vs. Formalin	0	<0.001
Methanol vs.formalin and detergent buffer	2339	0.861
Formalin and detergent buffer vs. Formalin	0	<0.001
Formalin and methanol vs. formalin	0	<0.001

[a] Sixty-nine cells were fixated with formalin, methanol, formalin with a detergent buffer or formalin followed by methanol

[b] The statistical differences between number of PLA foci in the nucleus by use of Mann-Whitney Rank Sum Test.

[c] The probability value of the statistical analysis

5.3 Use of PLA to explore protein interactions

5.3.1 Proximity of CKS2 and CDK proteins

PLA foci of CKS2-CDK1 were distributed in the nucleus and throughout the cytoplasm (figure 30). Large foci in the nucleus occurred mainly in the dark areas of the nucleus. This was the regions where CKS2 were located by immunocytochemistry.

PLA foci in mitotic cells were to a large extent localized outside the nucleus with a few foci occurring within the DNA in the various developmental phases (figure 30 F, I and L). It seemed to be more PLA foci in the nucleus of the early mitotic cell (prometaphase) than in the later phases.

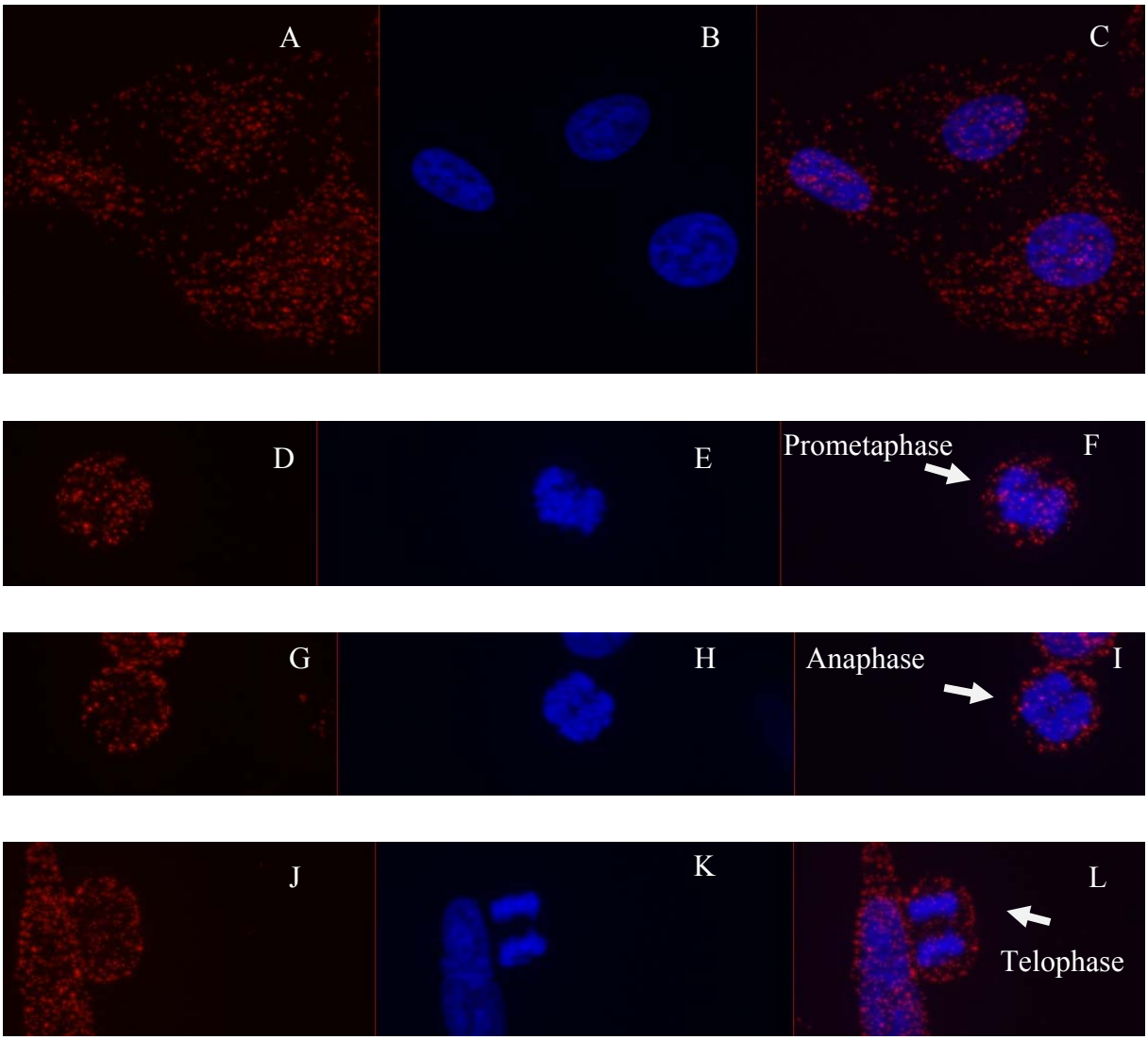

Figure 30. Localization of PLA foci (proximity of proteins) in methanol fixated HeLa cells in interphase and mitosis. The distribution of co-localized CKS2 and CDK1 (A, D, G and J), DNA in the nucleus (B, E, K and K), and PLA foci and nucleus superimposed on each other (C, F, I and L).

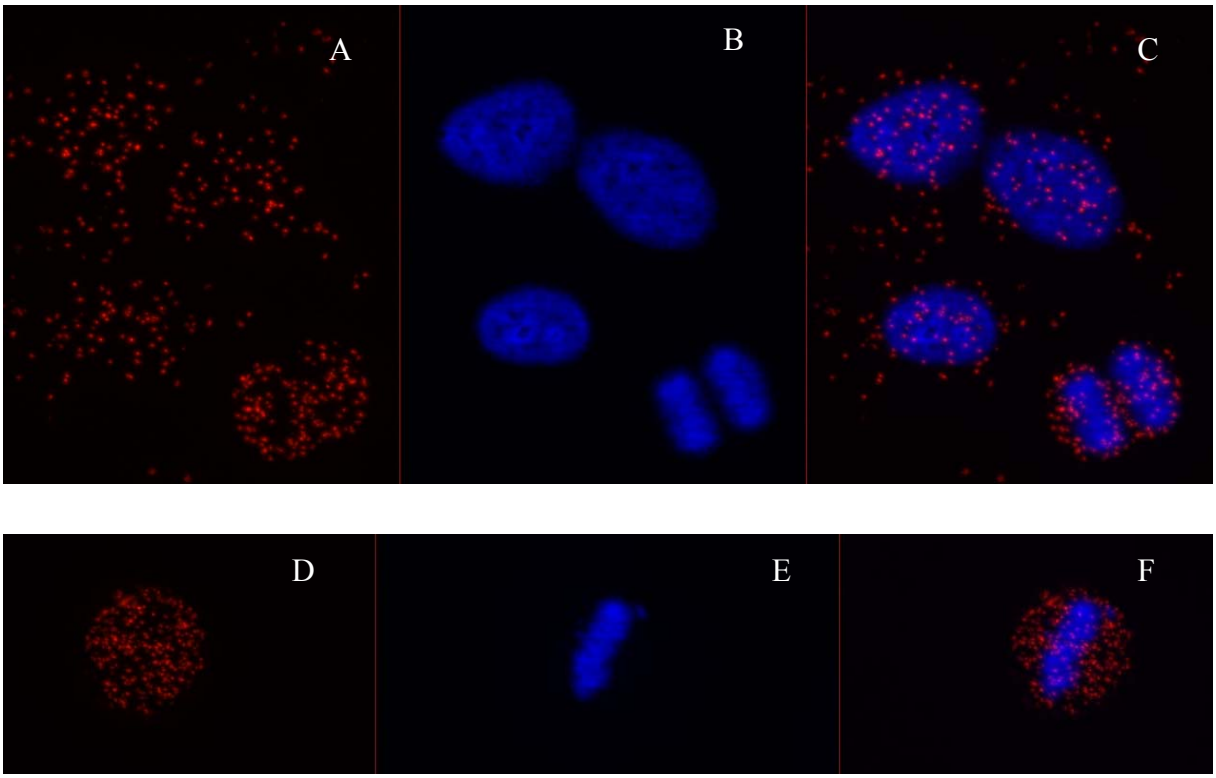

Figure 31. Localization of PLA foci (proximity of proteins) in methanol fixated HeLa cells in interphase and mitosis. The distribution of co-localized CKS2 and CDK2 (A and D), DNA in the nucleus (B and E), and PLA foci and nucleus superimposed on each other (C and F).

The similar pattern was seen for the CKS2-CDK2 PLA foci (figure 31). Also in this case were the PLA foci distributed in the nucleus and throughout the cytoplasm. Some PLA foci in the nucleus occurred in the dark areas and some occurred in the light blue areas. PLA foci in mitotic cells showed a tendency to localize outside the nucleus.

By immunocytochemistry, it was observed that CKS2 (red stained areas in figure 21B) was to a large extent localized to dark areas of the nucleus, except for the three nucleoli in this cell. The PLA signal from associated CKS2 and CDK1 (red signals) was distributed over the nucleus, except for the nucleoli (figure 32). Large CKS2-CDK1 foci were often located in dark areas of the nucleus. PLA signals were also distributed elsewhere in the nucleus, but were usually less dense. The PLA signals from associated CKS2 and CDK2 (red signals) were also distributed over the entire nucleus, except for the nucleoli (figure 33). However, there was no clear association between the localization of PLA foci and dark areas of the nucleus.

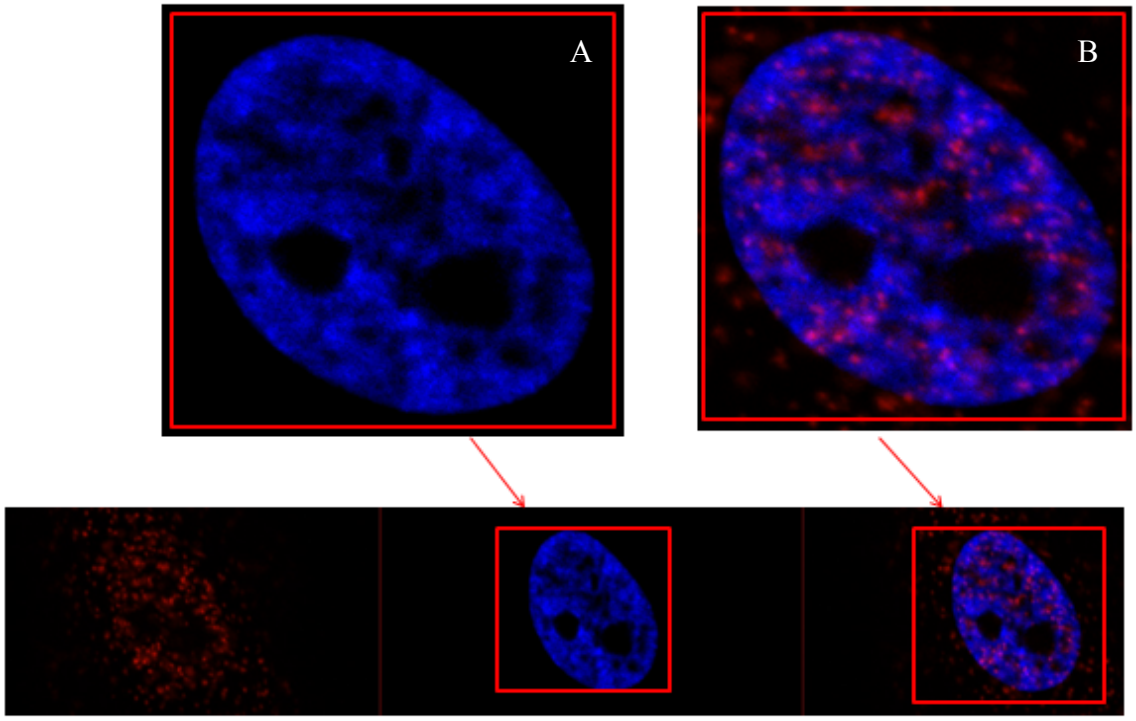

Figure 32. Distribution of CKS2-CDK1 PLA foci in the nucleus of a formalin and methanol fixated HeLa cell. A. Magnified nucleus with stained DNA (blue). B. Magnified nucleus with CKS2-CDK1 PLA foci (red).

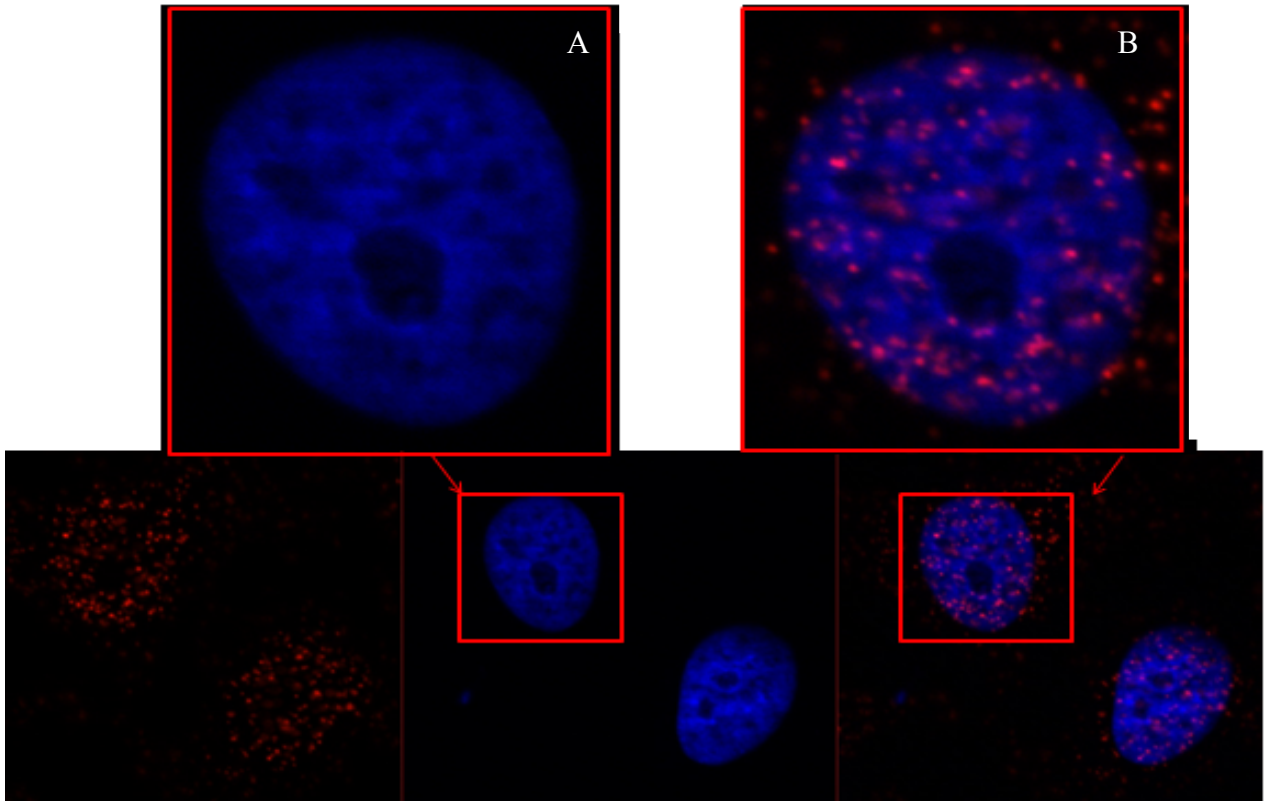

Figure 33. Distribution of CKS2-CDK2 PLA foci in the nucleus of a formalin and methanol fixated HeLa cell. A. Magnified nucleus with stained DNA (blue). B. Magnified nucleus with CKS2-CDK2 PLA foci (red).

5.3.2 Proximity of CKS2 and CDK1 with SSBP1

The CKS2-SSBP1 PLA signals were distributes in foci, mainly in the cytoplasm of the cells (figure 34). Most of the cytoplasmic signals occurred close to the nucleus. Sometimes signals occurred near the edges within the nucleus. This was the regions where SSBP1 were located by immunocytochemistry.

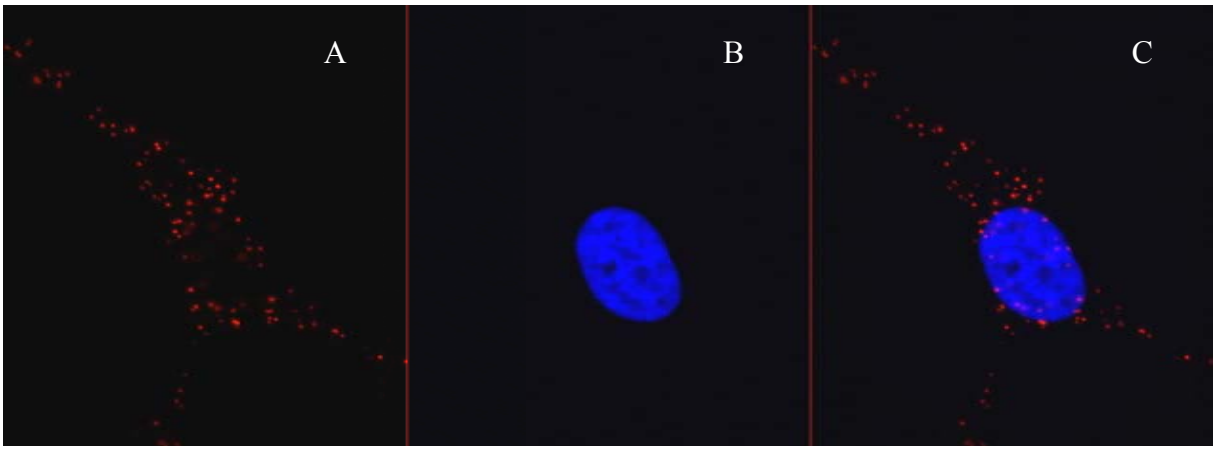

Figure 34. Localization of PLA foci in formalin and methanol fixated HeLa cells in interphase. The PLA foci of CKS2-SSBP1 (A), DNA in the nucleus (B), and PLA foci and nucleus superimposed on each other (C).

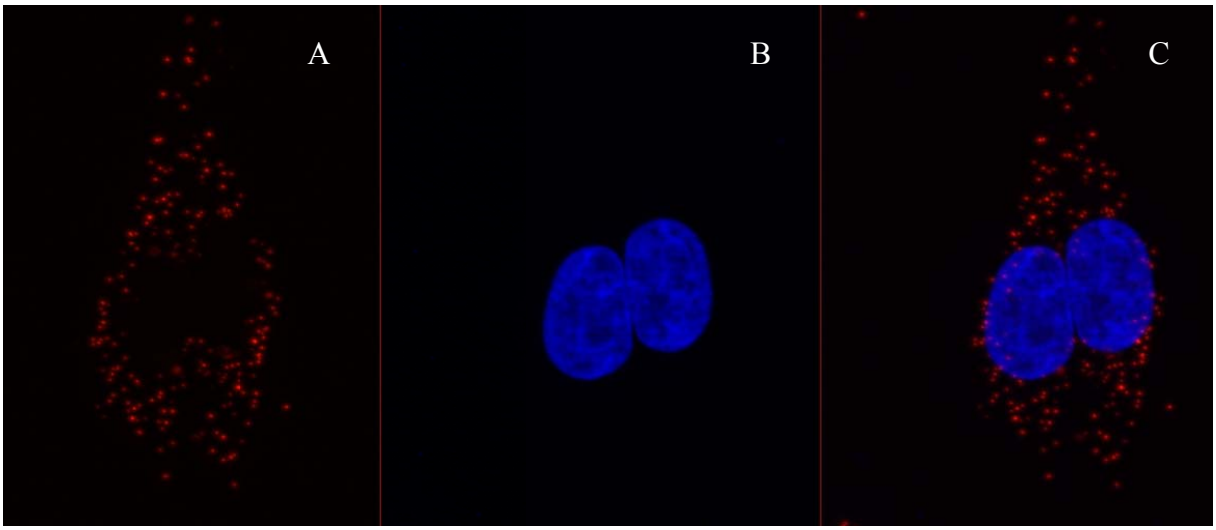

Figure 35. Localization of PLA foci in formalin and methanol fixated HeLa cells in interphase. The PLA foci of CDK1-SSBP1 (A), DNA in the nucleus (B), and PLA foci and nucleus superimposed on each other (C).

Also in the case of the CDK1-SSBP1, the PLA signals were mainly found in the cytoplasm and sometimes signals occurred near the edges within the nucleus (figure 35). This was the regions where SSBP1 were located by immunocytochemistry.

5.3.3 Controls for the PLA experiments

Images of the technical, negative controls are shown in Appendix 8. The negative control cells were incubated with secondary PLA probes (figure 9), secondary PLA probes with mouse anti-CKS2 (figure 10) or secondary PLA probes with rabbit anti-SSBP1 (figure 11). The control cells exhibited very weak or no signals showing that both primary antibodies had to be present to produce PLA signals.

6 Discussion

6.1 Methodology

6.1.1 Suitability of the methods

Immunofluorescence is a powerful technique for localization of proteins in cells [16]. To compare the localization of two proteins, double labelings of two primary and two secondary antibodies are needed. Furthermore, the method assumes proper fixation of cells, which depends on the sensitivity of the epitope and the working conditions for the antibody[120]. Care should be taken that the antibodies do not cross react when two or more antibody combinations are used [16].

In this thesis, the conditions for each antibody have been explored. The antibodies have been tested with both formalin and methanol fixation. Moreover, the antibodies have been tested in a range of dilutions for these two fixation methods to ensure that the antibody concentration used produced good staining with minimum background staining. A qualitative evaluation of the various antibody stainings in formalin and methanol fixation was performed. The qualitative evaluation was subjective, as explained in chapter 4.2.6.

Technical, negative controls were employed in the experiments. They assessed cross-reactivity between combinations of antibodies and unspecific binding of the secondary antibody. The negative controls exhibited very little or no fluorescence signal. The experiments lacked, however, a biological negative control where the proteins of interest were absent. Thus, unspecific binding of the primary antibodies to other epitopes, but the one of interest, have not been assessed. The use of the PLA relieved this problem.

PLA is a sensitive and specific method for studying protein-protein interactions in tissue or cell samples [15]. It provides a unique opportunity to study both stable and transient interactions directly in cells, because the fixation reagent “freezes” the cells [121, 122]. Each individual protein-interaction event ensures that every signal is visible as a distinct spot in the microscope. The signal is physically linked to its target and remains in the correct cellular location where the interaction took place. The present samples were fixed and incubated with the primary antibodies according to the best conditions as assessed by immunocytochemistry. In addition, the cells were permeabilized in methanol. Methanol was added as permeabilizing

agent because the antibody produced good signals, in the immunocytochemistry and the PLA experiments, in this solvent. All proteins studied in PLA have earlier been shown to bind to each other [6, 35]. Thus, the PLA signals produced show locations where the proteins probably interact. The studied proteins must be in proximity of 30-40 nm or less in order to produce a PLA signal [104]. Therefore, the probability of receiving false signals, due to unspecific binding, is reduced compared to immunocytochemistry co-localizing experiments.

Technical, negative controls were included in the PLA experiments in which primary antibodies were omitted. This assessed the PLA probe background. Also, controls with only one of the primary and two secondary antibodies were included. The controls comprised either primary antibody produced in rabbit or mouse. The negative controls exhibited very little or no fluorescence signal, suggesting that the signals were not caused by interactions between two identical primary antibodies or because of unspecific binding of the secondary PLA probes.

Alternatives to PLA for studying protein-protein interactions include förster resonance energy transfer (FRET [123]), fluorescence cross-correlation spectroscopy (FCCS), bimolecular fluorescence complementation (BiFC) and yeast-two hybrid (Y2H) technology [124, 125]. Some of these methods require expression of modified proteins, and can therefore not be used on clinical material. Although the method was used for cell samples in this thesis, PLA can be used on natural tissue and cell samples. When used on clinical material, this method may give a more accurate image of the proteins present *in vivo*. The FRET method detects protein interactions in both living and fixated cells. Furthermore, FRET can be used to study more than two proteins at the time. On the other hand, with FRET it is difficult to distinguish background signals from weak protein signals. PLA is more sensitive. Due to amplification, a single protein interaction is enough to produce a PLA signal. Also, the FRET method requires that the antibodies are correctly oriented in relation to each other to produce a signal. In addition, several correction factors must be calculated, making the use more complicated [124]. Y2H is a useful method for studying protein interactions [125]. A disadvantage, however, is that not all proteins shown to have an affinity for each other using this method, interact under normal conditions. PLA requires no extra equipment in addition to immunocytochemistry. The PLA interactions can be visualized by microscopy, providing insight to where the interactions are located in the cells [125]. Therefore, there are good reasons for selecting the PLA for studying protein-protein interactions in the cells.

6.1.2 Fixation

Number of PLA foci in the nucleus of HeLa cells representing the proximity of CKS2 and CDK1, differed when various fixation reagent were used. No PLA foci were observed in the nucleus of formalin fixated cells. However, foci in the nucleus were observed when formalin fixation was followed by detergent buffer (median value of 64 PLA foci). Thus, the lack of signals in formalin fixated cells was probably not because of chemical alterations of the epitope caused by the fixation method, but rather by lack of permeabilization of the antibodies. This may be due to the cross-linking properties of formalin, which may reduce antigenicity of some cell components by obstruction of antibody binding [107]. The detergent buffer contained Igepal ca-630, which is a non-ionic amphiphile (a compound that possess lipophilic and hydrophilic properties) that solubilizes membrane lipids [111]. The compound is efficient at breaking lipid-lipid and lipid-protein interactions in membranes. Thus, the use of detergent buffer probably permeabilizes the membrane and allows penetration of the antibodies inside the nucleus with subsequent production of PLA signals.

Combined formalin and methanol fixation yielded the highest amount of PLA foci in the nucleus. This method, in contrast with the combined formalin and detergent buffer fixation method, used methanol for permeabilization instead of the detergent buffer. Methanol solubilizes and extracts lipids in the membranes and cytoplasm, and thereby permeabilizes the cell [18]. Additionally, the solvent breaks hydrogen bonds disrupting the three-dimensional structure of proteins. Thus, methanol appeared to either permeabilize the cells more efficiently than the detergent buffer, or alter the epitope (*e.g.* denaturates) in a way that allowed more efficient recognition of the antigen by the antibodies. Formalin and methanol fixated cells probably maintained nuclear structures better than fixation in methanol alone. The nucleoli appeared more distinct, the outskirts of the nucleus were less dishevelled and the structures in the chromatin were more intact. However, number of PLA foci observed varied more among cells fixated in formalin and methanol than when the other methods were used. The variation may be caused by differences in penetration among cells when two fixation reagents were used. Neighboring cells could exhibit quite different PLA signals, possibly due to differences in the spatial orientation of the cells. Some cells were more closely packed than others and could be differently fixated by the reagents.

Methanol fixated cells produced fewer PLA foci in the nucleus than when both formalin and methanol were used (median value of 66 versus 94 PLA foci). This may be a consequence of

methanol induced antigen extraction [126]. The antigen extraction appeared to be reduced when formalin was used before methanol. However, the addition of formalin led to a larger variation in the number of PLA foci, and the result was therefore less reproducible. Since the purpose of the experiments was to detect PLA signals and not to quantify maximum number of PLA foci, methanol was chosen alone as fixative because this led to the most reproducible results. Furthermore, this method has been applied in other CKS2 studies performed in our laboratory, making the present results comparable to the previous ones [127, 128].

The distributions of PLA signals for methanol fixated cells and formalin and detergent buffer fixated cells, exhibited a peak at approximately 50 PLA foci. Since the G1-phase of the cell cycle is the most time-consuming cell cycle phase of HeLa cells [129], it is tempting to speculate that the peaks in the histograms represent cells in this phase. The histogram for formalin and methanol fixated cells, on the other hand, exhibited two peaks at approximately 50 and 100 PLA foci. This may represent cells with poor and good penetration of antibodies, respectively. However, the first suggestion cannot with certainty be drawn without further analysis, such as flow cytometric sorting of cell cycle phases with subsequent quantification of PLA foci in the different cell cycle phases.

6.2 Biological part

The localization of CKS2 proteins in the nucleus and cytoplasm, analyzed by immunocytochemistry, is similar to the finding of Urbanowicz-Kachnowicz et al [130]. The PLA signals generated by the proximity of CKS2 with CDK1, CDK2 and SSBP1 and of CDK1 with SSBP1 indicate locations where the proteins are closely located. The signals are therefore termed interactions, however, the proteins could possible also be in a complex with each other without a direct binding. CKS2 has previously been shown to bind to CDK1, CDK2 and SSBP1 and CDK1 have been shown to bind to SSBP1 [6, 35]. It is therefore plausible that the PLA signals observed represent binding between the proteins. In the following, possible functions for the interactions between the proteins will be discussed.

6.2.1 Binding of CKS2 to CDK1 and CDK2 in the nucleus and cytoplasm

Crystallographic investigations have suggested that CKS proteins bind CDKs after being activated by CCNs and cdk-activating kinases (CAKs) [31, 130]. CKS proteins are assumed to direct CDKs to their substrates [31, 34, 35]. The first hypothesis is supported by the observation that the binding of CKS2 to CDK1 is stimulated by CCNB [36]. *In vivo,* CKS proteins are expressed in the same cellular compartments as phosphorylated, potentially active CDK1 and CDK2 [130]. In addition, many studies indicate that CKS2 and CKS2 homologs bind to monomeric CDK1 (not bound to a CCN) as well [36, 131, 132]. Studies indicate that these interactions are weak and transient [36]. Active CDK-CCN complexes are predominantly nuclear in localization [133, 134]. However, active CDK1-CCNB is also observed in the cytoplasm in the mitosis [135]. Some of the present nuclear PLA signals may therefore indicate locations where CKS2 interact with active CDK1 and CDK2 and their CCNs, which are best known to participate in cell cycle progression [19]. Possible effects of CKS2 binding to CDK2, other than in cell cycle progression, are poorly known.

If active CDK1 and CDK2 mainly were located in the nucleus, what were the functions of the same proteins in the cytoplasm? One possibility is that these proteins are inactive. However, CDKs have a role in mitochondrial replication [6]. Thus, the cytoplasmic PLA foci can represent CKS2-CDK interactions involved in cellular functions, such as in mitochondrial replication, or perhaps the cytoplasmic PLA foci also represent stored, inactive CKS2 and CDKs.

6.2.2 A possible role of CKS2 in gene transcription

Immunocytochemistry staining of CKS2 showed that large CKS2 foci in the nucleus were associated with weakly Hoechst stained dark-blue areas of the DNA, which did not constitute nucleoli. Also, in the PLA experiments, signals produced by proximity of CKS2 with CDK1 were often associated with weakly DAPI stained areas. A similar clear association was not observed for the proximity of CKS2 with CDK2. A prominent part of the signals apparently occurred outside these lightly stained areas.

Hoechst and DAPI preferentially bind AT-rich DNA, which is typically enriched in heterochromatin (tightly coiled and mainly genetically inactive DNA), suggesting that DNA in the weakly stained areas are packed as euchromatin, *i.e*. partially or fully uncoiled DNA

[136-141]. Euchromatin is gene-rich and transcriptionally competent [142]. Martinsson-Ahlzén et al [2] have shown that CKS2 and CDK1 associate with chromatin. Moreover, they observed that CKS2 association with the promoter regions and ORF of *CCNB1* and *CDK1* genes increased during transcription of these genes. Depletion of CKS proteins by siRNA led to a significant reduction in *CCNB1* and *CDK1* mRNAs.

In yeast, CKS1 and CDK1 bind to promoters and ORF of several genes and promote their transcription [143]. CKS1 and CDK1 associate with the 19S proteasome, to induce efficient transcription, by reducing nucleosome density of chromatin [144]. CKS1 shows 81 % sequence similarity with CKS2 [5]. Based on the localization of CKS2 and the CKS2-CDK1 PLA signals in the nucleus, along with the association of CKS2 with chromatin, promoters and ORF, it is tempting to speculate that CKS2 may contribute to the expression of genes in a similar way as CKS1.

6.2.3 CKS2 at the centrosome

CKS2 immunocytochemistry showed that some cells exhibited an intensively stained double-point outside the nucleus. The double-point co-localized with a large focus stained by the rabbit CDK1 antibody. The double-point was split in the mitosis, and in the promethaphase, each point was located on opposite sides of the condensed chromatin. The other CDK1 antibody, produced in mouse, stained similar double-points as well as single points.

The position of the CKS2 stained points, their size (0.9 μm) and co-localization with CDK1 suggest that CKS2 localizes at the centrosome. Also, the C
KS2 stained double-points co-localized with γ-tubulin stained centrosomes. The centrosome ranges in diameter from 0.5 to 3 μm, with centrosomes typically 1μm in diameter [145]. CDK1 is known to interact with the centrosome in HeLa cells in all cell cycle phases [146].

In *Drosophila* embryos and HeLa cells the disappearance of CCNB in mitosis starts at the centrosomes [49, 50]. CCNB is degraded by a 26 S proteasome after ubiquitylation by APC/C, which recruits CCNB in a CKS-dependent manner in promethaphase [34]. Also, a CKS2 homolog in *Xenopus* has been proposed to be involved in the activation of the CDK1-CCNB complex at the G2/M transition, which involves dephosphorylation of the complex by CDC25 [38]. The initial dephosphorylation of CDK1-CCNB by CDC25 occurs at the

centrosome [41]. Thus, this may be functions of the centrosomal CKS2, and lend support to the finding that CKS2 proteins are associated with the centrosome.

6.2.4 A mitochondrial function of CKS2 and CDK1

The PLA foci for the interaction of CKS2 and CDK1 with SSBP1 were distributed in the cytoplasm, and in the outskirt of the cytoplasm they sometimes appeared to lie in lanes. Garrido et al [147] reported that SSBP1 localizes in distinct foci within mitochondria in human cells. They showed co-localization of SSBP1 foci with mitochondrial PEO1, mitochondrial transcription factor A (mtTFA) and mtDNA. This strongly suggests that SSBP1 is present in mitochondrial nucleoids [148, 149]. A nucleoid is a region in the mitochondria, which organizes multiple mitochondrial DNA molecules in discrete protein-DNA complexes. The known SSBP1 distribution in cells fits the localization of SSBP1 in the present immunocytochemistry experiments. Thus, the PLA foci produced by interaction of CKS2 and CDK1 with SSBP1 are most likely localized within or in proximity of mitochondrial nucleoids.

SSBP1 binds in a complex with CKS and CDK proteins, and is a substrate for CDK phosphorylation [6]. Knockdown of CKS proteins results in abrogation of SSBP1 phosphorylation, suggesting that the phosphorylation of SSBP1 is dependent on CKS. Further, CKS knockdown leads to compromised mtDNA replication observed as changed mitochondrial morphology and reduced mtDNA content. Thus, CKS proteins and CDK are probably involved in replication of mtDNA by participating in the same pathway as SSBP1 in the cells. This supports the hypothesis that CKS2-SSBP1 and CDK1-SSBP1 interact within or in proximity of mitochondrial nucleoids.

SSBP1 appears to play a role in several other cellular functions [74], for instance in the fission of mitochondria during the morphological dynamics of mitochondria, continuously occurring within cells [150]. Whether mitochondrial CKS2 is involved in these functions, appear still unknown.

6.2.5 CKS2 overexpression and progression of cancer

CKS2 has been found to be overexpressed in a broad spectrum of human malignancies [1, 7, 8, 151, 152]. Based on the previous observations and literature, possible mechanistical links between CKS2 and cancer progression will be discussed.

Initiation, progression and completion of the cell cycle are regulated by various CDKs, and they are therefore critical for cell growth [153]. Aberrant expression of CDK proteins is implicated in many human cancers [154, 155]. CKS2 binds to CDK1 and CDK2, and elevated CKS2 levels have been linked to increased proliferation in normal and malignant lymphoid cells [130]. The stimulating effect of CKS proteins on cell proliferation is assumed to be caused by the association of CKS proteins with CDKs [2, 6, 27]. If CKS2 direct cell cycle progression through interactions with CDK1 and CDK2, one might assume that overexpression of CKS2 lead to increased proliferation. In addition, if CKS2 has a role in transcription of genes, such as *CDK1* and *CCNB*, CKS2 overexpression may cause perturbations of normal gene transcription [2], perhaps with a subsequent increase in their levels.

Furthermore, CKS2 overexpression has been associated with overriding the S-phase checkpoint in cancer cells [27]. When overexpressed, CKS2 kept CDK2 in an active state capable of phosphorylating substrates, even though CDK2 were inhibited by phosphorylations on Tyr15 triggered by activated S-phase checkpoint. The evasion of the S-phase checkpoint constitutes a mechanism whereby cells may continue to replicate DNA under replicative stress, thereby contributing to tumor progression.

Phosphorylation of a CDK2 substrate, RB1, has been associated with centrosome duplification [156]. Moreover, accidental activation of CDK2 with concomitant CCNE overexpression and mutated/lossed TP53 seem to be one possible explanation for centrosome amplification [156-158]. CDK2-CCNE is often deregulated in cancer cells [159]. It is tempting to speculate that CKS2 overexpression in TP53 defective cells may lead to aberrant CDK2 activation and thereby promote centrosome amplification, which constitutes a major mechanism leading to chromosomal instability and aneuploidy [160]. However, for this to occur, high CDK2 activity must be accompanied by CCNE overexpression. A strong correlation between high CCNE and high CKS2 levels have indeed been noted in human breast tumor samples [27]. In these experiments the overexpression of CCNE did not effect on

the protein level of CKS2 in the cells, and overexpression of CKS2 did not affect the levels of CCNE. Thus, the protein levels appear to be independent of each other. It is possible that high CCNE levels must be followed by high CKS2 levels in these cancer cells to achieve full-blown cancerous growth.

Mitochondrial biogenesis may drive tumor growth [161, 162]. This hypothesis is supported by observations that increased mitochondrial biogenesis promotes tumorigenesis, and loss of mtDNA leads to decreased tumorigenesis [163, 164]. A proposed explanation is that increased ATP production, together with enhanced glycolytic gene transcription, provides bioenergetic resources essential for tumor growth [163].

Increased mitochondrial biogenesis is observed in several cancers [165], and is believed to be induced by prolonged hypoxia [72]. The hypoxia can induce HIFs, which in turn increase the expression of oncogenes, such as MYC. MYC promotes the transcription of genes involved in mitochondrial biogenesis [166], which is associated with increased production of ROS [72]. ROS promotes and amplifies genomic damage and instability, provides greater potential for genetic mutations, which leads to cell transformation and malignancy in a vicious vortex.

The interaction of CKS2 with SSBP1 appears essential for mitochondrial replication [6]. Since SSBP1 is involved in mitochondrial biogenesis, one might assume that CKS2 overexpression may lead to increased mitochondrial biogenesis, at least in MYC overexpressed cancers. Interestingly, the *CKS2* gene is a target for the MYC induced transcription [167], and thus may provide a link between MYC activity and CKS2 levels.

A contrasting finding is that many cancers exhibit decreased, not increased, mitochondrial contents [165], and that increased mitochondrial biogenesis can impair carcinogenesis in some cases [168]. Apparently, there are differences in mitochondrial metabolism in various cancers [161], and this may contribute to the heterogeneity in mitochondrial content among them. Possibly, the metabolic state of a tumor is important for the pathogenesis of different tumor subtypes. So far, the understanding of the mitochondrial function of tumors remains far from complete.

6.2.6 Further research

The next step would be to test if CDK2 interacts with SSBP1. PLA is a suitable method to investigate this. In addition, the presence and localization of the PLA foci for CKS2-

CDK1/CDK2/SSBP1 interactions should be explored in clinical patient samples derived from cervical cancers. Then, localization and abundances of the PLA signals can be compared among samples derived from different clinical stages of the cancer and for aggressive and slow-growing cancers. Such experiments could reveal which interactions that are associated with cancer aggressiveness, and whether some of them are particularly active at certain stages of the cancer. If so, one has a good basis for commencing functional analyses of the interactions in order to clarify the mechanism underlying the role of CKS2 in development of an aggressive tumor phenotype.

6.2.7 Conclusions

The fixation method used for preparing cells for immunofluorescence cytochemistry and PLA, has large impacts on the signals observed in the microscope. The fixative should be chosen based on the properties of the antibodies and the cellular compartments studied. For the CKS2-CDK co-localizations and PLA experiments, methanol fixation seems to provide the strongest and most reproducible signals. The signals in CKS2-SSBP1 and CDK1-SSBP1 co-localization experiments appear denser in formalin fixated cells.

CKS2 is localized in foci in the nucleus and cytoplasm in interphase cells and mainly in the cytoplasm in mitotic cells. In the nucleus, large foci probably locate in euchromatin. CKS2 co-localizes with CDK1 and CDK2 in the nucleus and with CDK1, CDK2 and SSBP1 in the cytoplasm. Immunofluorescence cytochemistry also reveals that CKS2 and CDK1 locate at the centrosomes. The PLA experiments suggest that CKS2 interacts with CDK1 in euchromatin. However, it is not apparent whether CKS2 interacts with CDK2 in this area. CKS2 also interacts with CDK1 and CDK2 in the cytoplasm. Some of the cytoplasmic CKS2 foci probably occur within the mitochondria. Interactions of CKS2 with the mitochondrial protein, SSBP1, demonstrate this. Also CDK1 interacts with SSBP1 and this lends support to the hypothesis that SSBP1 interacts with CKS2 in a CDK-dependent manner in the mitochondria.

PLA is a very useful method for studying CKS2 interactions. This method appears to identify weak and transient interactions. Because of strong signal amplification, even single protein interactions are identified, making the method sensitive.

7 Reference List

1. Chen, R., C. Feng, and Y. Xu, *Cyclin-dependent kinase-associated protein Cks2 is associated with bladder cancer progression.* Journal of International Medical Research, 2011. **39**(2): p. 533-540.
2. Martinsson-Ahlzén, H.-S., et al., *Cyclin-dependent kinase-associated proteins Cks1 and Cks2 are essential during early embryogenesis and for cell cycle progression in somatic cells.* Molecular and Cellular Biology, 2008. **28**(18): p. 5698-5709.
3. Demetrick, D.J., H. Zhang, and D.H. Beach, *Chromosomal mapping of the human genes CKS1 to 8q21 and CKS2 to 9q22.* Cytogenetics and Cell Genetics, 1996. **73**(3): p. 250-254.
4. Parge, H.E., et al., *Human CksHs2 atomic structure: a role for its hexameric assembly in cell cycle control.* American Association for the Advancement of Science, 1993. **262**(5132): p. 387-395.
5. Richardson, H.E., et al., *Human cDNAs encoding homologs of the small p34Cdc28/Cdc2-associated protein of Saccharomyces cerevisiae and Schizosaccharomyces pombe.* Genes & Development, 1990. **4**(8): p. 1332-1344.
6. Radulovic, M., et al., *CKS protein protect motochondrial genome integrity by interacting with mitochondrial single-stranded DNA-binding protein.* Molecular & Cellular Proteomics, 2010. **9**(1): p. 145-152.
7. Tanaka, F., et al., *Clinicopathological and biological significance of CDC28 protein kinase regulatory subunit 2 overexpression in human gastric cancer.* International Journal of Oncology, 2011. **39**: p. 361-372.
8. Lyng, H., et al., *Gene expression and copy numbers associated with metastatic phenotypes of uterine cervical cancer.* BMC Genomics, 2006. **7**(268).
9. Jung, Y., et al., *Clinical validation of colorectal cancer biomarkers identified from bioinformatics analysis of public expression data.* Clinical Cancer Research, 2011. **17**(4): p. 700-709.
10. Shen, D.Y., et al., *Clinical significance and expression of cyclin kinase subunits 1 and 2 in hepatocellular carcinoma.* Liver International, 2010. **30**(1): p. 119-125.
11. Martha, V.S., et al., *Constructing a robust protein-protein interaction network by integrating multiple public databases.* BMC Bioinformatics, 2011. **12**(10): p. 7.
12. Chu, L.H. and B.S. Chen, *Construction of a cancer-perturbed protein-protein interaction network for discovery of apoptosis drug targets.* BMC Systems Biology, 2008. **30**(2): p. 56.
13. Helmuth, J.A., G. Paul, and I.F. Sbalzarini, *Beyond co-localization: inferring spatial interactions between sub-cellular structures from microscopy images.* BMC Bioinformatics, 2010. **11**: p. 372.
14. Leuchowius, K.J., I. Weibrecht, and O. Söderberg *In situ proximity ligation assay for microscopy and flow cytometry*. Current Protocols in Cytometry, 2011. **9**, 9.36-9.36.
15. Landegren, U., et al., *Molecular tools for a molecular medicine: analyzing genes, transcripts and proteins using padlock and proximity probes.* Journal of Molecular Recognition, 2004. **17**(3): p. 194-197.
16. Donaldson, J.G. *Immunofluorescence Staining.* Current Protocols in Cell Biology., 2001. 4.3.1-4.3.6.
17. Olink Bioscience. *Duolink II fluorescence user manual*. [cited 25.01. 2012]; Available from:

http://www.olink.com/sites/default/files/files/0650%20v2.2%20Duolink%20II%20Fluorescence%20User%20Manual.pdf.
18. Melan, M.A., *Overview of cell fixation and permeabilization.* Methods in Molecular Biology, 1994. **34**: p. 55-66.
19. Campbell, N.A. and J.B. Reece, *Biology*. 7th ed2005, San Francisco: Benjamin Cummings-Pearson Education, Inc.
20. Vermeulen, K., D.R.V. Bockstaele, and Z.N. Berneman, *The cell cycle: a review of regualtion, deregulation and therapeutic targets in cancer.* Cell Proliferation, 2003. **36**(3): p. 131-149.
21. Carr, A.M., et al., *The chk1 pathway is required to prevent mitosis following cell-cycle arrest at 'start'.* Current Biology, 1995. **5**(10): p. 1179-1190.
22. Alberts, B., et al., *Essential cell biology*. 2nd ed 2004, New York: Garland Science.
23. Malumbres, M. and M. Barbacid, *Mammalian cyclin-dependent kinases.* Trends in Biochemical Sciences, 2005. **30**(11): p. 630-641.
24. Aleem, E., H. Kiyokawa, and P. Kaldis, *Cdc2-cyclin E complexes regulate the G1/S phase transition.* Nature Cell Biology, 2005. **7**(8): p. 831-836.
25. Santamaría, D., et al., *Cdk1 is sufficient to drive the mammalian cell cycle.* Nature, 2007. **448**(7155): p. 811-815.
26. Kim, S. and H. Yu, *Mutual regulation between the spindle checkpoint and APC/C.* Seminars in Cell and Developmental Biology, 2011. **22**(6): p. 551-558.
27. Liberal, V., et al., *Cyclin-dependent kinase subunit (cks) 1 or Cks2 overexpression overrides the DNA damage response barrier triggered by activated oncoproteins.* Proceedings of the National Academy of Sciences of the United States of America, 2011: p. 1-6.
28. Wong, Y.-F., et al., *Genome-wide gene expression profiling of cervical cancer in Hong Kong women by oligonucleotide microarray.* International Journal of Cancer, 2006. **118**(10): p. 2461-2469.
29. Donovan, P.J. and S.I. Reed, *Germline exclusion of Cks1 in the mouse reveals a metaphase I role for Cks proteins in male and female meiosis.* Cell Cycle, 2003. **2**(4): p. 275-276.
30. Seeliger, M.A., et al., *Folding and association of the human cell cycle regulatory proteins ckshs1 and ckshs2.* Biochemistry, 2002. **41**(4): p. 1202-1210.
31. Bourne, Y., et al., *Crystal structure and mutational analysis of the human CDK2 kinase complex with cell cycle-regulatory protein CksHs1.* Cell, 1996. **84**(6): p. 863-874.
32. Rousseau, F., et al., *Stability and folding of the cell cycle regulatory protein, p13(suc1).* Journal of Molecular Biology, 1998. **284**(2): p. 503-519.
33. Watson, M.A., et al., *A mutation in the human cyclin-dependent kinase interacting protein, cksHs2, interferes with cyclin-dependent kinase binding and biological function, but preserves protein structure and assembly.* Journal of Molecular Biology, 1996. **261**(5): p. 646-657.
34. Zon, W.v., et al., *The APC/C recruits cyclin B1-Cdk1-Cks in prometaphase before D box recognition to control mitotic exit.* The journal of Cell Biology, 2010. **190**(4): p. 587-602.
35. Pines, J., *Cell cycle: reaching a role for cks proteins.* Current Biology, 1996. **6**(11): p. 1399-1402.
36. Egan, E.A. and M.J. Solomon, *Cyclin-stimulated binding of cks proteins to cyclin-dependent kinases.* Molecular and Cellular Biology, 1998. **18**(7): p. 3659-3667.

37. Ruiz, E.J., M. Vilar, and A.R. Nebreda, *A two-step inactivation mechanism of Myt1 ensures CDK1/cyclin B activation and meiosis entry.* Current Biology, 2010. **20**(8): p. 717-723.
38. Patra, D., et al., *The Xenopus Suc1/Cks protein promotes the phosphorylation of G2/M regulators.* The Journal of Biological Chemistry, 1999. **274**(52): p. 36839-36842.
39. Moreno, S., J. Hayles, and P. Nurse, *Regulation of p34^{cdc2} protein kinase during mitosis.* Cell, 1989. **58**: p. 361-372.
40. Petra, D. and W. Dunphy, *Xe-p9, a Xenopus suc1/cks homolog, has multiple essential roles in cell cycle control.* Genes & Development, 1996. **10**(12): p. 1503-1515.
41. Cazales, M., et al., *CDC25B phosphorylation by Aurora-A occurs at the G2/M transition and is inhibited by DNA damage.* Cell Cycle, 2005. **4**(9): p. 1233-1238.
42. Wang, Y., et al., *Centrosome-associated regulators of the G2/M checkpoint as targets for cancer therapy.* Molecular Cancer, 2009. **8**: p. 8.
43. Wolthuis, R., et al., *Cdc20 and Cks direct the spindle checkpoint-independent destruction of cyclin A.* Molecular Cell, 2008. **30**(3): p. 290-302.
44. Kraft, C., et al., *Mitotic regulation of the human anaphase-promoting complex by phosphorylation.* The EMBO Journal, 2003. **22**(24): p. 6598-6609.
45. Hershko, A., *Mechanisms and regulation of the degradation of cyclin B.* Philosophical Transactions of The Royal Society, 1999. **354**(1389): p. 1571-1575.
46. Golan, A., Y. Yudkovsky, and A. Hershko, *The cyclin-ubiquitin ligase activity of cyclosome/APC is jointly activated by protein kinases Cdk1-cyclin B and Plk.* The Journal of Biological Chemistry, 2002. **277**(18): p. 15552-15557.
47. Hagting, A., et al., *Human securin proteolysis is controlled by the spindle checkpoint and reveals when the APC/C switches from activation by Cdc20 to Cdh1.* The journal of Cell Biology, 2002. **157**(7): p. 1125-1137.
48. Deveraux, Q., et al., *Inhibition of ubiquitin-mediated proteolysis by the Arabidopsis 26 S protease subunit S5a.* The Journal of Biological Chemistry, 1995. **270**(50): p. 29660-29663.
49. Wakefield, J.G., J.-y. Huang, and J.W. Raff, *Centrosomes have a role in regulating the destruction of cyclin B in early Drosophila embryos.* Current Biology, 2000. **10**(21): p. 1367-1370.
50. Clute, P. and J. Pines, *Temporal and spatial control of cyclin B1 destruction in metaphase.* Nature Cell Biology, 1999. **1**(2): p. 82-87.
51. Elzen, N.d. and J. Pines, *Cyclin A is destroyed in prometaphase and can delay chromosome alignment and anaphase.* The journal of Cell Biology, 2001. **153**(1): p. 121-136.
52. Fiore, B.D. and J. Pines, *How cyclin A destruction escapes the spindle assembly checkpoint.* The journal of Cell Biology, 2010. **190**(4): p. 501-509.
53. Schultz, R.A., et al., *Differential expression of mitochondrial DNA replication factors in mammalian tissues.* Journal of Biological Chemistry, 1998. **273**(6): p. 3447-3451.
54. Cancer Registry of Norway. *Cancer in Norway 2009*. Cancer incidence, mortality, survival and prevalence in Norway 2011.
55. Kristensen, G.B. *Livmorhalskreft*. 09.12.2010 [cited 13.02 2012]; Available from: http://www.oncolex.no/GYN/Diagnoser/Livmorhals.aspx.
56. Schiffman, M.H., et al., *Epidemiologic evidence showing that human papillomavirus infection causes most cervical intraepithelial neoplasia.* Journal of the National Cancer Institute, 1993. **85**(12): p. 958-964.
57. Kristensen, G.B. *Årsaker*. 09.01.2012 [cited 13.02 2013]; Available from: http://www.oncolex.no/GYN/Diagnoser/Livmorhals/Bakgrunn/Arsaker.aspx.

58. Carter, J., Z. Ding, and B. Rose, *HPV infection and cervical disease: a review.* The Australian and New Zealand Journal of Obstetrics and Gynaecology, 2011. **51**(2): p. 103-108.
59. Echelman, D. and S. Feldman, *Management of cervical precancers: a global perspective.* Hematology/Oncology Clinics of North America, 2012. **26**(1): p. 31-44.
60. Cox, J.T., *Epidemiology of cervical intraepithelial neoplasia: the role of human papillomavirus.* Baillière's Clinical Obstetrics and Gynaecology, 1995. **9**(1): p. 1-37.
61. Moody, C.A. and L.A. Laimins, *Human papillomavirus oncoproteins: pathways to transformation.* Nature Reviews Cancer, 2010. **10**: p. 550-560.
62. Carew, J.S. and P. Huang, *Mitochondrial defects in cancer.* Molecular Cancer, 2002. **1**: p. 9-9.
63. Heo, J.-M. and J. Rutter, *Ubiquitin-dependent mitochondrial protein degradation.* International Journal of Biochemistry & Cell Biology, 2011. **43**(10): p. 1422-1426.
64. Chatterjee, A., S. Dasgupta, and D. Sidransky, *Mitochondrial subversion in cancer.* Cancer Prevention Research, 2011. **4**(5): p. 638-654.
65. Lindahl, M., A. Mata-Cabana, and T. Kieselbach, *The disulfide proteome and other reactive cysteine proteomes: analysis and functional significance.* Antioxidants & Redox Signalling, 2011. **14**(12): p. 2581-2642.
66. McCord, J.M. and I. Fridovich, *Superoxide dismutase. An enzymic function for erythrocuprein (hemocuprein).* Journal of Biological Chemistry, 1969. **244**(22): p. 6049-6055.
67. Liu, P. and B. Demple, *DNA repair in mammalian mitochondria: much more than we thought?* Environmental and Molecular Mutagenesis, 2010. **51**(5): p. 417-426.
68. Boesch, P., et al., *DNA repair in organelles: pathways, organization, regulation, relevance in disease and aging.* Biochimica et Biophysica Acta, 2010: p. 186-200.
69. Souza-Pinto, N.C.d., et al., *Mitochondrial DNA, base excision repair and neurodegeneration.* DNA Repair, 2008. **7**(7): p. 1098-1109.
70. Nakagawa, Y., et al., *A new mitochondrial DNA mutation associated with non-insulin-dependent diabetes mellitus.* Biochemical and Biophysical Research Communications, 1995. **209**(2): p. 664-668.
71. Abdin, A.A. and N.I. Sarhan, *Intervention of mitochondrial dysfunction-oxidative stress-dependent apoptosis as a possible neuroprotective mechanism of α-lipoic acid against rotenone-induced parkinsonism and L-dopa toxicity.* Neuroscience Research, 2011. **71**(4): p. 387-395.
72. Ralph, S.J., et al., *The causes of cancer revisited: "Mitochondrial malignancy" and ROS-induced oncogenic transformation - Why mitochondria are targets for cancer therapy.* Molecular Aspects of Medicine, 2010. **31**(2): p. 145-170.
73. Franovic, A., et al., *Human cancers converge at the HIF-2α oncogenic axis.* Proceedings of the National Academy of Sciences of the United States of America, 2009. **106**(50): p. 21306-21311.
74. Wong, T.S., et al., *Physical and functional interactions between human mitochondrial single-stranded DNA-binding protein and tumour suppressor p53.* Nucleic Acids Research, 2009. **37**(2): p. 568-581.
75. Broderick, S., et al., *Genome stability and human diseases*, in *Eukaryotic single-stranded DNA binding proteins: central factors in genome stability*, H.-P. Nasheuer, Editor 2010, Springer Science+Business Media B.V.: Dordrecht.
76. Korhonen, J.A., M. Gaspari, and M. Falkenberg, *TWINKLE Has 5′ -> 3′ DNA helicase activity and is specifically stimulated by mitochondrial single-stranded DNA-binding protein.* Journal of Biological Chemistry, 2003. **278**(49): p. 48627-48632.

77. Genuario, R. and T.W. Wong, *Stimulation of DNA polymerase gamma by a mitochondrial single-strand DNA binding protein.* Cellular & Molecular Biology Research, 1993. **39**(7): p. 625-634.
78. Farr, C.L., et al., *Physiological and biochemical defects in functional interactions of mitochondrial DNA polymerase and DNA-binding mutants of single-stranded DNA-binding protein.* Journal of Biological Chemistry, 2004. **279**(17): p. 17047-17053.
79. Ruhanen, H., et al., *Mitochondrial single-stranded DNA binding protein is required for maintenance of mitochondrial DNA and 7S DNA but is not required for mitochondrial nucleoid organisation.* Biochimica et Biophysica Acta, 2010. **1803**(8): p. 931-939.
80. Kasiviswanathan, R., T.R. Collins, and W.C. Copeland, *The interface of transcription and DNA replication in the mitochondria.* Biochimica et Biophysica Acta, 2011.
81. Takamatsu, C., et al., *Regulation of mitochondrial D-loops by transcription factor A and single-stranded DNA-binding protein.* EMBO reports, 2002. **3**(5): p. 451-456.
82. Strachan, T. and A.P. Reas, *Human Molecular Genetics*. 2nd ed1999, New York: Bios Scientific Publishers.
83. Steen, K.W., et al., *mtSSB may sequester UNG1 at mitochondrial ssDNA and delay uracil processing until the dsDNA conformation is restored.* DNA Repair, 2011: p. 82-91.
84. Mignotte, B., M. Barat, and J.C. Mounolou, *Characterization of a mitochondrial protein binding to single-stranded DNA.* Nucleic Acids Research, 1985. **13**(5): p. 1703-1716.
85. Chen, C.-H. and Y.-C. Cheng, *The role of cytoplasmic deoxycytidine kinase in the mitochondrial effects of the anti-human immunodeficiency virus compund, 2',3'-dideoxycytidine.* The Journal of Biological Chemistry, 1991. **267**(5): p. 2856-2859.
86. Achanta, G., et al., *Novel role of p53 in maintaining mitochondrial genetic stability through interaction with DNA Pol gamma.* The EMBO Journal, 2005. **24**(19): p. 3482-3492.
87. Kamenisch, Y., et al., *Proteins of nucleotide and base excision repair pathways interact in mitochondria to protect from loss of subcutaneous fat, a hallmark of aging.* The Journal of Experimental Medicine, 2010. **207**(2): p. 379-390.
88. Visnes, T., et al., *Uracil in DNA and its processing by different DNA glycosylases.* Philosophical Transactions of the Royal Society, 2009. **364**(1517): p. 563-568.
89. Bohr, V.A., T. Stevnsner, and N C de Souza-Pinto, *Mitochondial DNA repair of oxidative damage in mammalian cells.* Gene, 2002. **286**(1): p. 127-134.
90. Behlke, M.A., et al. *Fluorescence and fluorescence applications*. 2005; Available from: http://biophysics.idtdna.com/pdf/Fluorescence_and_Fluorescence_Applications.pdf.
91. Johnson, I. and M.T.Z. Spence, *The molecular probes handbook. A Guide to fluorescent probes and labeling technologies*, I. Johnson and M. Spence, Editors. 2010, Life Technologies Corporation.
92. Herman, B. *Fluorescence microscopy*. Current Protocols in Cell Biology, 1998. **48**, 4.2.1-4.2.10.
93. Life technologies. *Fluorescence spectraviewer*. Available from: http://www.invitrogen.com/site/us/en/home/support/Research-Tools/Fluorescence-SpectraViewer.html.
94. Parham, P., *The immune system*. 3rd ed2009, New York: Garland Science.
95. Thermo Scientific. *Choosing a secondary antibody: a guide to fragment specificity*. 2007 [cited 20.05 2012]; Available from: http://www.piercenet.com/files/TR0059-Choose-second-Ab.pdf.

96. Thermo Scientific. *Secondary antibodies as detection probes*. [cited 16.05. 2011]; Available from: http://www.piercenet.com/browse.cfm?fldID=4A93DDB6-5056-8A76-4E38-E54A3C46D750.
97. Lichtman, J.W. and J.-A. Conchello, *Fluorescence microscopy.* Nature Methods, 2005. **2**(12): p. 910-919.
98. Davidson, M.W. *Configuring a microscope for Köhler illimunation*. [cited 08.02. 2012]; Available from: http://zeiss-campus.magnet.fsu.edu/articles/basics/kohler.html.
99. Davidson, M.W. *Fundamentals of metal halide arc lamp*. [cited 08.02. 2012]; Available from: http://zeiss-campus.magnet.fsu.edu/articles/lightsources/metalhalide.html.
100. Kapitza, H.G., *Microscopy from the very beginning*, S. Lichtenberg, Editor 1997, Carl Zeiss: Jena.
101. Rost, F.W.D., *Fluorescence microscopy*, F.W.D. Rost, Editor 1992, Cambridge University Press: Cambridge.
102. Gines, T.B. and M.W. Davidson. *Structured illumination: ZEISS ApoTome*. [cited 04.02. 2012]; Available from: http://zeiss-campus.magnet.fsu.edu/tutorials/opticalsectioning/apotome/index.html.
103. Söderberg, O., et al., *Direct observation of individual endogenous protein complexes in situ by proximity ligation.* Nature Methods, 2006. **3**(12): p. 995-1000.
104. Olink Bioscience. *Technology related questions*. [cited 25.1. 2012]; Available from: http://www.olink.com/sites/default/files/files/FAQ_Duolink_Technology%20related.pdf.
105. Llewellyn, B. *Introduction to fixation*. 2009 [cited 20.12. 2011]; Available from: http://stainsfile.info/StainsFile/prepare/fix/fixintro.htm.
106. Rogers, S. *Cell biology applications of fluorescence microscopy*. [cited 20.12. 2011]; Available from: http://www.ihcworld.com/_protocols/immunofluorescence/specimen_preparation1.htm.
107. Burry, R.W., *Immunocytochemistry: A Practical Guide for Biomedicinal Research*, 2010, Springer Science + Business Media, LLC: New York.
108. Price, R.L. and W.G. Jerome, *Basic confocal microscopy*, R.L. Price and W.G. Jerome, Editors. 2011, Springer Science + Business Media, LLC: New York.
109. IHC World. *Immunocytochemistry methods, techniques and protocols*. [cited 20.12. 2011]; Available from: http://www.ihcworld.com/_protocols/general_ICC/fixation.htm.
110. Opas, M., *Fluorescence tracing of intracellular proteins.* Biotechnic & Histochemistry, 1999. **74**(6): p. 294-310.
111. Sánchez-Ferrer, A., R. Bru, and F. García-Carmona, *Phase separation of biomolecules in polyoxyethylene glycol nonionic detergents.* Critical Reviews in Biochemistry and Molecular Biology, 1994. **29**(4): p. 275-313.
112. Masters, J.R., *HeLa cells 50 years on: the good, the bad and the ugly.* Nature Reviews Cancer, 2002. **2**(4): p. 315-319.
113. Ugarte, D.A.D., et al., *Comparison of multi-lineage cells from human adipose tissue and bone marrow.* Cells Tissues Organs, 2003. **174**(3): p. 101-109.
114. ATCC. *Product description*. [cited 20.01. 2012]; Available from: http://www.atcc.org/ATCCAdvancedCatalogSearch/ProductDetails/tabid/452/Default.aspx?ATCCNum=CCL-2&Template=cellBiology.
115. Bottone, M.G., et al., *Multiple effects of paclitaxel are modulated by a high c-myc amplification level.* Experimental Cell Research, 2003. **290**(1): p. 49-59.

116. Graham, D.Y. and M.K. Estes, *Proteolytic enhancement of rotavirus infectivity: Biological mechanisms.* Virology, 1979. **101**(2): p. 432-439.
117. Graham, M.D., *The coulter principle: foundation of an industry.* The Journal of the Association for Laboratory Automation, 2003. **8**(6): p. 72-81.
118. Life technologies. *ProLong® gold antifade reagent*. [cited 25.01. 2012]; Available from: http://www.invitrogen.com/site/us/en/home/brands/Molecular-Probes/Key-Molecular-Probes-Products/ProLong-Antifades-Brand-Page.html.
119. Zeiss. *Fluorescence dye and filter database*. [cited 08.02. 2012]; Available from: https://www.micro-shop.zeiss.com/us/us_en/spektral.php?f=fa.
120. Abcam. *Fixation and permeabilization in IHC/ICC*. [cited 04.03. 2012]; Available from: http://www.abcam.com/ps/pdf/protocols/fixation_permeabilization.pdf.
121. Duolink. *In-cell Co-IP for visualization of protein interactions in situ*. [cited 03.03. 2012]; Available from: http://www.olink.com/sites/default/files/files/0876%20v1.2%20Duolink%20Application%20Note.pdf.
122. Godin, F., et al., *A fraction of neurofibromin interacts with PML bodies in the nucleus of the CCF astrocytoma cell line.* Biochemical and Biophysical Research Communications, 2012. **418**(4): p. 689-694.
123. Schäferling, M. and S. Nagl, *Förster resonance energy transfer methods for quantification of protein-protein interactions on microarrays.* Methods in Molecular Biology, 2011. **723**: p. 303-320.
124. Leuchowius, K.J., et al., *Flow cytometric in situ proximity ligation analyses of protein interactions and post-translational modification of the epidermal growth factor receptor family.* Cytometry Part A, 2009. **75**(10): p. 833-839.
125. Söderberg, O., et al., *Characterizing proteins and their interactions in cells and tissues using the in situ proximity ligation assay.* Methods, 2008. **45**(3): p. 227-232.
126. Hoetelmans, R.W., et al., *Effects of acetone, methanol, or paraformaldehyde on cellular structure, visualized by reflection contrast microscopy and transmission and scanning electron microscopy.* Applied Immunohistochemistry & Molecular Morphology, 2001. **9**(4): p. 346-351.
127. Mirzaei, M., *Deteksjon og lokalisasjon av CKS2-proteinet i ulike cellesyklusfaser i livmorhalskarsinomer*, in *Farmasøytisk insitutt*2008, University of Oslo: Oslo.
128. Caspersen, E.F., *Cell cycle distribution and CKS2 protein content in cervical carcinoma cell lines after exposure to ionizing radiation*, in *School of Pharmacy*2006, University of Oslo: Oslo.
129. Volpe, P. and T. Eremenko, *A method for measuring cell cycle phases in suspension cultures.* Methods in Cell Biology, 1973. **6**: p. 113-126.
130. Urbanowicz-Kachnowicz, I., et al., *ckshs expression is linked to cell proliferation in normal and malignant human lymphoid cells.* International Journal of Cancer, 1999. **82**(1): p. 98-104.
131. Booher, R.N., et al., *The fission yeast cdc2/cdc13/suc1 protein kinase: regulation of catalytic activity and nuclear localization.* Cell, 1989. **58**(3): p. 485-497.
132. Ducommun, B., P. Brambilla, and G. Draetta, *Mutations a sites involved in suc1 binding inactivate cdc2.* Molecular and Cellular Biology, 1991. **11**(12): p. 6177-6184.
133. Obaya, A.J. and J.M. Sedivy, *Regulation of cyclin-Cdk activity in mammalian cells.* Cellular and Molecular Life Sciences, 2002. **59**(1): p. 126-142.
134. Moore, J.D., et al., *Nuclear import of cdk/cyclin complexes: identification of distinct mechanisms for import of cdk2/cyclin e and cdc2/cyclin b1.* The journal of Cell Biology, 1999. **144**(2): p. 213-224.

135. Gavet, O. and J. Pines, *Activation of cyclin B1–Cdk1 synchronizes events in the nucleus and the cytoplasm at mitosis.* The journal of Cell Biology, 2010. **189**(2): p. 247-259.
136. Shimi, T., et al., *The A- and B-type nuclear lamin networks: microdomains involved in chromatin organization and transcription.* Genes & Development, 2008. **22**(24): p. 3409-3421.
137. Bancaud, A., et al., *Molecular crowding affects diffusion and binding of nuclear proteins in heterochromatin and reveals the fractal organization of chromatin.* The EMBO Journal, 2009. **28**(24): p. 3785-3798.
138. Wheeler, L.L. and L.C. Altenburg, *Hoechst 33258 banding of Drosophila nasutoides metaphase chromosomes.* Chromosoma, 1977. **62**(4): p. 351-360.
139. Lee, J.-H. and D.G. Skalnik, *CpG-binding Protein Is a Nuclear Matrix- and Euchromatin-associated Protein Localized to Nuclear Speckles Containing Human Trithorax.* The Journal of Biological Chemistry, 2002. **277**(44): p. 42259-42267.
140. Görisch, S.M., et al., *Histone acetylation increases chromatin accessibility.* Journal of Cell Science, 2005. **118**(24): p. 5825-5834.
141. Schweizer, D., *DAPI fluorescence of plant chromosomes prestained with actinomycin D.* Experimental Cell Research, 1976. **102**(2): p. 408-413.
142. Kwon, S.H. and J.L. Workman, *The changing faces of HP1: From heterochromatin formation and gene silencing to euchromatic gene expression: HP1 acts as a positive regulator of transcription.* BioEssays, 2011. **33**(4): p. 280-289.
143. Yu, V.P.C.C., et al., *A kinase-independent function of cks1 and cdk1 in regulation of transcription.* Molecular Cell, 2005. **17**(1): p. 145-151.
144. Chaves, S., et al., *Cks1, cdk1, and the 19 S proteasome collaborate to regulate gene induction-dependent nucleosome eviction in yeast.* Molecular and Cellular Biology, 2010. **30**(22): p. 5284-5294.
145. Lukasiewicz, K.B. and W.L. Lingle, *Aurora A, centrosome structure, and centrosome cycle.* Environmental and Molecular Mutagenesis, 2009. **50**(8): p. 602-619.
146. Pockwinse, S.M., et al., *Cell cycle independent interaction of CDC2 with the centrosome, which is associated with the nuclear matrix-intermediate filament scaffold.* Proceedings of the National Academy of Sciences of the United States of America, 1997. **94**(7): p. 3022-3027.
147. Garrido, N., et al., *Composition and dynamics of human mitochondrial nucleoids.* Molecular Biology of the Cell, 2003. **14**(4): p. 1583-1596.
148. Bogenhagen, D.F., et al., *Protein components of mitochondrial DNA nucleoids in higher eukaryotes.* Molecular & Cellular Proteomics, 2003. **2**(11): p. 1205-1216.
149. Sumitani, M., et al., *Association of a novel mitochondrial protein M19 with mitochondrial nucleoids.* The Journal of Biochemistry, 2009. **146**(5): p. 725-732.
150. Arakaki, N., et al., *Regulation of mitochondrial morphology and cell survival by Mitogenin I and mitochondrial single-stranded DNA binding protein.* Biochimica et Biophysica Acta, 2006. **1760**(9): p. 1364-1372.
151. Menghi, F., et al., *DNA microarray analysis identifies CKS2 and LEPR as potential markers of meningioma recurrence.* The Oncologist, 2011. **16**(10): p. 1440-1450.
152. Jain, S., et al., *Molecular genetics of hepatocellular neoplasia.* American Journal of Translational Research, 2010. **2**(1): p. 105-118.
153. Fischer, P.M. and D.P. Lane, *Inhibitors of cyclin-dependent kinases as anti-cancer therapeutics.* Current Medicinal Chemistry, 2000. **7**(12): p. 1213-1245.
154. Deshpande, A., P. Sicinski, and P.W. Hinds, *Cyclins and cdks in development and cancer: a perspective.* Oncogene, 2005. **24**(17): p. 2909-2915.

155. Malumbres, M. and M. Barbacid, *Cell cycle, CDKs and cancer: a changing paradigm.* Nature Reviews Cancer, 2008. **9**(3): p. 153-166.
156. Fukasawa, K., *Centrosome amplification, chromosome instability and cancer development.* Cancer Letters, 2005. **230**(1): p. 6-19.
157. Cai, Y., et al., *Cyclin E overexpression and centrosome amplification in squamous cell carcinoma of oral cavity.* Zhonghua Bing Li Xue Za Zhi, 2007. **36**(6): p. 375-378.
158. Weroha, S.J., et al., *Specific overexpression of cyclin E·CDK2 in early preinvasive and primary breast tumors in female ACI rats induced by estrogen.* Hormones and Cancer, 2010. **1**(1): p. 34-43.
159. Hwang, H.C. and B.E. Clurman, *Cyclin E in normal and neoplastic cell cycles.* Oncogene, 2005. **24**(17): p. 2776-2786.
160. Chan, J.Y., *A clinical overview of centrosome amplification in human cancers.* International Journal of Biological Sciences, 2011. **7**(8): p. 1122-1144.
161. Martinez-Outschoorn, U.E., et al., *Mitochondrial biogenesis drives tumor cell proliferation.* The American Journal of Pathology, 2011. **178**(5): p. 1949-1952.
162. Shapovalov, Y., et al., *Mitochondrial dysfunction in cancer cells due to aberrant mitochondrial replication.* The Journal of Biological Chemistry, 2011. **286**(25): p. 22331-22338.
163. Samper, E., et al., *Increase in mitochondrial biogenesis, oxidative stress, and glycolysis in murine lymphomas.* Free Radical Biology & Medicine, 2009. **46**(3): p. 387-396.
164. Yu, M., et al., *Depletion of mitochondrial DNA by ethidium bromide treatment inhibits the proliferation and tumorigenesis of T47D human breast cancer cells.* Toxicology Letters, 2007. **170**(1): p. 83-93.
165. Bai, R.K., et al., *Mitochondrial DNA content varies with pathological characteristics of breast cancer.* Journal of Oncology, 2011. **2011**: p. 496189-496189.
166. Li, F., et al., *Myc stimulates nuclearly encoded mitochondrial genes and mitochondrial biogenesis.* Molecular and Cellular Biology, 2005. **25**(14): p. 6225-6234.
167. Guo, Q.M., et al., *Identification of c-myc responsive genes using rat cDNA microarray.* Cancer Research, 2000. **60**(21): p. 5922-5928.
168. Wang, X. and C.T. Moraes, *Increases in mitochondrial biogenesis impair carcinogenesis at multiple levels.* Molecular Oncology, 2011. **5**(5): p. 399-409.

Appendices

Appendix 1: Cell splitting protocol

Appendix 2: Coulter counter protocol

Appendix 3: Immunocytochemistry protocol

Appendix 4: *In situ* proximity ligation assay protocol

Appendix 5: Detergent buffer formula

Appendix 6: Zeiss Imager.z1 fluorescence microscope protocol

Appendix 7: Immunocytochemistry signal from formalin fixated cells

Appendix 8: Controls for the immunocytochemistry and PLA experiments

Appendix 9: Reagents used in the experiments

Appendix 1

Cell splitting protocol

1. Fresh growth medium, PBS and trypsin were warmed up to 37 °C in a water bath for at least 30 minutes.
2. Wipe down the LAF bench and equipment with 70 % ethanol.
3. Examine the cells under the microscope and determine what the split ratio should be.
4. Remove the old DMEM + GlutaMAX medium using a 10 mL stripette
5. Wash the cell surface with 5 mL PBS to eliminate remnants from the growth medium
6. Add 1 mL trypsin to the T75 cell bottle. Gently rotate the bottle to ensure that the entire cell surface is covered
7. Incubate for 5 minutes at 37 °C
8. Prepare a new bottle by adding 10 mL fresh DMEM + GlutaMAX medium
9. Remove the bottle from the incubator and make sure that the cells are detached
10. Add DMEM + GlutaMAX, usually 8-9 mL (1:9 and 1:10 dilution respectively) to the old cell bottle and mix
11. Transfer 1 mL from the old T75 to the new T75 bottle and mix

Appendix 2

Coulter counter protocol

1. Turn on the coulter counter
2. Lower the sample platform and insert a small cup of isotone water and submerge the aperture
3. Flush the instrument by pushing the functions button, use "<" and ">" to flush aperture can be visualized in the display and then push start/stop button
4. Repeat the flushing step
5. Dilute 100 µl cell suspension with 10 000 µL isotone water (1:100)
6. Adjust the dilution factor by pushing: output→ 100
7. Push set-up and change the upper size and lower size of the particles the coulter counter should count
8. Choose lower size = 8 µm and upper size = 24 µm
9. Stir in the cup of cells using a pipette tip, ensuring that the cells have not sunk to the bottom
10. Lower the sample platform, remove the isotone water , place the sample in the slot and submerge the aperture in the solution
11. Push the start/stop button to count cells.
12. Replace the sample with Coulter Clenz® cleaning agent and flush the aperture by pushing functions and then the start/stop button
13. Turn off the coulter counter and dispose the sample

Appendix 3

Immunocytochemistry protocol

1. Seed adherent cells on coverslips

a) Place 3-4 autoclaved coverslips (12 mm) suitable for fluorescence microscopy (No. 1.5) in a 35 mm tissue culture dish
b) Add 2.5 mL cell suspension containing 60 000 cells/mL over the coverslips
c) Grow the cells overnight at 37 °C in a CO_2 incubator
d) Wash the cells carefully with warm (37 °C) PBS prior to fixation. Do not let the cells dry out.

2. Fixation/permeabilization

e) Fix the cells with one of the two methods:
   i. 2 mL cold methanol (-20°C) for 10 minutes and wash three times with PBS. Leave the cells in PBS for 2-3 minutes for rehydration
   ii. 1 mL fresh neutral buffered 10 % formalin solution (room temperature) for 10 minutes, and wash three times with PBS.
f) Place the coverslips on parafilm in a humidified chamber
g) Wash each coverslip wih 1 mL PBS by pipetting and aspirating at the same time
h) Block and permeabilize cells in PBS-AT (1% BSA, 0.5 % Triton-X100 in PBS) for 15 minutes at room temperature

3. Antibody incubations and mounting

i) Dilute the primary antibodies in PBS-AT according to table 1. Add 40 µL antibody solution to each coverslip (12 mm diameter) and incubate for 2 hours at room temperature
j) Wash each coverslip with 1 mL PBS (pipetting and aspiration)
k) Dilute the fluorophore-conjugated secondary antibodies in PBS-AT according to table 1 and apply 40 µL to each coverslip. Incubate with secondary antibody for 40-60 minutes at room temperature, away from light
l) Wash each coverslip with 1 mL PBS (pipetting and aspiration)
m) Counterstain DNA with Hoechst 33258 (0,6 µg/mL in PBS) for 1-2 minutes
n) Wash each coverslip with 1 mL PBS (pipetting and aspiration)
o) Rinse coverslips to remove PBS by dipping coverslips 10 x into ddH_2O
p) Briefly dry coverslips and add a drop of mounting medium (ProLong Gold) on the slide. Place each coverslip on the mounting medium, with the cell-side facing down. Try to avoid getting air bubbles under the coverslip
q) Visualize the cells using a fluorescence microscope with appropriate filters

The slides can be stored at -20°C in the dark

Table 1. The dilution factors and concentrations of the various antibodies for immunocytochemistry

	Primary antibodies					Secondary antibodies		DNA stain
Antibody	Mouse anti-CKS2	Mouse anti-CDK1	Rabbit anti-SSBP1	Rabbit anti-CDK1	Rabbit anti-CDK2	Donkey anti-mouse 549	Donkey anti-rabbit 488	Hoechst 33258
Antibody concentration prior to dilution	0,5 mg/mL	0.2 mg/mL	0.12 mg/mL	1 mg/mL	0.2 mg/mL	1.4 mg/mL	1.5 mg/mL	0.6 mg/mL
Dilution factor	1:25	1:200	1:300	1:100	1:200	1:1000	1:1000	1:1000
Antibody concentration after dilution	20 µg/mL	1 µg/mL	0.4 µg/mL	10 µg/mL	1 µg/mL	1.4 µg/mL	1.5 µg/mL	0.6 µg/mL

Appendix 4

In situ proximity ligation assay protocol

All incubations are performed in a humidified chamber

1. Cell culture:

a) Seed HeLa cells on glass slides and incubate overnight

2. Fixation/permeabilization:

a) Wash the cells carefully with warm PBS prior to fixation

b) Fix the cells with one of the four protocols:

i. Fix the cells in fresh, neutral buffered 10% formalin solution for 10 minutes (room temperature)
ii. Fix the cells in fresh, neutral buffered 10 % formalin solution for 10 minutes (room temperature) and permeabilize cells with a detergent buffer for 1 hour on ice
iii. Fix the cells in fresh, neutral buffered 10 % formalin solution for 10 minutes and permeabilize with cold (-20 °C) methanol for 10 minutes (-20 °C)
iv. Fix and permeabilize the cells with cold (-20 °C) methanol for 10 minutes (-20°C)

c) Wash cells thrice with PBS, and leave the methanol fixated cells in PBS for 2-3 minutes

3. Delimit the reaction area (about 1 cm^2) with a grease pen or silicone mask, *e.g.* ImmEdge™ Pen from Vector Laboratories

4. Transfer the slides to a humidified chamber and wash with PBS

5. Blocking and antibody incubations:

a) Block the cells in duolink blocking solution for 30 minutes at 37 °C

b) Dilute the primary antibodies in antibody diluent according to table 1.

c) Tap off blocking solution from slides and add 40 µL primary antibody solution. Incubate for 2 hours at room temperature.

d) Vortex and dilute PLA probe PLUS and MINUS 1:5 in antibody dilution

e) Tap off primary antibody solution from slides and wash them in a container with at least 70 mL room tempered wash buffer A on a shaker with gentle orbital shaking.

f) Vortex and add 40 µL of the diluted PLA probes and incubate in a pre-heated chamber for 1 hour at 37 °C

6. Ligation:

a) Dilute the ligation stock 1:5 in milliQ water and mix

b) Tap off the PLA probes from the slides and wash the slides in 1x Wash Buffer A for 2 x 5 minutes with gentle agitation

c) Remove the ligase from the freezer using a freeze block, vortex and add the ligase to the ligation solution from step a) at a 1:40 dilution. Vortex before applying the solution to the cells

d) Add 40 µL ligation-ligase solution to the cells and incubate in a pre-heated humidified chamber for 30 minutes at 37 °C

7. Amplification:
NB! Light sensitive reagents

a) Dilute the amplification stock 1:5 in milliQ water and mix

b) Tap off the ligation-ligase solution from the slides and wash the slides in 1x Wash Buffer A for 2 x 2 minutes with gentle agitation

c) Remove the polymerase from the freezer using a freeze block, vortex and add the polymerase to the amplification solution from step a) at a 1:80 dilution. Vortex before applying the solution to the cells

d) Add 40 µL amplification-polymerase solution to the cells and incubate in a pre-heated humidified chamber for 100 minutes at 37 °C

8. Wash and DNA staining step:
NB! Light sensitive slides. Wash and dry the slides protected from light

a) Tap off the Amplification-Polymerase solution from the slides

b) Wash the slides for 2 x 10 minutes with 1x Wash Buffer B

c) Wash the slides for 1 minute with 0,01x Wash Buffer B

d) Mount with 5 µL duolink mounting medium with DAPI. Be careful not to trap air bubbles under the coverslip

h) Use nail polish to seal the edges of the coverslip

The slides can be stored in the dark at -20°C

Table 1. The dilution factors and concentrations of the various antibodies for PLA

	Primary antibodies				
Antibody	Mouse anti-CKS2	Mouse anti-CDK1	Rabbit anti-SSBP1	Rabbit anti-CDK1	Rabbit anti-CDK2
Antibody concentration prior to dilution	0.5 mg/mL	0.2 mg/mL	0.12 mg/mL	1mg/mL	0.2 mg/mL
Dilution factor	1:25	1:200	1:300	1:100	1:200
Antibody concentration after dilution	20 µg/mL	1 µg/mL	0.4 µg/mL	10 µg/mL	1 µg/mL

Table 2. The reagents included in the duolink II orange starter kit.

Reagents	Function[a]
PLA probe anti-mouse minus	Secondary antibody that binds to mouse primary antibodies. It is linked to an oligonucleotide which serves as a template for circularization of so-called connector oligonucleotides by enzymatic ligation
PLA probe anti-rabbit plus	Secondary antibody that binds to rabbit primary antibodies. It is linked to an oligonucleotide which serves as a template for circularization of so-called connector oligonucleotides by enzymatic ligation
Blocking solution	The blocking solution prevents unspecific binding of the antibodies
Antibody diluent	It is used to dilute primary and secondary antibodies. According to duolink, it contains salt, blocking solution and detergents
Ligation solution	Consists of two different connector-oligonucleotides which hybridize to the two PLA probe oligonucleotides and form a closed circle
Ligase	An enzyme that ligates the oligonucleotides together to form a closed circle which serves as a template for rolling circle amplification
Amplification solution	Consists of nucleotides labeled with a fluorophore used to produce a single-stranded product during rolling circle amplification. The fluorophore is excitated at 554 nm and emits fluorescence of 579 nm
Polymerase	An enzyme that uses the ligated circle as a template for rolling circle amplification

Wash buffer A and B for fluorescence	Wash buffer A was used after incubation with primary antibodies, PLA probes and ligation-ligase solution. Wash buffer B was used after incubation with the amplification-polymerase solution
Mounting medium with DAPI	A mounting medium that preserves the PLA signals. It contains DAPI nuclear stain with excitation of 360 nm and emission of 460 nm

[a] The functions the reagents have in the assay [17]

Appendix 5

Detergent buffer formula

Formula for 500 mL detergent buffer:

-0.1% Igepal CA-630. Do not store the detergent buffer with this component. Therefore, add this component immediately before use.

-6.5 mM Na_2HPO_4 x 2 H_2O

-2.7 mM KCl

-137 mM NaCl

-0.5 mM EDTA

Na2HPO4 x 2 H_2O has a molar mass of 177.99 g/mol. 0.00325 mol (per 500 mL) x 177.99 g/mol x 1000mg/g = 578.47 mg. One will need 578.47 mg to produce a 6.5 mM Na2HPO4 x 2 H_2O solution in 500 mL distilled water.

KCl has a molar mass of 74.55 g/mol. 0.00135 mol (per 500 mL) x 74.55 g/mol x 1000 mg/g = 100.64 mg. One will need 100.64 mg to produce a 2.7 mM KCl solution in 500 mL distilled water.

NaCl has a molar mass of 58.44 g/mol. 0.0685 mol (per 500 mL) x 58.44 g/mol x 1000 mg/g = 4003 mg. One will need 4003 mg to produce a 137 mM NaCl solution in 500 mL distilled water.

EDTA (= $C_{10}H_{14}N_2O_8Na_2$ x $2H_2O$) has a molar mass of 372.2 g/mol. 2.5 x 10^{-4} mol (per 500 mL) x 372.2 g/mol x 1000 mg/g = 93 mg. One will need 93 mg to produce a 0.5 mM EDTA solution in 500 mL distilled water.

1. Weigh out the correct amount of each salt on an analytical balance.
2. Add the salts, one of a time, to a 500 mL bottle with some of the distilled water. Add a magnet into the beaker and stir with a magnetic stirrer until the solids dissolve.
3. Fill the remainder of the 500 mL volume with distilled water
4. Adjust the pH to 7.5 using NaOH and store at 4 °C

Appendix 6

Zeiss Axio Imager.z1 fluorescence microscope protocol

1. Preparations:

a) Turn on the instruments in the following order: HXP 120 (mercury lamp) → Power supply→ ApoTome → Microscope → Computer

b) Then log in (the username is stokke) and double click on the AxioVision Rel. 4.8 icon on the desktop

2. The Microscope:

a) Adjust the intraocular distance between the binoculars

b) Press in the plunger which controls the light path. When the plunger is pressed in all the light transfers to the eyepieces whereas when it is out all the light transfers to the camera

c) Lower the stage by pushing switches which are on the right side of the microscope and place a sample slide on the stage with the coverslip facing the objective. Apply a small drop of immersion oil directly on the coverslip when using the objectives 63x or 100x and raise the stage

d) Push "Microscope", "FL" and "RL shutter open" on the touch screen

e) Use the focus knob until the specimen is clearly in focus

f) Pull out the plunger. The light from the microscope will then be transmitted to the camera instead of the binoculars

3. The Computer:

a) To set up channels click "multidimentional acquisition" followed by "multidimentional acquisition" in the work area. Click on the C tab, then "channel pool" and select the channels you need from the list of dyes. Click on "add to experiment" and close the window

b) Inactivate "1" by right-clicking on the channel

c) Click on "ApoTome Mode" in the toolbar, go to the settings tab and choose "raw data mode" and "grid visible"

d) Click on the "measure" button in the work area and let the camera decide the optimal exposure level. Use the focus knob to check if the image is overexposed. If any red spots appear in the image, adjust the exposure manually using the top slider control. Repeat this for the rest of the channels as well.

4. Push the ApoTome slider into the microscope

a) If you want to capture a photo without a z-stack, press start.

b) Z-stack is a series of images acquired at different focus positions. To capture a photo with a z-stack then go to the z tab under "multidimentional acquisition". Check the tick box for z-stack. If you would like to capture photos of all channels before changing z, check the "All Channels per slice" tick box and click on the "start/stop" button. Press the upper "…" and focus the microscope to the top stage position, then press OK. Click on the lower "…", focus the microscope to the bottom stage position and press OK.

c) Click on “optimal distance”. The number of sections will update automatically depending on the interval between the top and bottom stage position. Adjust the number of sections if desirable and press “start”.
d) To create a projection of the z-stack click on the following buttons in the work area: sim converter → choose “optical selection” (combine mode) → turn on “display normalization” and make sure that “filter” and “image normalization” is turned off. Uncheck the “enable channel selection” tick box and press “start”. A new image will appear on the screen. Click on “image processing” in the work area, then “geometric”, “orthoview” and XY (parameters) and press “start”
e) The splitter window can be used to view all the channels of the image separately. Click the “splitter” button at the toolbar. Click the “gallery” button and select images for each pane. Choose which channels you want to view in each pane and click “create image”

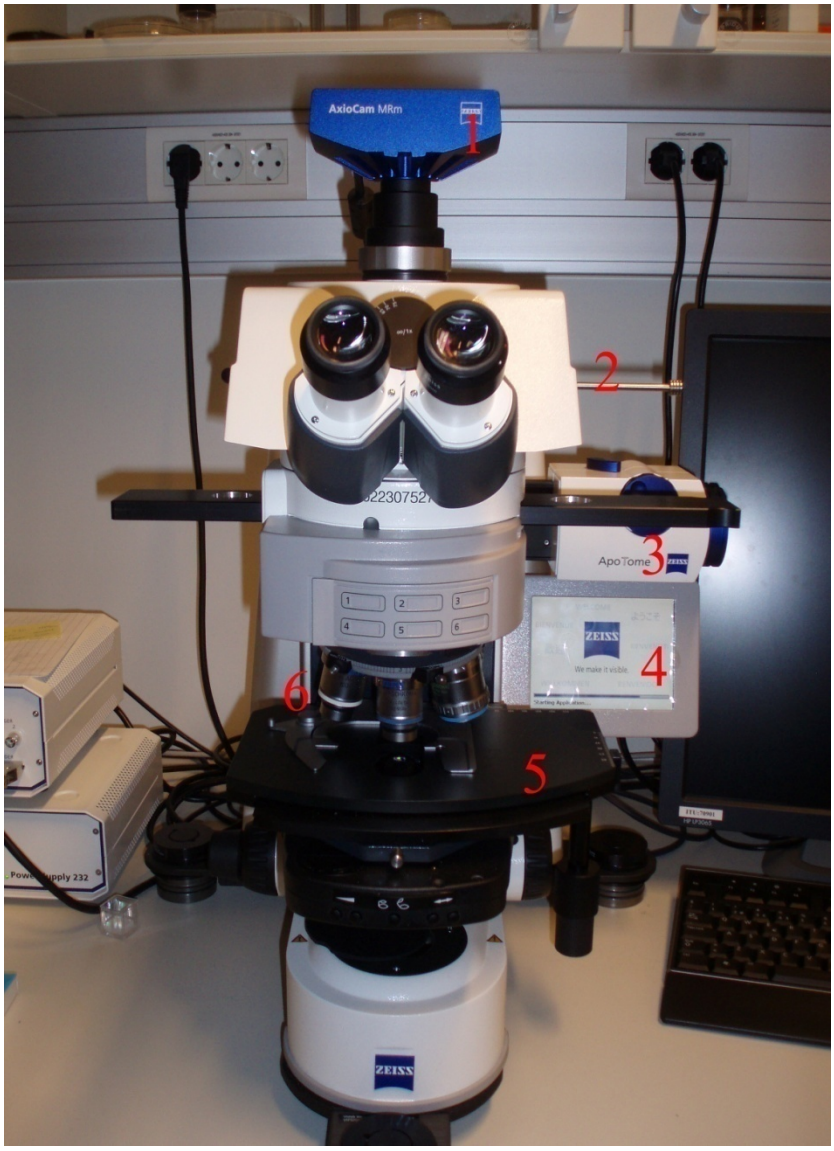

Figure 1. Some of the components of the fluorescence microscope 1. Camera. 2. Plunger that controls the light path. 3. ApoTome. 4. Touch screen. 5. Sample platform. 6. Objectives.

Appendix 7

Immunocytochemistry signal from formalin fixated cells

Formalin fixated cells stained with CKS2 and CDK1 antibody produced a good signal (figure 1). Some cells exhibited a green CDK1 dot outside the nucleus, but many cells did not display any of these. Formalin fixation displayed a yellow signal in the cytoplasm and the nucleus (figure 1 D) formed by co-localization of the red CKS2 and green CDK1 signals. No fluorescence signal was spotted in the nucleoli.

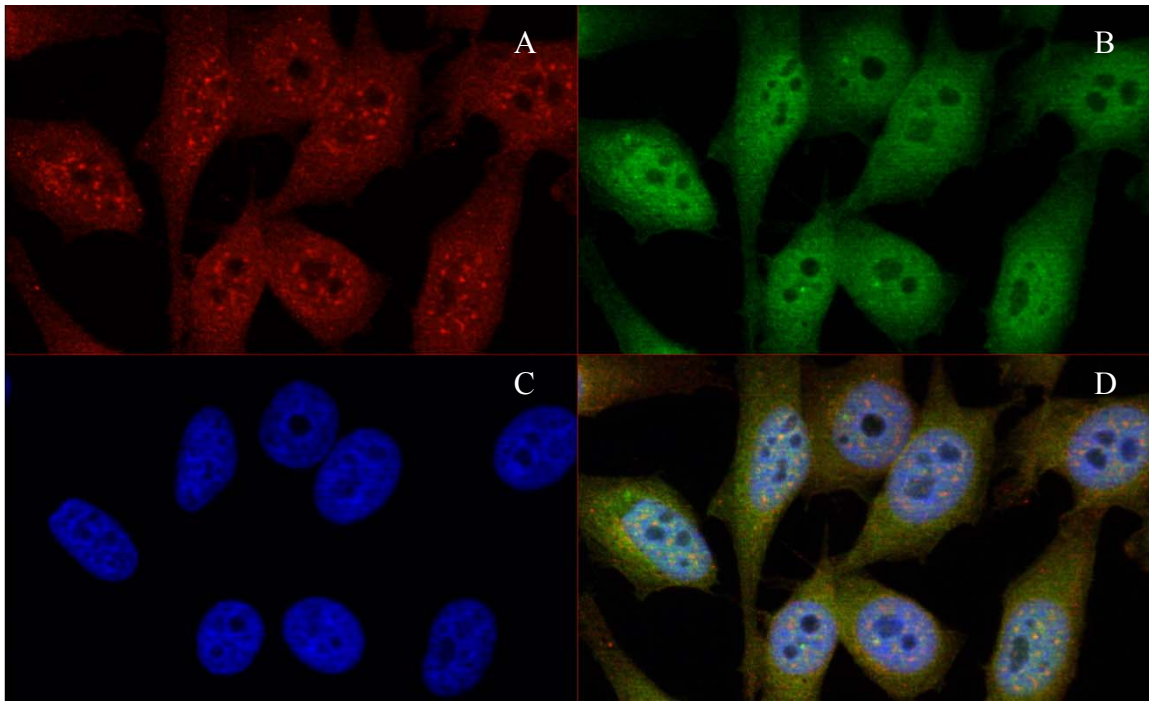

Figure 1. Signal of mouse anti-CKS2 antibody and rabbit anti-CDK1 antibody in formalin fixated HeLa cells. A. Signal obtained from binding of CKS2antibody. B. Signal from CDK1 antibody. C. Signal from stained DNA. D. Signals from A-C superimposed on each other

Formalin fixated cells stained with CKS2 and CDK2 antibody produced a good signal (figure 2). The signal from CKS2 stained foci in the nucleus are apparent, but they differ less in fluorescence intensity from those in the cytoplasm compared to methanol fixated cells. Formalin fixation displayed a pronounced yellow signal (figure 2 D) formed by co-localization of the red CKS2 and green CDK2 signals. No fluorescence signal was spotted in the nucleoli.

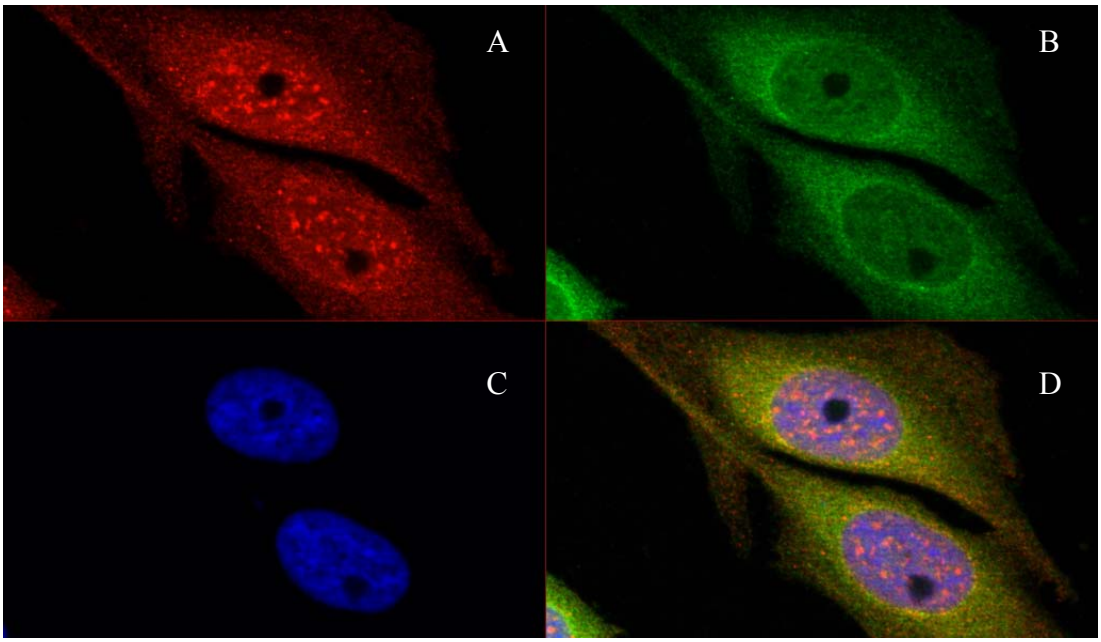

Figure 2. Signal of mouse anti-CKS2 antibody and rabbit anti-CDK2 antibody in formalin fixated HeLa cells. A. Signal obtained from binding of CKS2 antibody. B. Signal from CDK2 antibody. C. Signal from stained DNA. D. Signals from A-C superimposed on each other.

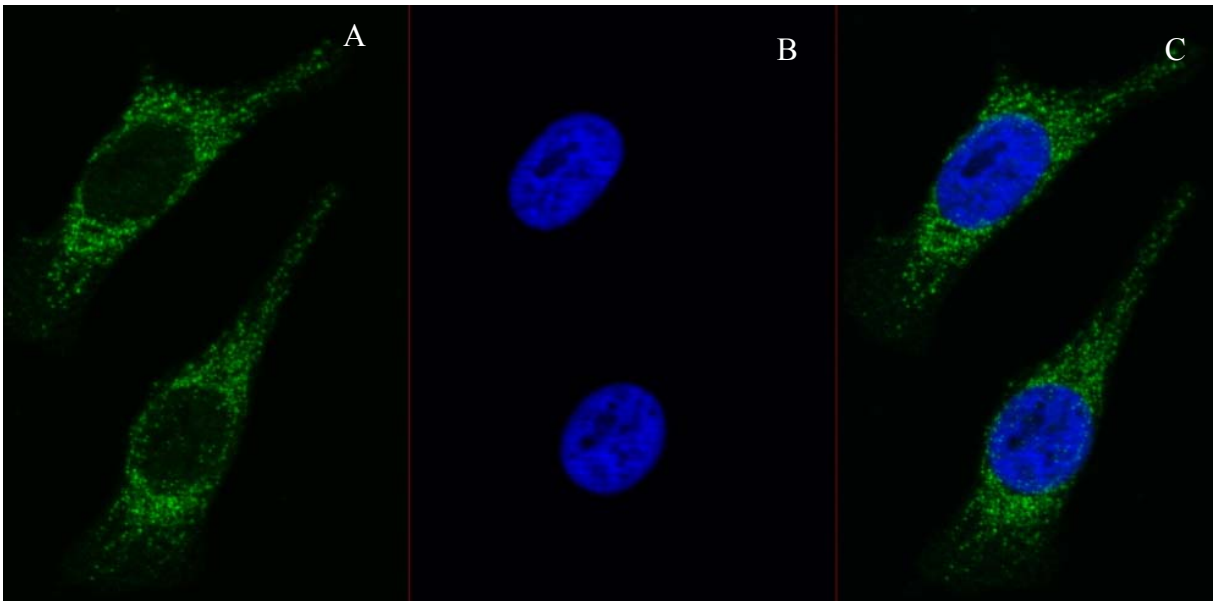

Figure 3. Signal of rabbit anti-SSBP1 antibody in formalin fixated HeLa cells. A. Signal obtained from binding of SSBP1 antibody. B. Signal from stained DNA. C. A and B superimposed on each other.

Formalin fixated cells stained with SSBP1 antibody produced a good signal (figure 3). The signaling came mainly from the cytoplasm, although weak signals occurred also in the nucleus of certain cells. The structure of the stained proteins in the outskirts of the cytoplasm was thread-like.

Formalin fixated cells stained with CKS2 and SSBP1 antibody produced a good signal (figure 4). The signal from CKS2 stained foci in the nucleus are apparent, but they differ less in fluorescence intensity from those in the cytoplasm compared to methanol fixated cells. Formalin fixation displayed some yellow signals in the cytoplasm (figure 4 D) formed by co-localization of the red CKS2 and green SSBP1 signals. No fluorescence signal was spotted in the nucleoli.

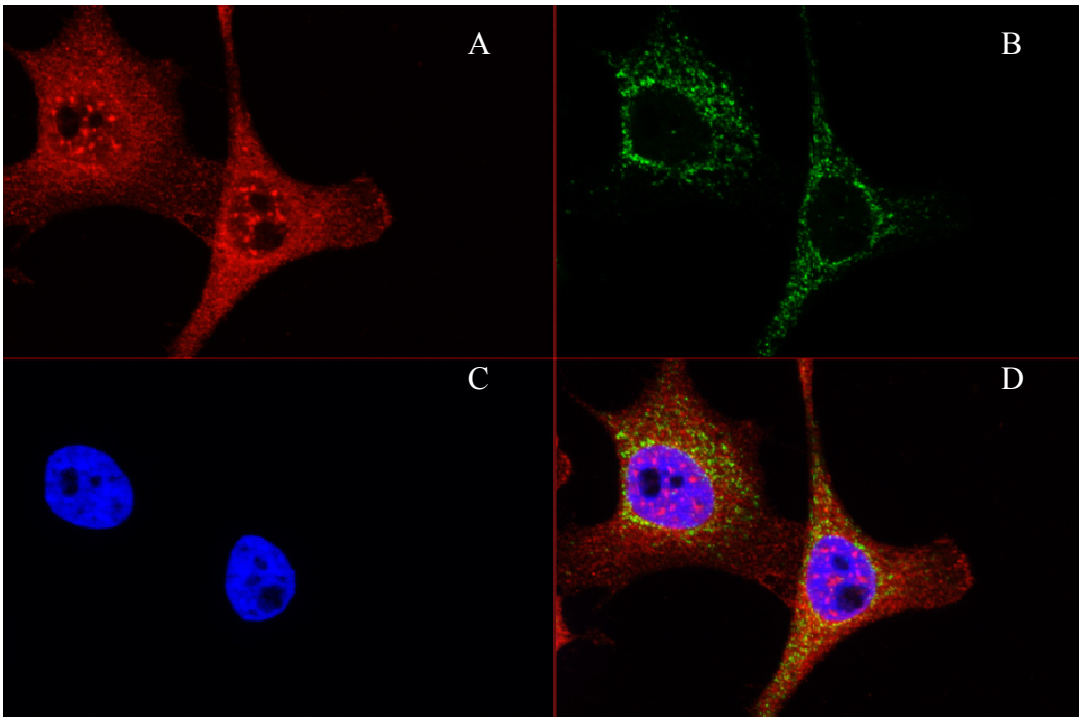

Figure 4. Signal of mouse anti-CKS2 and rabbit anti-SSBP1 antibody in formalin fixated HeLa cells. A. Signal obtained from binding of CKS2antibody. B. Signal from SSBP1 antibody. C. Signal from stained DNA. D. Signals from A-C superimposed on each other.

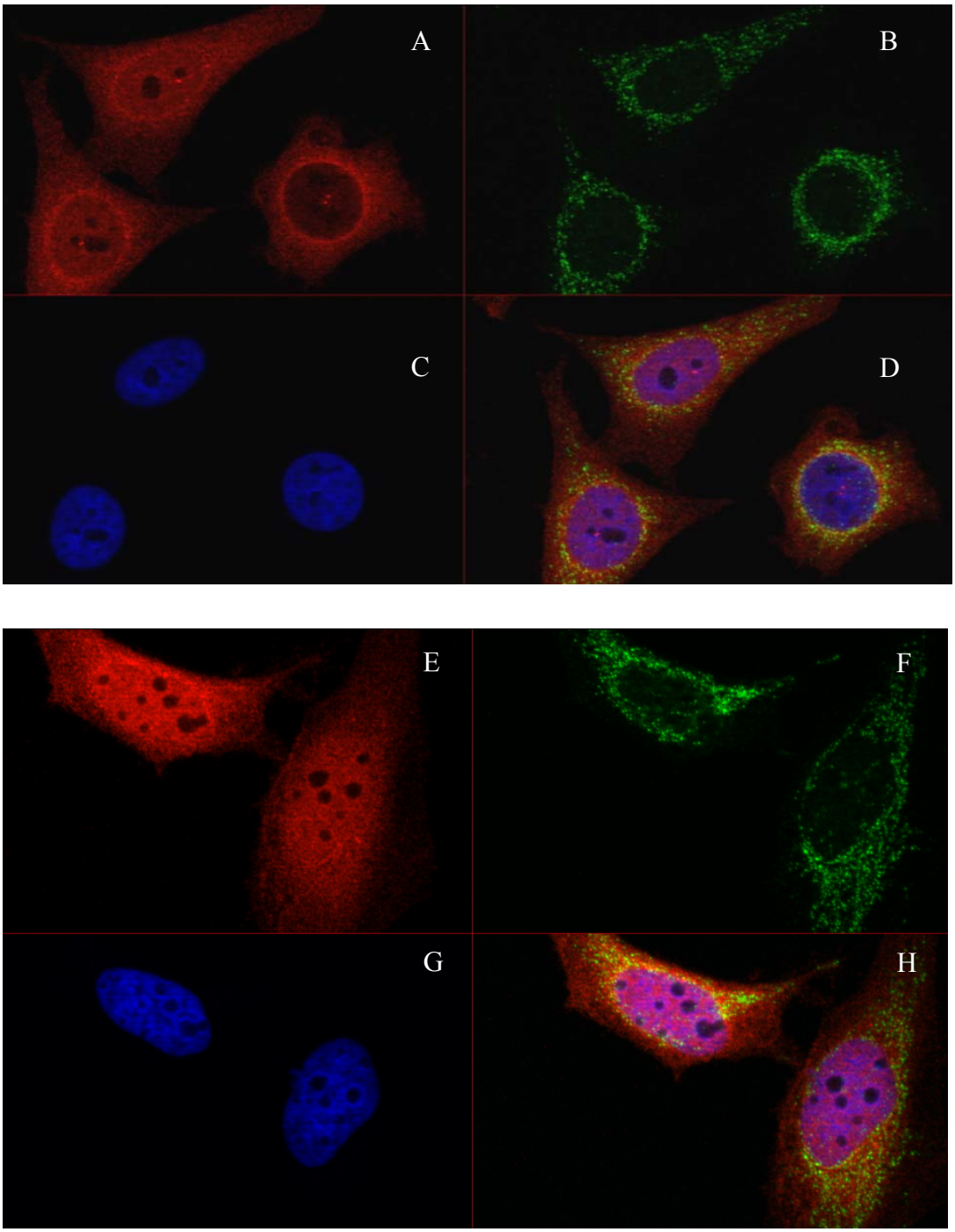

Figure 5. Signal of rabbit anti-SSBP1 antibody and mouse anti-CDK1 antibody in formalin fixated HeLa cells. A and E. Signal obtained from binding of CDK1antibody. B and F. Signal from SSBP1 antibody. C and G. Signal from stained DNA. D and H. Respective signals from A-C and E-G superimposed on each other.

Formalin fixated cells stained with SSBP1 and CDK1 antibody also produced a good signal (figure 5). The signal from CDK1 staining varied among cells. Some cells exhibited conspicuous dots outside the nucleus (Figure 5 A), whereas other cells showed no similar dots

(figure 5 E). Formalin fixation displayed a yellow signal (figure 5 D and H) formed by co-localization of the red CDK1 and green SSBP1 signals. No fluorescence signal was spotted in the nucleoli.

Appendix 8

Controls for the immunocytochemistry experiments

As control for possible reaction between primary antibodies obtained from mice with secondary antibodies reactive for primary antibodies produced in rabbit, HeLa cells were stained for CKS2 anti-mouse and secondary anti-rabbit (figure 1). A. shows a very weak signal corresponding to signals from unstained cells. Most likely, this is caused by autofluorescence of the cells.

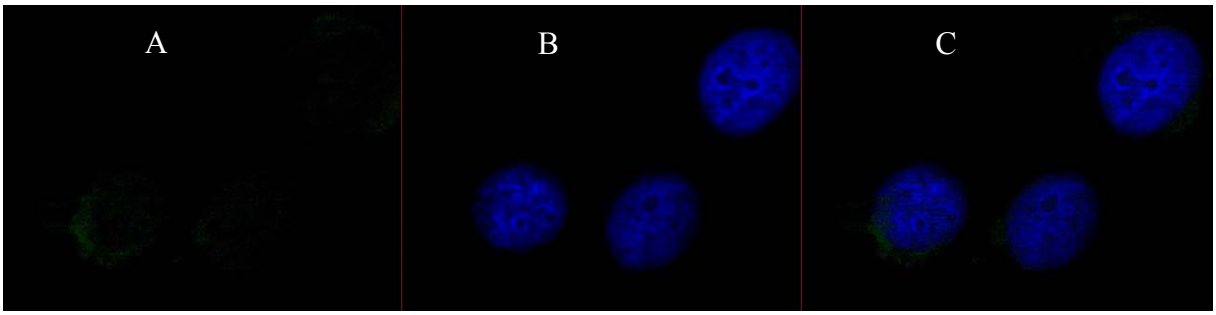

Figure 1 Control of cross reaction between CKS2 anti-mouse and secondary donkey anti-rabbit antibody in methanol fixated HeLa cells. A. Signal obtained from CKS2 stained cells, which have received secondary antibody reactive for primary antibody produced in rabbits. B. Signal from stained DNA. C. A and B superimposed on each other.

As control for possible reaction between primary antibodies obtained from rabbit with secondary antibodies reactive for primary antibodies produced in mouse, HeLa cells were stained for CDK1 anti-rabbit and secondary anti-mouse (figure 2). A. shows a very weak signal corresponding to signals from unstained cells. Most likely, this is caused by autofluorescence of the cells.

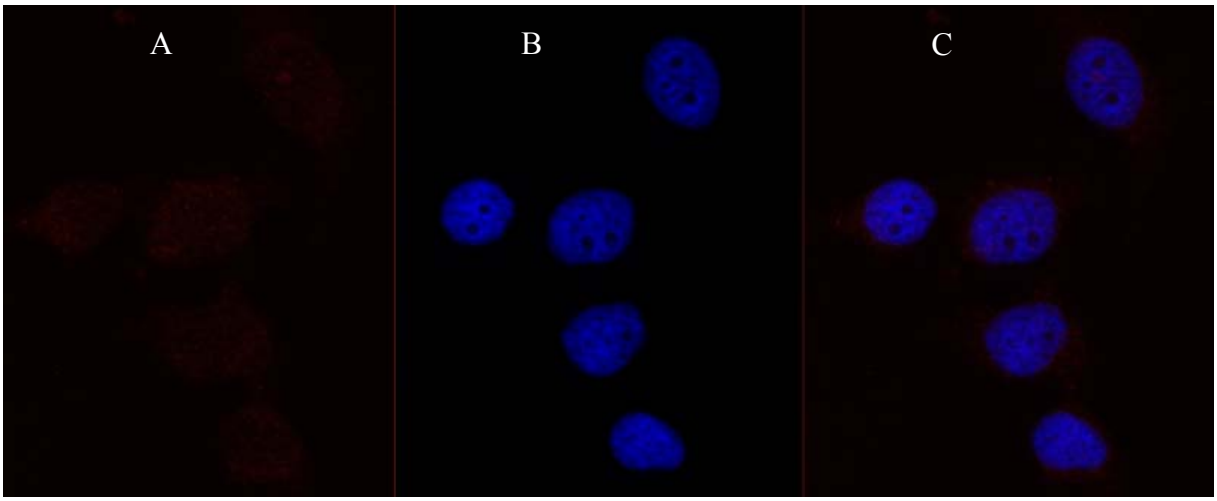

Figure 2 Control of cross reaction between CDK1 anti-rabbit and secondary donkey anti-mouse antibody in methanol fixated HeLa cells. A. Signal obtained from CDK1 stained cells, which have received secondary antibody reactive for primary antibody produced in mouse. B. Signal from stained DNA. C. A and B superimposed on each other.

As control for possible reaction between primary antibodies obtained from rabbit with secondary antibodies reactive for primary antibodies produced in mouse, HeLa cells were stained for CDK2 anti-rabbit and secondary anti-mouse (figure 3). The cells showed a very weak signal corresponding to signals from unstained cells. Most likely, this is caused by autofluorescence of the cells.

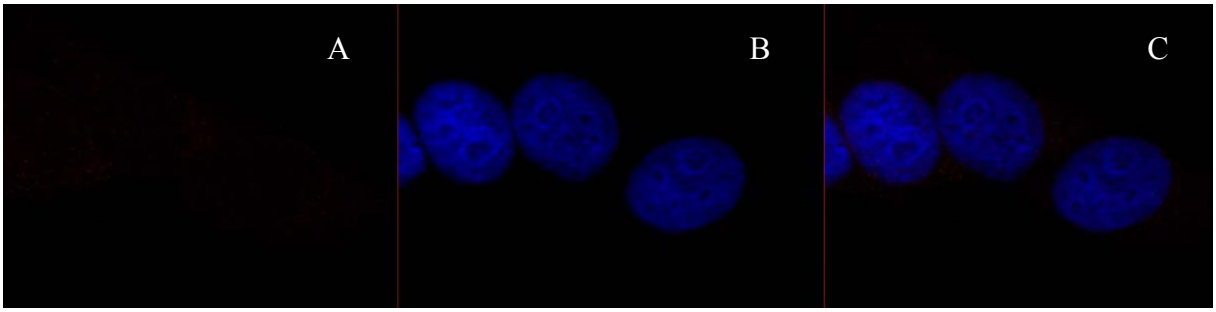

Figure 3 Control of cross reaction between CDK2 anti-rabbit and secondary donkey anti-mouse antibody in methanol fixated HeLa cells. A. Signal obtained from CDK2 stained cells, which have received secondary antibody reactive for primary antibody produced in mouse. B. Signal from stained DNA. C. A and B superimposed on each other.

As control for possible reaction between primary antibodies obtained from rabbit with secondary antibodies reactive for primary antibodies produced in mouse, HeLa cells were stained for SSBP1 anti-rabbit and secondary anti-mouse (figure 4). The cells showed a very

weak signal corresponding to signals from unstained cells. Most likely, this is caused by autofluorescence of the cells.

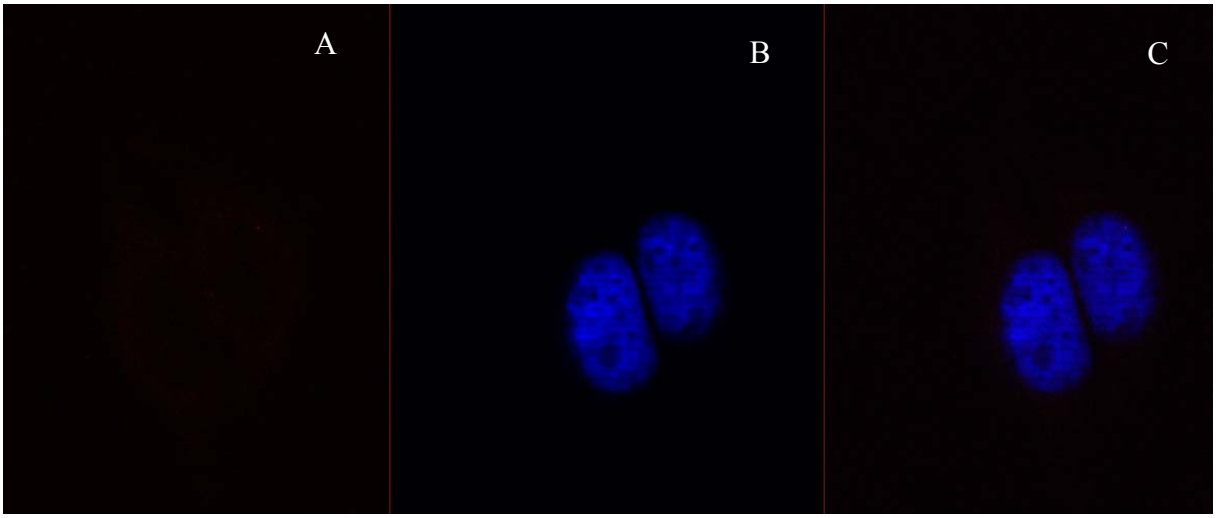

Figure 4 Control of cross reaction between SSBP1 anti-rabbit and secondary donkey anti-mouse antibody in methanol fixated HeLa cells. A. Signal obtained from SSBP1 stained cells, which have received secondary antibody reactive for primary antibody produced in mouse. B. Signal from stained DNA. C. A and B superimposed on each other.

As control for possible reaction between primary antibodies obtained from rabbit with secondary antibodies reactive for primary antibodies produced in mouse, HeLa cells were stained for CDK1 anti-mouse and secondary anti-rabbit (figure 5). The cells showed a very weak signal corresponding to signals from unstained cells. Most likely, this is caused by autofluorescence of the cells.

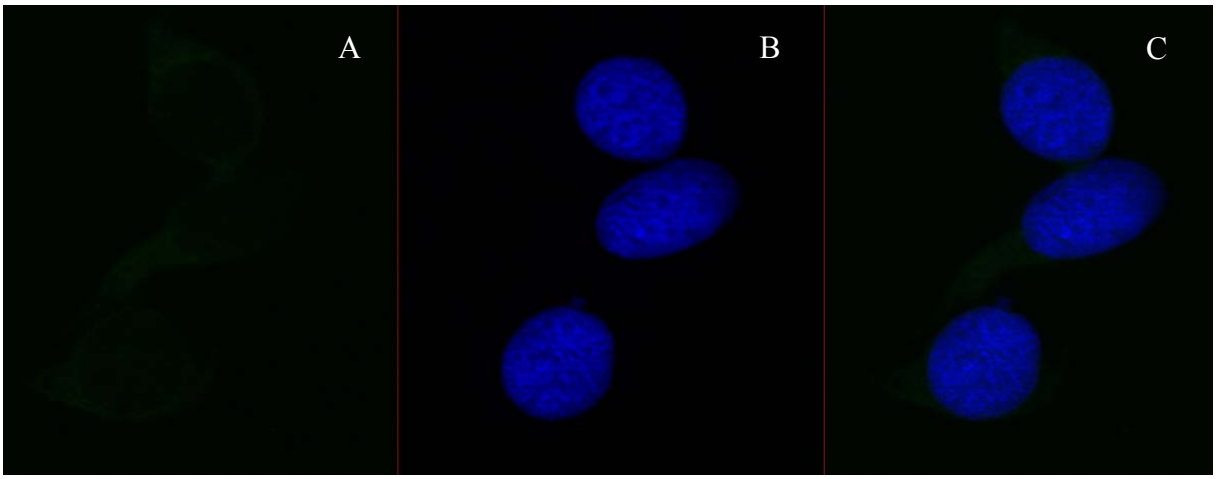

Figure 5 Control of cross reaction between CDK1 anti-mouse and secondary donkey anti-rabbit antibody in methanol fixated HeLa cells. A. Signal obtained from CDK1 stained cells, which have received secondary antibody reactive for primary antibody produced in rabbit. B. Signal from stained DNA. C. A and B superimposed on each other.

As control for possible signal obtained from unspecific binding of secondary antibody, HeLa cells were stained for secondary anti-rabbit (figure 6). The cells showed a very weak signal corresponding to signals from unstained cells. Most likely, this is caused by autofluorescence of the cells.

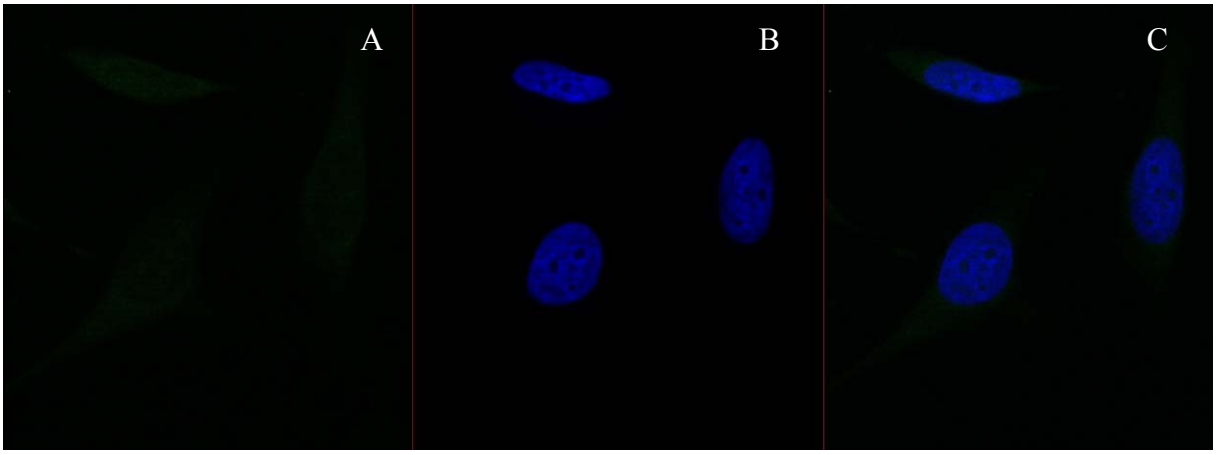

Figure 6 Control of unspecific binding of secondary donkey anti-rabbit antibody in methanol fixated HeLa cells. A. Signal obtained from donkey anti-rabbit in unstained cells. B. Signal from stained DNA. C. A and B superimposed on each other.

As control for possible signal obtained from unspecific binding of secondary antibody, HeLa cells were stained for secondary anti-mouse (figure 7). The cells showed a very weak signal corresponding to signals from unstained cells. Most likely, this is caused by autofluorescence of the cells.

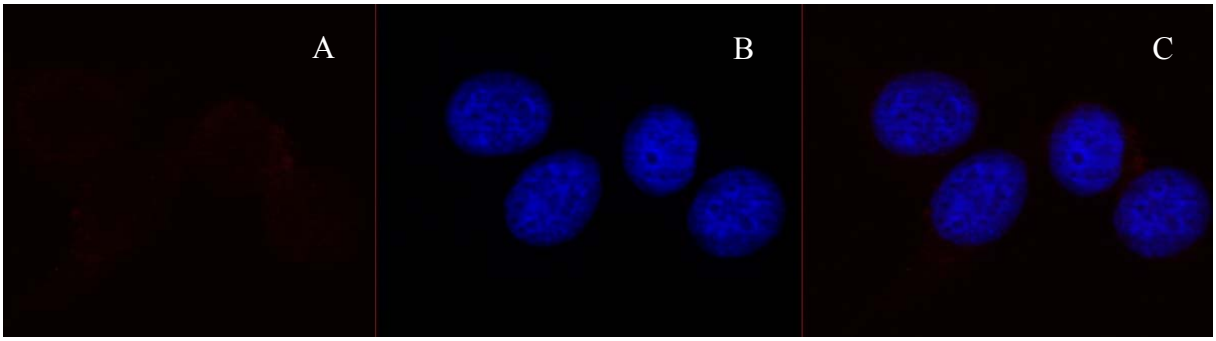

Figure 7 Control of unspecific binding of secondary donkey anti-mouse antibody in methanol fixated HeLa cells. A. Signal obtained from donkey anti-mouse in unstained cells. B. Signal from stained DNA. C. A and B superimposed on each other.

As a control for possible reaction between primary antibodies obtained from rabbit with secondary antibodies reactive for primary antibodies produced in mice, HeLa cells were

stained for γ-tubulin anti-mouse and secondary anti-rabbit (figure 8). The control cells showed a very weak signal corresponding to signals from unstained cells. Most likely, this is caused by autofluorescence of the cells.

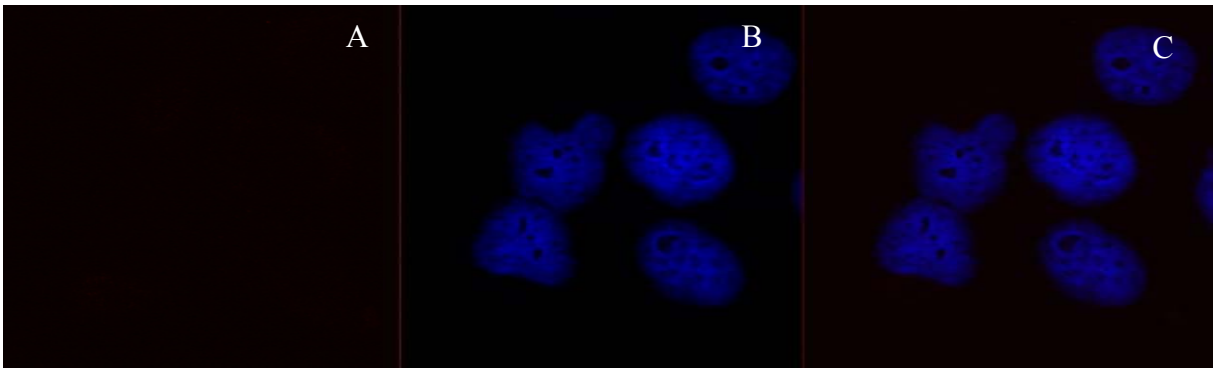

Figure 8 Control of cross reaction between mouse anti-γ tubulin and secondary donkey anti-mouse antibody in methanol fixated HeLa cells. A. Signal obtained from γ tubulin stained cells, which have received secondary antibody reactive for primary antibody produced in mouse. B. Signal from stained DNA. C. A and B superimposed on each other.

Controls for the PLA experiments

As control for possible signal obtained from binding of secondary antibodies, HeLa cells were incubated with secondary PLA probes (antibodies) (figure 9). A. shows almost no signal. Most likely, this was caused by pollution during washing.

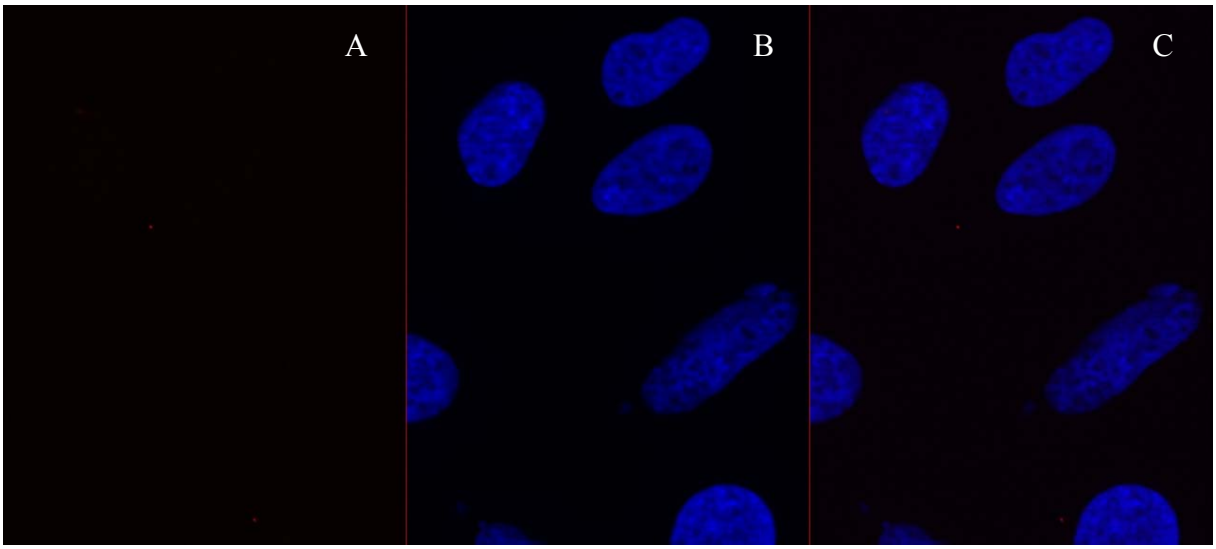

Figure 9 Control for possible PLA signal of secondary antibodies in methanol fixated HeLa cells. A. Signal obtained from secondary antibodies in unstained cells. B. Signal from stained DNA. C. A and B superimposed on each other.

As control for possible signal obtained from binding of secondary antibodies to one primary antibody, HeLa cells were incubated with CKS2 primary antibody and two secondary PLA probes (antibodies) (figure 10). A. shows almost no signal. Most likely, this was caused by pollution during washing.

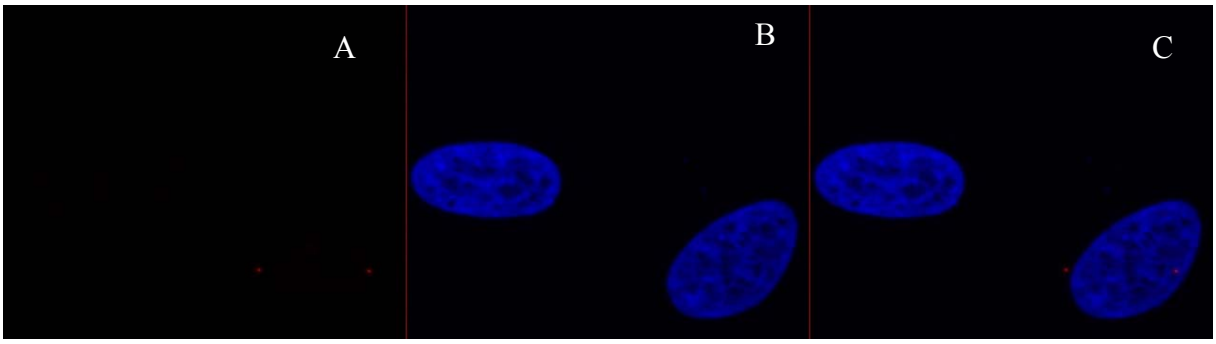

Figure 10 Control for possible PLA signal of primary CKS2anti-mouse antibody and both secondary antibodies (PLA probe mouse and rabbit) in methanol fixated HeLa cells. A. Signal obtained from binding of both secondary antibodies to one of the primary antibodies. B. Signal from stained DNA. C. A and B superimposed on each other.

As control for possible signal obtained from binding of secondary antibodies to one primary antibody, HeLa cells were incubated with SSBP1 primary antibody and two secondary PLA probes (antibodies) (figure 11). A. shows almost no signal. Most likely, this was caused by pollution during washing.

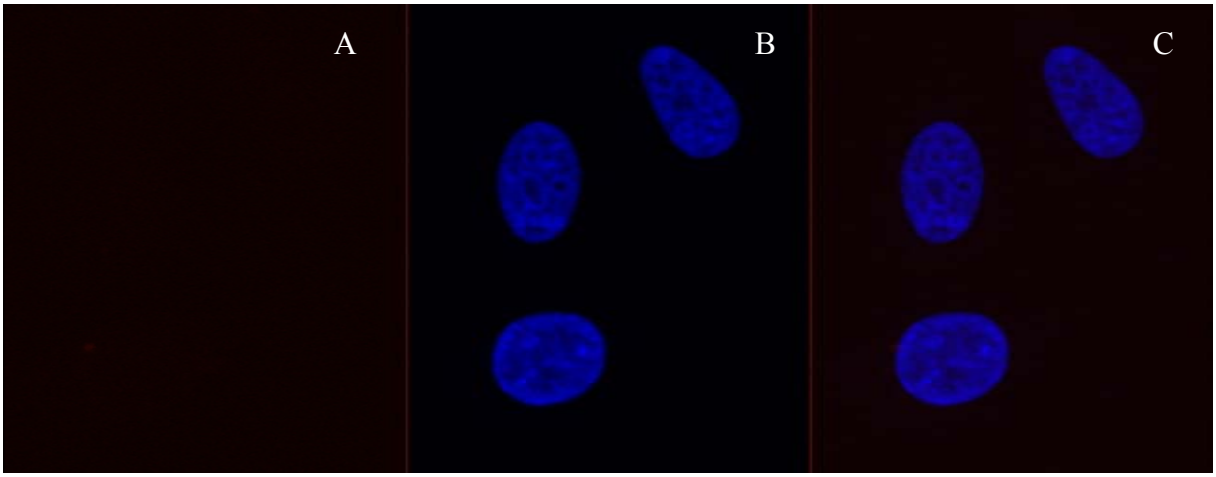

Figure 11 Control for possible PLA signal of primary SSBP1anti-rabbit antibody and both secondary antibodies (PLA probe mouse and rabbit) in methanol fixated HeLa cells. A. Signal obtained from binding of both secondary antibodies to one of the primary antibodies. B. Signal from stained DNA. C. A and B superimposed on each other.

Appendix 9

Reagents used in the experiments

Reagent	Company	Concentration
Albumin, from bovine serum	Sigma-Aldrich	
CDK1 mouse antibody: sc-54	Santa Cruz Biotechnology	0.2 mg/mL
CDK1 rabbit anti-Human polyclonal antibody (Catalog ID LS-C123204)	Lifespan Biosciences	1 mg/mL
CDK2(M2) sc-163 rabbit polyclonal antibody	Santa Cruz Biotechnology	0.2 mg/mL
CKS2 mouse antibody (Catalog No 37-0300)	Life Technologies	0.5 mg/mL
Coulter clenz cleaning agent	Beckman Coulter	
Coulter isoton II diluent	Beckman Coulter	
Duolink II amplification solution	Olink Bioscience	5X
Duolink II blocking solution	Olink Bioscience	
Duolink II ligase	Olink Bioscience	
Duolink II ligation	Olink Bioscience	5X
Duolink II mounting medium with DAPI	Olink Bioscience	
Duolink II polymerase	Olink Bioscience	
Duolink II PLA probe minus	Olink Bioscience	5X
Duolink II PLA probe plus	Olink Bioscience	5X
Duolink II wash buffer A	Olink Bioscience	
Duolink II wash buffer B	Olink Bioscience	
DMEM + Glutamax ™ growth medium (catalog number 31966-021)	Life Technologies	

Dulbecco's PBS without calcium and magnesium (catalog number H-15-002)	PAA Laboratories	1x
Dylight 549-conjugated affinipure donkey anti-mouse	Jackson ImmunoResearch	1.4 mg/mL
Dylight 488- conjugated affinipure donkey anti-rabbit	Jackson ImmunoResearch	1.5 mg/mL
EDTA, disodium salt dihydrate	Sigma-Aldrich	
Formalin solution, neutral buffered	Sigma-Aldrich	10 %
Gibco fetal bovine serum	Life Technologies	
γ-tubulin antibody	Kind gift of Stephen Doxsey, University of Massachusetts Medical School, Worcester, MA (U.S.A)	
Hoechst 33258	Sigma-Aldrich	
Igepal CA-630 (for molecular biology)	Sigma-Aldrich	
Immersion oil	Zeiss	
KCl	Sigma-Aldrich	
L-glutamine	PAA Laboratories	200 mM
Methanol	VWR	
Na_2HPO_4 x 2 H_2O	Merck	
NaCl	Sigma-Aldrich	
NaOH	Sigma-Aldrich	
Penicillin/Streptomycin	PAA Laboratories	100X
ProLong® Gold antifade reagent	Life Technologies	
SSBP1 rabbit antibody Catalog number HPA002866	Sigma-Aldrich	0.12mg/mL

Triton X-100	Sigma-Aldrich	Triton X-100
Trypsin-EDTA solution	Sigma-Aldrich	1X